STUDY OF ANISOTROPIC BEHAVIOR AT JOINTED ROCKS FOR BIG SPAN UNDERGROUND STRUCTURES WITH NATM PHILOSOPHY

by

Mustafa KOÇ

B.S., in Civil Engineering, Istanbul Technical University, 2003

B.S., in Geological Engineering, Istanbul Technical University, 2004

M.S., in Civil Engineering, Istanbul Technical University, 2006

Submitted to the Institute for Graduate Studies in
Science and Engineering in partial fulfillment of
the requirements for the degree of
Doctor of Philosophy

Graduate Program in Civil Engineering

Boğaziçi University

2019

Dedicated to Engineering

ACKNOWLEDGEMENTS

The author of this study wishes to gratefully acknowledge the following supervisors who have contributed to this study through their physical, mental and emotional support over the past fifteen years: Prof. Erol Güler, Prof. Mahir Vardar. He is also grateful to his family for their backup on a complimentary basis.

ABSTRACT

STUDY OF ANISOTROPIC BEHAVIOR AT JOINTED ROCKS FOR BIG SPAN UNDERGROUND STRUCTURES WITH NATM PHILOSOPHY

Underground structures mainly composed in rock environment may be defined as the load-bearing structures under all loading cases. The behavior of the rock environment is the critical component in understanding the behavior of the underground structure and the design procedures. NATM that is accepted as a philosophy rather than a design method is the primary conception in underground rock engineering. The behavior of the rock environment under principal stresses is going to be affected, utilizing secondary and tertiary stresses. The physical dimensions of the technical interference (can be accepted as tunnel structure) which is to be the main issue in the classical design should be designated due to their orientation, joint structures and its surrounding environment properties.

The main goal of this study is to examine the relationship between the dimensions of the excavated area with its surrounding environment for anisotropic behavior to define the problem more accurately. Physical and numerical modeling tools were used, and the dimensionless interactions in the design of underground structures were tried to be built. Base friction method was selected and bricks from sugar were used for physical modelling. The ratio of joint openings to tunnel diameter was varied between six to twelve with changing inclination of joints from horizontal to ninety degrees (gradually with 15 degrees each set) with respect to horizontal were provided simultaneously. One of the goals was to determine the influence distance of number of joints at the heading part of the tunnel. Moreover, the variation of influence zone due to the effect of the anisotropy was also studied. The results of total 49 numbers of tests were interpreted, and an analytical variation was derived. The findings of the study were aimed to gain the effectiveness of the excavating strategies in the light of NATM philosophy to find out the correct phenomena in design for big span underground structures.

ÖZET

NATM FELSEFESI YAKLAŞIMI ILE BÜYÜK AÇIKLIKLI YERALTI YAPILARI IÇIN KIRIKLI ÇATLAKLI KAYA ORTAMIN ANIZOTROPIK DAVRANIŞLARI ÜZERINE BIR ÇALIŞMA

Yeraltında özellikle kaya içerisinde açılan yapılar, yeraltı kaya yapıları açıldıktan sonra ortaya çıkan yükleme koşullarında mühendislik açısından yeterli ve güvenli yapılar olarak nitelendirilebilir. Kaya ortamın özellikleri ve davranışı taşıyıcı sistemin davranışı tasarım için anahtar girdilerdir. NATM (Yeni Avusturya Tünel Yöntemi) kaya mühendisliğinde bir metodolojiden öte tünel açım felsefesi olarak görülmektedir. Birincil gerilmeler etkisindeki kaya ortama temas ile, kaya ve çevre yapılar ikincil ve üçüncül gerilmelerden etkilenmektedir. Klasik tasarımda teknik girişimin fiziksel boyutları (tünel olarak değerlendirilebilir) süreksizliklerin yönelimi, yapısı ve çevre yapı ile ilişkisi dikkate alınmalıdır.

Bu çalışmanın temel amacı açılan boyutların çevredeki süreksizlikler ile ilişkisini ortaya koyarak problemi daha anlaşılır bir hale getirmektir. Fiziksel ve nümerik araçlar kullanılarak boyutsuz etkileşimlerin elde edilmesine gayret edilmiştir. Taban sürtünme modeli kullanılarak kesme şekerden oluşan model malzemesi ile deneyler gerçekleştirilmiştir. Kırık çatlak takımlarının tünel çapına oranı altı ila on iki arasında değiştirilmiş ve aynı zamanda kırık çatlak sistemlerinin dalım açısı yataydan doksan dereceye kadar 15 derece aralıklar ile değiştirilerek deneyler tamamlanmıştır. Elde edilen sonuçlarda tünelin ilk açıldığı anda etki mesafesini bulmak amaçlanmıştır. Bu kapsamda kırık çatlak sistemlerinin anizotropisinin bu etki mesafesine etkisi belirlenmiştir. Toplam 49 adet deneyin sonuçları incelenmiş olup analitik bir değişimi gösteren etki türetilmiştir. Bu tezin sonuçları ile süreksizliklerin bulunduğu ortamda büyük çaplı yeraltı yapıları içinde NATM felsefesi ile kazı stratejilerini belirlemeye yönelik hedefler gaye edinilmiştir.

TABLE OF CONTENTS

LIST OF FIGURES

1 INTRODUCTION

Tunneling or underground structures are becoming very popular since civilization has been growing up rapidly in the last century. Tunnels have been dug for access, transportation, defense, shelter, drainage, water supply, and mining. By development of the energy and defense necessities and new lines for urban traffic, the underground got a vital role in daily life. The limits are forced by the human being day by day to maintain bigger spaces underground for various requirements. Hence it is a part of engineering combining Civil, Geological, and Mining Engineering, there is no conventional technique to solve the encountered problems. Rock is mainly discontinuous material and the anisotropic behavior of the rock environment has not been studied well as in soil mechanics. Hence the problem is not a well-defined structure as being used in the civil engineering, or the loading scheme is not the usual which is increasing with time, rock mechanics or underground structures are unique in every Project. The main difference beyond all is that the loading is becoming lower than the existing conditions by any technical interference (Primary stresses) at first, then it is reloaded afterward (Secondary stresses).

Whenever a tunnel or an underground structure is to be designed and constructed, the engineer is faced with the problem of estimating the expected loads on the tunnel support, both in magnitude and direction, and the corresponding deformations and the extent of loosening of the rock mass around the tunnel. This information forms the basis of the design and dimensioning of the tunnel. Estimation of these loads and deformations is not easy even for the smaller tunnels. In the case of big diameter tunnels, the influence of the joint structures makes the problem even more complicated, since the stresses increase with the growing diameter (Vardar, 1979). In fact, engineers try to minimize the opening size at each step to maintain the required deformation and design so that effects the time for the construction. Some attempts have been made in the past to study this problem.

Rock masses, in general, are not only inhomogeneous and anisotropic but are also jointed. These joints often have a major influence on the rock mass behavior, and this characteristic should be considered if analysis and design for constructions in rock is to be relevant and useful for engineering purposes.

While excavating big span structures for growing necessities, engineers do not have a common understanding and some special and local solutions can be seen in Italy in the literature (Karakus, 2004). The methodology and the technical procedure to build such structures are not clearly defined. Hence the importance of general rules for mechanical behavior in jointed rock environment come across, and the solution that will come up will help the scientists, designers, and engineers at the site. The main idea is that the interfered behavior of the environment with geology and the dimensions may limit the construction methods and help engineers to build safe and economical designs.

This thesis describes an interaction of mechanical behavior of big span underground structures (tunnels) with NATM philosophy by means of physical model investigation using base friction apparatus and numerical model with Finite Element Analysis modelling. The main goal is to examine the use of NATM philosophy by studying the problem of tunnels in anisotropic jointed rocks. Scope and aim of the investigation beside the strength and deformation characteristics of the individual rock elements, the aspects of the joints in rock (e.g. orientation, spacing, degree of joint continuity, etc.) and the geometry of the mass with tunnel (e.g. diameter of the structure, shape of the structure, location of the tunnel with respect to the topography) has been considered as the possible parameters having influence on the problem. In the investigation described the number of parameters is proposed to be limited to two important ones:

i. the orientation of the joints,
ii. the diameter of the tunnel.

Further, the problem was treated as two-dimensional, assuming the geological and geomechanical characteristics parallel to the ground surface to be constant. The investigation aims to understand the mechanical behavior of the rock mass around the tunnel opening as influenced by the above parameters.

This understanding should help in predicting more accurately the deformation patterns and the development of "zones of loosening" and thereby in estimating the likely loading on the tunnel support. Resultantly, a new analytical approach and results for tunnel excavation in jointed rock concerning the number of joint sets influencing on the diameter of the tunnel which NATM shall also be used as philosophy may help in terms of economy and the safety in tunnel design. It is believed that the result of this study may help the designers to analyze dimensions of tunnel structure with its surrounding rock environment, especially in jointed rocks. It is also expected for future studies that this kind of studies shall be varied and practiced in daily engineering projects.

2 LITERATURE REVIEW

Rock mass, which is prescribed as a rock formation, is generally made up of many (small to large scales) elements of rock fragments. This kind of jointed fragmented material is much more complicated than most other materials for engineers those have to deal with. It is more polymorphic, more inhomogeneous, and changing from place to place. The main characteristic of mechanical behavior for this material can be defined by the two basic properties, its anisotropy, and discontinuity. Anisotropy, concerning its mechanical behavior is the rock material itself which constitutes the rock mass whose strength and deformation behavior depend on the direction.

Vardar (1979), pointed out that the behavior of underground structures can be divided into three eras. The first era was named as classical era beginning from the 1850's. Researchers; Ritter (1879), Engesser (1882), Heim (1905), Trompeter (1899), Wiesmann (1912) etc. can be given as the names for this period. These researchers were assuming that the equal forces were acting in every direction to the tunnel structure. Also, they proposed that the plastic zones were exposed nearby the tunnel structure. The experimental studies at the end of the classical era disclosed that a protective zone occurred with elastic and plastic zones. The second era was named as the transition era where the mathematical solutions were tried to be built instead of experimental approaches. Schmid (1926), Fenner (1938) can be given as names for this period. The later era which the modern tunneling studies started was named as the modern era in tunneling researches. By means of Rabcewicz (1944 and 1962), Stini (1955), Pacher (1963), Müller (1963,1978), Egger (1973), Sauer (1975), and Vardar (1977), modern approaches for tunneling started and also named as NATM (New Austrian Tunneling Method) since the methods were named with country assumptions and methods at that time.

The studies in the first era gave an initial form of tunneling philosophy to the scientists in the modern era where modern era researchers worked on more detailed cases employing more observation and mathematical solutions. The anisotropy and the more complex geometries were highly studied by Prof Müller and his team in Karlsruhe (Müller et al.,

1973) and resulted in huge expertise by means of experimental and observational studies. The result is that the leading theory by Trompeter and Wiesmann (1912) were the base of tunneling behavior, and the details were formed by the Modern era researches.

One of the methods to understand the basic behavior and the interaction of material of jointed media is physical models to test the material law of this rock mass in experiments so that finally these more complex parameters can be used as input values for a (simpler) calculation (Müller, 1969)

A variety of modeling techniques have been developed by researchers to study ground anisotropy and the behavior of these jointed/fractured media. These methods range from easy two-dimensional (partially three-dimensional) designs to miniature tunnel boring machines that mimic in a centrifuge set-up the process of tunnel excavation and lining.

Anisotropic strength behavior of the rock was studied utilizing physical models many times, and a summary was given by John (1969) in his thesis. According to John (1969) and Müller (1972), Kuznecov (1947, 1958 and 1963) was one of the pioneer researchers where Oberti (1962) and Fumagalli (1968) were some others worked on the issue. Prof Müller and Pacher (1965) had written a paper on the experiments that were explicitly related to the determination of the influence of anisotropy on the structure of rock masses. The attempts of Hayashi (1966) and Lajtai (1967) were also directly keen on the anisotropic behavior of the rock. The same kind of experiments was performed many times in Karlsruhe Institute of Technology in Rock Mechanics Division under the lead of Prof Müller (Müller, 1969, 1978).

The joint sets were studied by Tess and Fecker (1973), and Reik (1978) in details and the findings indicated that the anisotropy is related with the principal stress ratios directly affected the strength of the rock environment. The researchers observed that the discontinuity sets almost behaved as isotropic, where the ratio of principal stresses was three and lower. The higher values of ratios gave a result that anisotropy in between 0-60 degrees with respect to horizontal have a significant effect on the ratio of singular strength to rock environment strength (Figure 2.2).

They used two models of rock blocks with two sets of joints. The main idea was to find effect of anisotropically distributed discontinuities on material strength and the reduction of strength as a function of angle between principal axes and joint orientation (Figure 2.1&Figure 2.2)

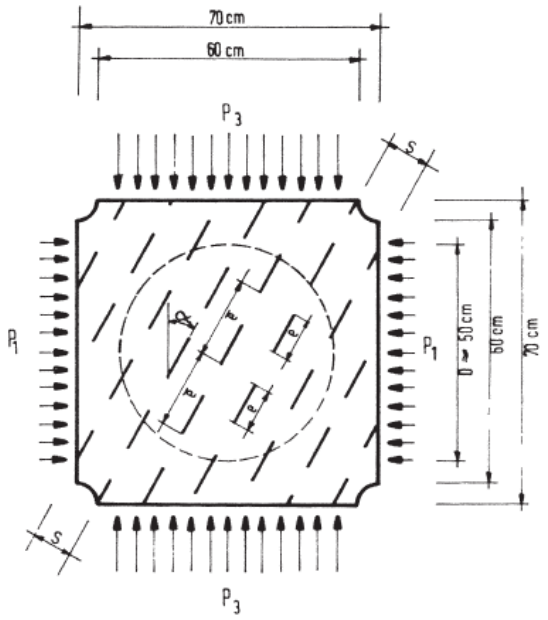

Figure 2.1. Two-dimensional model for investigating the behavior of fissured rock masses (Müller, 1965)

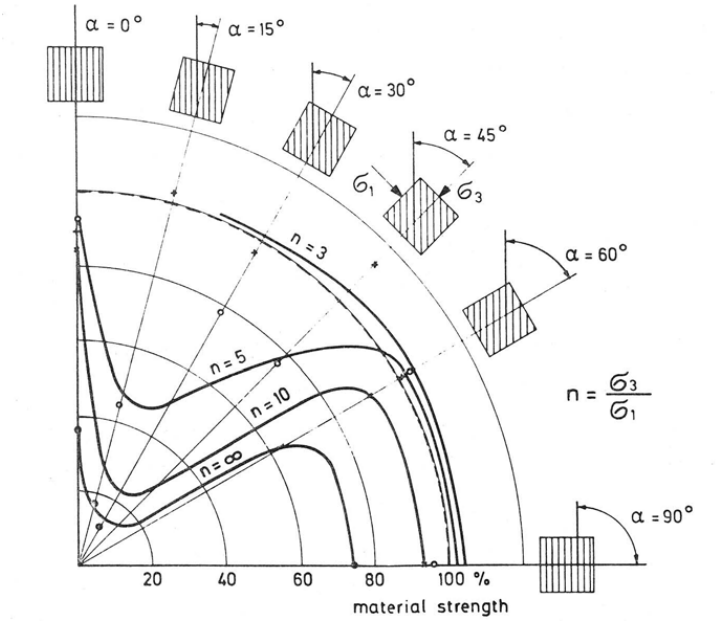

Figure 2.2. Test results; reduction of strength (above) and deformation in the direction of principal stresses (below) versus angle α. (Müller, 1965)

Discrete Element Method (DEM) and Discontinuous and Deformation Analysis (DDA) have been mostly used numerical tools for blocky rock formations whereas Hammah et al., (2006) described how to use discrete elements in Finite Element Analysis software especially in Phase2 by Rocscience Software Company.

Base friction technique was selected and reviewed in Part 3 with its methodology. Below some other researches for physical modelling techniques, were explained briefly. Different strategies to model tunnel surroundings in soil & rock is summarized in Meguid et.al (2008) and different strategies encountered as given in his paper can be summarized as;

i. Trap Door Technique; Terzaghi (1936, 1943), Ladanyi and Hoyaux, 1969) or dry sand (e.g. Vardoulakis et al., 1981)
ii. Rigid tube with flexible or movable face; Chambon et al., 1991; Sterpi et al., 1996; Sterpi et al., 1996; Kamata and Masimo, 2003;
iii. Pressurized air bags; Atkinson et al., 1975; Hagiwara et al., 1999; Wu and Lee, 2003; Lee et al., 2006)
iv. Polystyrene foam and organic solvent (Centrifuge modelling); Sharma et al. (2001)
v. Soil augering; Love (1984); Kim (1996); Champan et al. (2006);
vi. Miniature TBM; Nomoto et al. (1999)
vii. Mechanically adjustable tunnel diameter; Lee and Yoo (2006)
viii. Brick models under uniaxial, triaxial loading; Vardar 1977, Barton 1979,
ix. Simple models under gravitational forces; M. Kleepmek & K. Fuenkajorn 2011
x. Base Friction Technique; Hoek, 1971; Erguvanli & Goodman, 1972; Whyte, 1973; Egger and Gindroz, 1979; Bray and Goodman, 1981; Karaca 1991, Goricki 1999, Chi-hong.).

Base Friction technique, which can be simply summarized as two-dimensional modelling of gravitational forces, was selected as a tool for this study, and the results for the similar type of studies found in the literature review are given in sequence below. It is necessary to emphasize that no other research was done after these studies of which the latest was published in 1999, using base friction method. The reason for this could be the difficulty of this technique or using alternative methods.

The method was selected for the study since the existing techniques summarized by Meguid et al. (2008) cannot model rock environment in two dimensions. Vardar (1977) and Barton (1979) used three dimensional models in their study.

The main purpose of developing the base friction machine was to study the progressive failure processes of rock slopes. Using a base friction machine speed of movement of a model can be controlled and the post peak behavior of the model can be observed easily by controlling the motor that drives the machine. In addition, the ease of preparation of the models on a horizontal surface is another advantage of base friction modelling. The base friction modelling technique is one of the most effective experimental methods for analyzing complex movement patterns in discontinuous rock masses.

The advantages of base friction modelling include the ease of preparation of the model, slow movement of the model and that the effects of the gravitational force can be switched off at any time. However, like other methods, it has some limitations for certain problems.

Like any engineering tool, the base friction modeling technique has its limitations. Goodman (1976) pointed out that the base friction technique cannot simulate the response of the block acquiring horizontal momentum. During the failure process, if the model is completely linked and the blocks are in contact with each other, forces are transmitted through contacts, and the model should have the same failure behavior as the real structure under gravity. However, different parts of models may move independently, relative displacements in the models probably not the same as in real structures.

Sauer G., (1975), summarized the materials to be selected for the model material as follows if it shall be prepared as mixture;

i. Hard to plastic rock types: quartz sand, clay, chalk, heavy minerals, paraffin oil or silicone oil
ii. Soft and brittle rock types: barite, zinc oxide, paraffin oil or silicone oil
iii. Very brittle rock types: plaster, cork flour, water,
iv. Soils of all kinds: bentonite, mica, barite, powdered cork, paraffin oil

Bray J. W., R. E. Goodman (1981) gave the mixture as sand + floor + oil, where Barium Sulfate or Diatomite can be used instead of Barite in some cases. White Zinc can also be used for Zinc Oxide.

Goricki (1999) and Liu, Chi-hong (2003) worked with fine sand (0.063-1.0 mm), fine floor and cooking oil in their models. The ratios in weight were as; 5 x sand + 5 x floor + 1 oil. Karaca 1991; worked with %70 Barite powder, %21 Zinc powder and % 9 paraffin oil.

2.1 Previous Studies on Base Friction Technique

Base friction technique was selected to model the jointed rock mass under gravitation loads. There are various model tests for the tunnels with base friction which may be summarized as;

Goodman (1976) was one of the initial researches on the using base friction technique in University of California Berkeley (Hoek can be stated as the first researcher at Imperial College). Goodman has done a lot of models of slope engineering, dam safety, tunnel engineering with base friction.

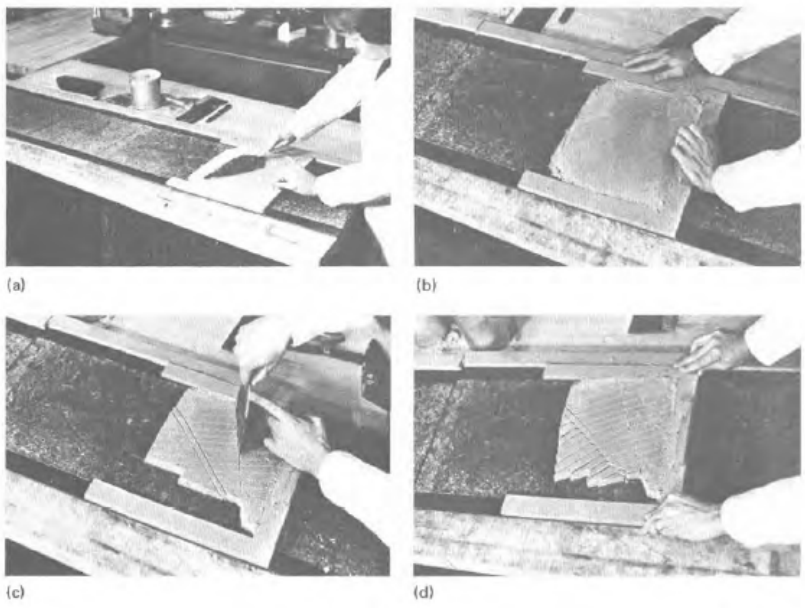

Figure 2.3. Initial Studies on Slope Engineering with Base Friction Apparatus at University of Berkeley (Goodman 1976)

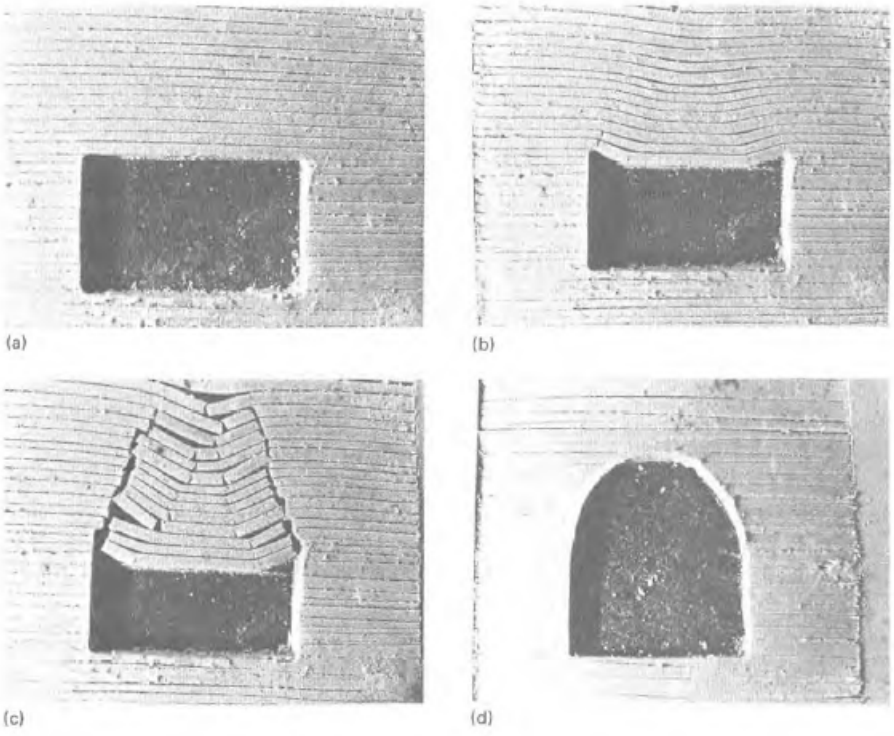

Figure 2.4. Initial studies on underground structures with base friction apparatus at University of California, Berkeley (Goodman 1976)

Karaca (1991) used base friction models and Distinct element models (software UDEC by ITASCA) models to investigate the failure phenomena of circular tunnel in a rock mass with bedding planes and staggered joints, they concluded that the shear zone developed along the path of the stagger joints and the minimum required bolt length is equal to the radius of the tunnel. Karaca studied the stability of circular tunnel with consideration of various properties including geometry of opening, inclination, and spacing of joint sets. They concluded that the failure mode of underground opening in a jointed rock mass is sliding, and the joint orientation affects the width of the failure zones and the size of the displacements.

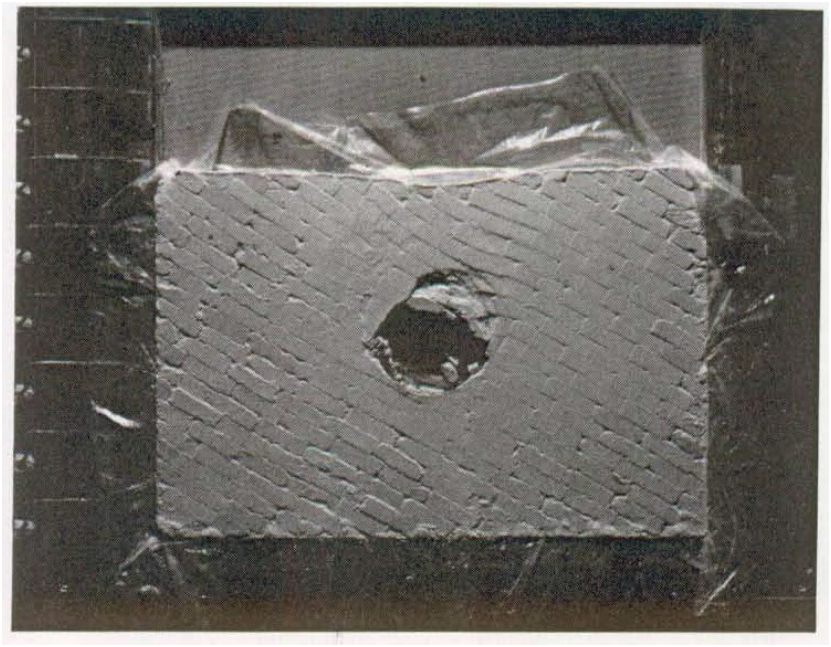

Figure 2.5. Studies of tunnel structure with base friction apparatus at EPFL, (Karaca 1991)

Goricki (1999) was one of the researchers who used the base friction apparatus to interpret failure mechanisms in rock formations. He noted that the subject was to describe the basics of modeling of defragmented rock in general. His first aim was declared to focus on the presentation and description of the most important mechanisms of failure of slopes and excavations (sliding, toppling, slumping; shear failure, roof failure) by means of the base friction experiment. Moreover, Discontinuous Deformation Analysis (DDA) was also used for particular mode of failure.

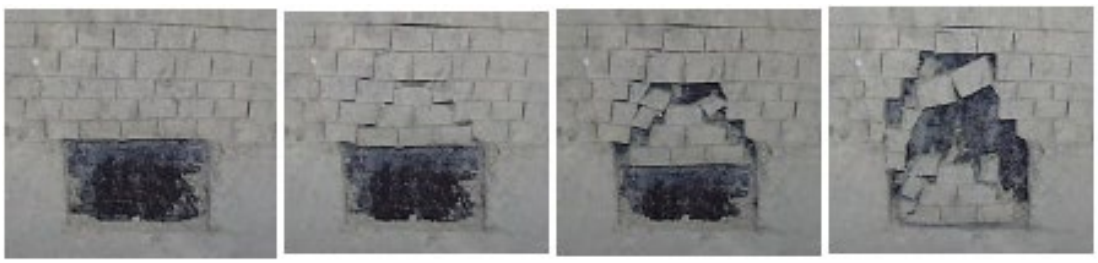

Figure 2.6. Studies of tunnel structure with base friction apparatus at TU Graz, Goricki (1999)

Liu Chi-hong (2003) used the base friction modeling for the analysis of discontinuous rock mass behavior. A large base friction machine was designed, constructed and used to examine the validity of a time-scale equation used to convert base-friction time to real time. He performed the tests under base friction and under gravity in which a block is placed on an incline and released.

He carried out a parametric study using base friction modeling and Discontinuous Deformation Analysis (DDA) for a tunnel in a jointed rock mass. The behavior of the tunnel and its surrounding rock blocks was studied with respect to various parameters including joint orientation, joint spacing and block size. Finally, an alternate rock bolting arrangement was investigated with base friction.

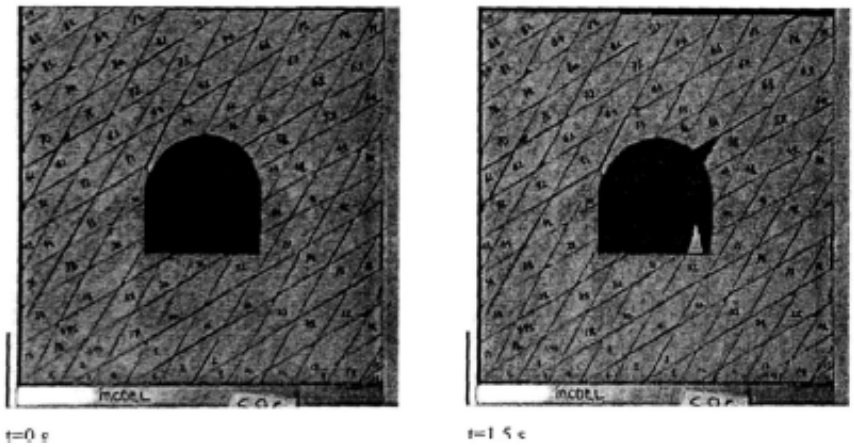

Figure 2.7. Studies of tunnel structure with base friction apparatus, (Chi-Hong 2002)

Yeung (1997), Conducted a parametric study using a two-dimensional DDA to research the impacts of joint characteristics in a rock mass on the stability of a tunnel excavated in a rock mass. Cases were analyzed using different combinations of tunnel depth (10 m and 25 m), joint orientation (0, 30, 60 and 90 degrees with respect to horizontal), joint spacing (2 to 5 m) and joint friction angle (30 and 40 degrees). They found that the size and shape of the block had an impact on tunnel stability.

Tsesarsky (2005) studied the stability of underground openings excavated in stratified and jointed rock using the Discontinuous Deformation Analysis method (Shi, 1988; 1993). His aim for his research were: i) validation of DDA using analytical solutions, physical models and case study; ii) investigation of fractured beam kinematics; and 3) development

of simplified design charts for assessment of rock over-break above excavations as a function of joint spacing and shear resistance along joints. He used both Shaking table and Centrifuges for his studies. He concluded that the height of the loosening zone is inversely proportional to joint density. He added that if the number of blocks per beam is greater than five, the beam tends to deform by inter-block shear, while rotation is minimal.

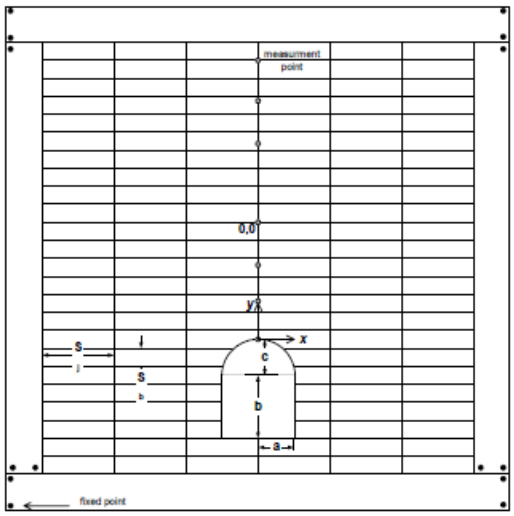

Figure 2.8. Geotechnical studies of Tsearsky (2005)

3 METHODOLOGY OF PROPOSED STUDY

Underground structures do not behave similarly as other engineering structures above ground, due to their loading mechanisms. Loading shall occur by adding extra loads and parts to the structure above ground whereas it is vice versa for underground structures.

The literature review showed that overwhelming attention has been paid to modeling tunnels in isotropic, homogeneous media, whether these models are empirical, analytical, physical or numerical. In nature, however, soils and specifically rocks are neither homogeneous nor isotropic. Therefore, the objective of this thesis was to examine the surrounding media (jointed rock)-tunnel interaction within an excavation in jointed rock with anisotropy by means of differing the diameter and joint patterns in a scaled model work. The reason to vary the parameters was subjected to study mechanical behavior of joint orientation for NATM philosophy to open big span tunnels and to see the effect of anisotropy on the tunnel influence zone. The use of NATM was subjected to be a design method where NATM should be defined as a philosophy rather than a method as seen in the previous works.

There are many engineering situations in which knowledge of the discontinuity characteristics of the rock mass is of importance and a variety of approaches can be used to analyze the stability and behavior of the rock mass using discontinuity characteristics. Physical model tests and numerical simulations offer the best alternatives to investigate the mechanism of failure for assessing strength and deformability of jointed rock masses. Physical modeling has played an important role in studies related to excavation of tunnels in soil and rock. A variety of modeling techniques have been developed by researchers all over the world to study interaction of ground response to tunneling.

3.1 Methodology

This study was based on the physical and numerical modelling of underground structures in anisotropic jointed rock conditions to evaluate the effect on big span underground structures in consideration of NATM philosophy. There are some researchers try to build the NATM with existing situations where the idea was mainly estimation of support. This thesis was to reexamine the validity of using NATM philosophy in big span tunneling. Base friction method was selected as the physical modelling where Finite Element Analysis with discontinuity sets was adopted to espouse the physical models.

3.1.1 Physical Model

The studied model was setup in two dimensional and worked with circular underground structures with various diameter in jointed rock conditions. The diameter and the orientation of the joints were the main variables. Model material was selected to realize the rock blocks in real world.

To simulate the gravitational effect on a rock material physical model, many researchers have used different methods, including centrifuge models, tilting experiments and base friction models. The base friction modelling which was first suggested by Erguvanlı and Goodman (1972) on a basis of sandpaper model is one of the common techniques for analyzing problems of complex movement patterns in a rock mass. This study adopts base friction model as a physical modelling tool since the method was used successfully and easy to interpret the rock-like environments.

3.1.2 Numerical Model

Software that were built with the idea of Finite Element Analysis and Discrete Element Analysis methods were commonly used for comparison. This thesis adopted semi discrete element method by means of FEA.

The choice between FEA and DEA depended on that the commercial software's with FEA can also consider the semi-discrete behavior with some special joint sets as interfaces.

The software RS2 by Rocscience was used in the modelling since it allows using two or more discontinuities and joint structures. Since the easiness for geometry input and complex geometry options, RS2 was selected as a tool to model the test results.

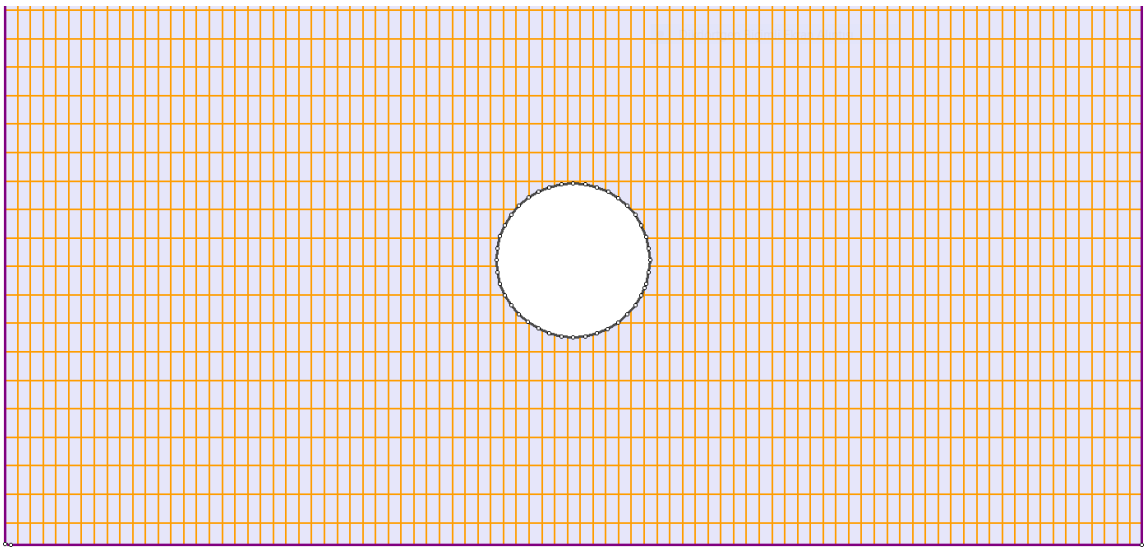

Figure 3.1. FEA example of Rocscience RS2

4 NATM PHILOSOPHY

New Austrian Tunneling method was named as “method” by tunneling community. On the other hand, the writer of this thesis thinks that NATM is not only method where it is better to be named as philosophy. The characteristic features are given step by step in order.

NATM is based on the concept that the ground around the tunnel not only acts as a load, but also as a load-bearing element. According to the present definition, the New Austrian Tunneling Method thus consists in stabilizing the ground around the excavation in the most safe and economic manner possible by making extensive use of the bearing capacity of the ground with the help of sprayed concrete and other support elements as well as through the use of measured data. (50 Jahre NÖT – Neue Österreichische Tunnelbaumethode).

Typically, the excavation and support activities are continuously adjusted during construction to suit the ground conditions, always considering the technical/design requirements. The ground reaction, in the form of lining displacements is measured to check the stability of the opening and to optimize excavation and support process. Depending on the project conditions (e.g. shallow soft ground tunnel, deep rock tunnel) and the results of the geotechnical measurements, the requirements for a specific support are determined.

The typical support elements in NATM are shotcrete and rock dowels. Steel ribs or lattice girders provide limited early support before the shotcrete hardens and ensure correct profile geometry. If ground conditions require support at or ahead of the excavation face, face dowels, shotcrete, spiles or pipe canopies are installed as required. If necessary, the excavation cross-section is subdivided into top heading, bench and invert depending on both ground conditions and logistical requirements (i.e. to facilitate the use of standard plant and machinery). Side drift galleries are provided to limit the size of large excavation faces and surface settlements. Some researchers interpreted their experience to excavate full face, central diaphragm and side drifts. They also give empirical relationships of tunnel spans with respect to strength/stress ratios (Figure 4.1)

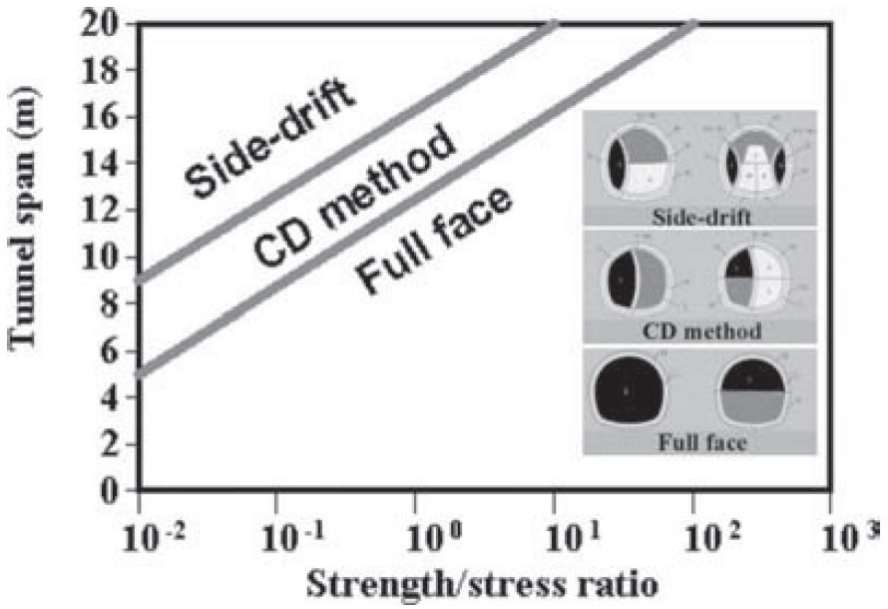

Figure 4.1. Optimized chart for selecting a suitable excavation procedure according to tunnel span and the strength stress ratio (Yu & Chern 2007)

Nowadays the diameter of the tunnel has been tried to be enlarged as much as possible which triggers the environment with its technical interference. Accordingly, the depth, diameter and the shape of the tunnel become the most important issue to be analyzed so that the system magnitude and technical interference would be the major factor in the design.

4.1 Definition & History of NATM

As explained in Part 2, the modern era of tunneling history started with Rabcewicz (1944). The term NATM (or New Austrian Tunneling Method) which was first named by Austrian engineer Rabcewicz (Salzburg 1962), points out a philosophy of applying a thin, temporary flexible support and allowing deformations in case the rock pressure could be reduced and distributed into the surrounding rock. By doing so, a new equilibrium shall be reached hence the final support will be less loaded and can be installed even later and as a much thinner structure. This shall be controlled by in-situ deformation measurements with a proper geometry.

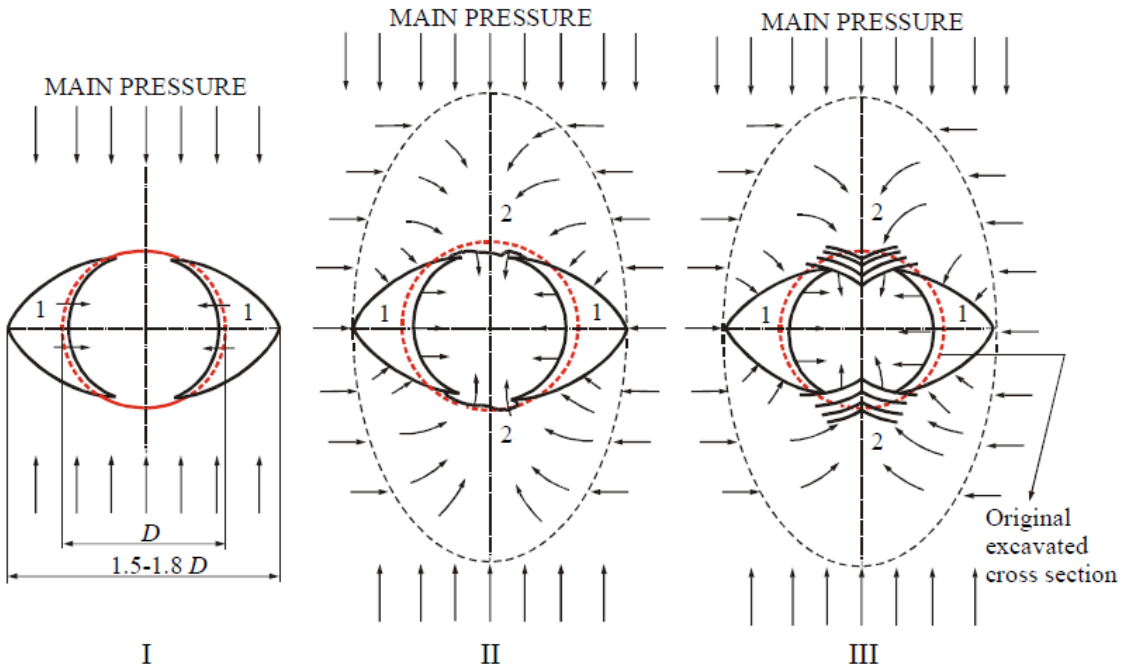

Figure 4.2. NATM philosophy by Rabcewicz (1963) (Karakus, 2004)

Rabcewicz (1963) combined his mining expertise with other theoretical and practical knowledge at his time and published the milestone book of NATM “Rock Pressure and Tunneling” in 1944. With the two decades after this book, Rabcewicz developed his ideas with the practical tunneling and proved a patent solution (1948) for excavation of underground structures. His main idea was the deformable support systems in the time domain where the surrounding rock also covers itself and starts to bear new loads as a result of the excavation. The introduction of shotcrete changed the approaches to the tunneling considerably. He first mentioned the term “NEW” instead of “Old” Austrian Method in 1962 during Geomechanics Colloquium where he has already used it in various projects. The main idea to give a new name is to mark off it from other old traditional methods.

Then Austrian/German Scientists and practitioners have worked on the principles of the new philosophy. The key components that were defined by Prof Müller-Salzburg (1978) in NATM philosophy are:

i. Mobilization of the Strength of the Rock Mass: The method relies on the inherent strength of the surrounding rock mass being conserved as the main component of tunnel support. Primary support is directed to enable the rock to support itself. It follows that the support must have suitable load-deformation characteristics and be placed at the correct time.

The strength of the ground around a tunnel should be deliberately mobilized to the maximum extent possible. Mobilization of ground strength is achieved by allowing deformation of the ground (Figure 4.3).

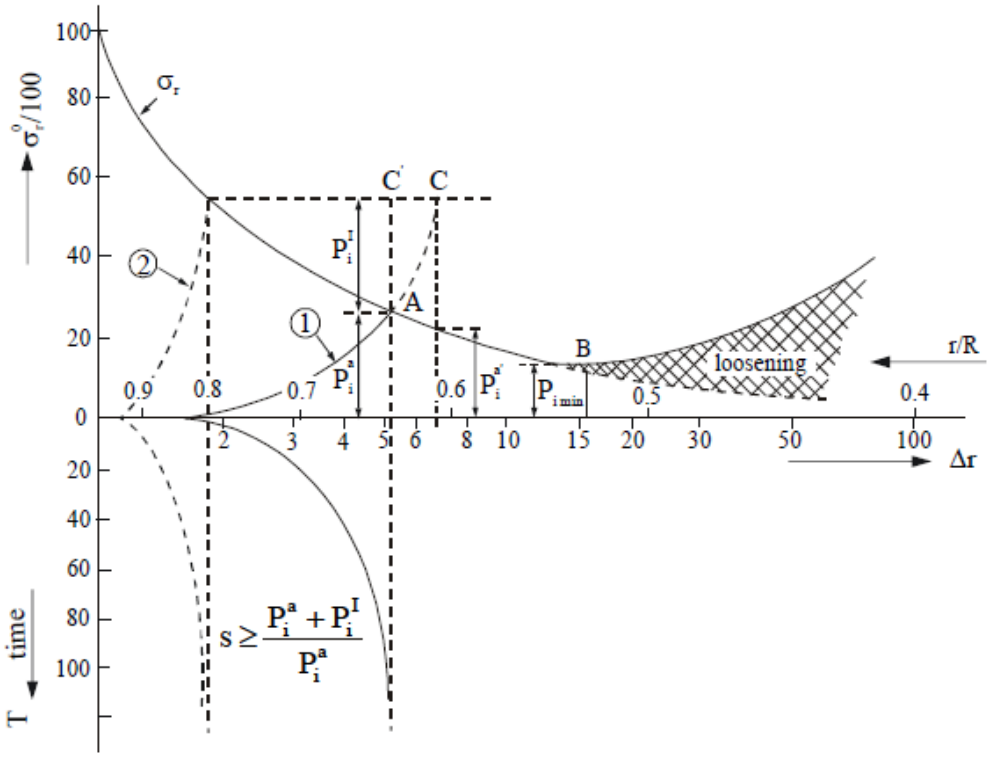

Figure 4.3. Ground Reaction Curve after Pacher (1963)

ii. Shotcrete Protection: In order to preserve the load-carrying capacity of the rock mass, loosening and excessive rock deformations must be minimized. This is achieved by applying a thin layer of shotcrete, most time together with a suitable system of rock bolting, immediately after face advance. It is essential that the support system used remains in full contact with the rock and deforms with it.

Initial or primary support, having load deformation characteristics appropriate to the ground conditions is installed. Permanent support works are normally carried out at a later stage.

iii. Measurements: The NATM requires the installation of sophisticated instrumentation at the time the initial shotcrete lining is placed, to monitor the deformations of the excavation and build-up of load in the support. This provides information on tunnel stability and permits optimization of the formation of a load bearing ring of rock strata.

Instrumentation is installed to monitor the deformations of the initial support system and the build-up of load upon it. Where appropriate, the results of this monitoring form the basis for varying the primary and permanent support, and the sequence of excavation.

iv. Flexible Support: The NATM is characterized by versatility and adaptability leading to flexible rather than rigid tunnel support. Thus, active rather than passive support is advocated, and strengthening is not by a thicker concrete lining but by a flexible combination of rock bolts, wire mesh, and steel ribs.

v. Closing of Invert: Since a tunnel is a thick-walled tube, the closing of the invert to form a load-bearing ring of the rock mass is essential. This is crucial in soft ground tunneling, where the invert should be closed quickly, and no section of the excavated tunnel surface should be left unsupported even temporarily. However, for tunnels in rock, support should not be installed too early since the load-bearing capability of the rock mass would not be fully mobilized. For rock tunnels, the rock must be permitted to deform sufficiently before the support takes full effect.

vi. Rock Mass Classification Determines Support Measures: Figure 4.4 is a good example of the main ground classes and comparison for rock mass and the support measure to adopt according with NATM.

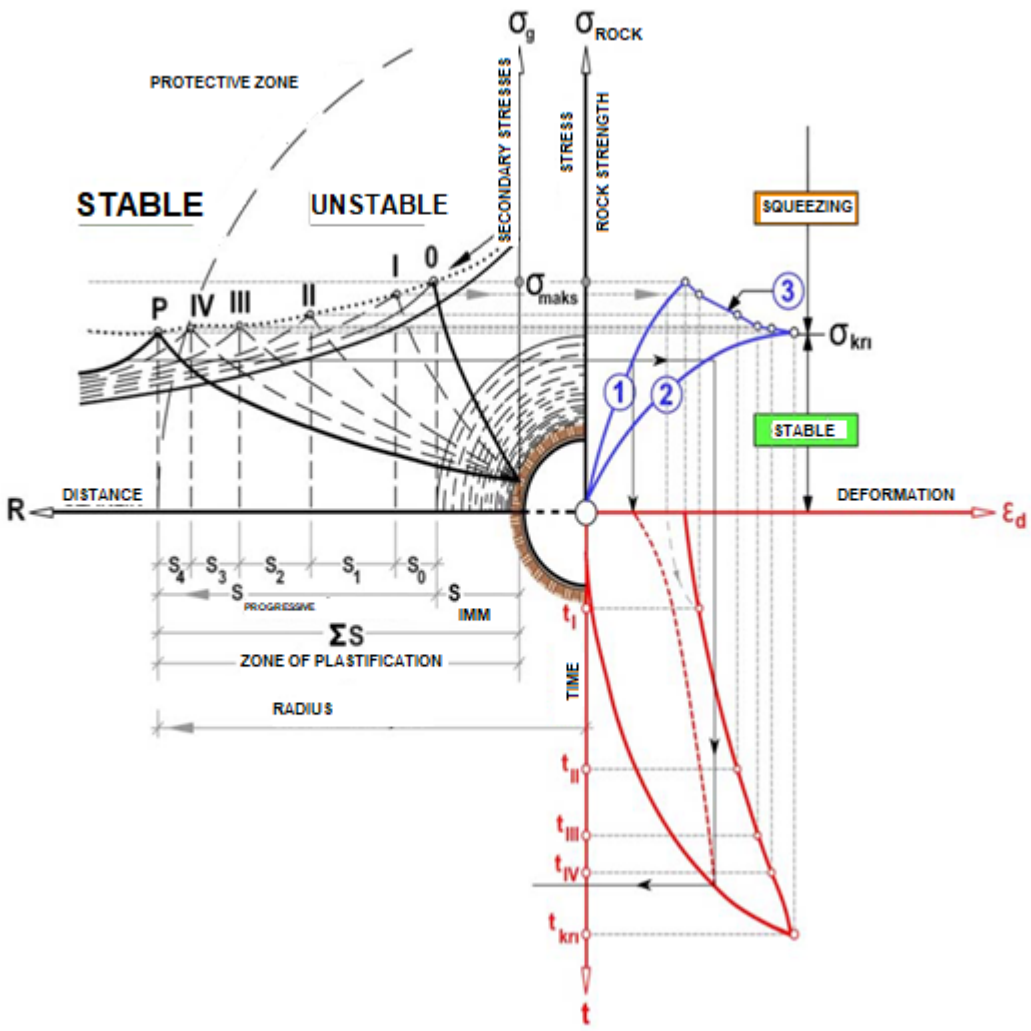

Figure 4.4 Secondary stress development with respect to time and rock-sample strength, (Vardar, 2004)

The difference of Figure 4.3 and Figure 4.4 can be summarized as that Pacher ground response curve is related with rock strength and the secondary stresses which builds a protective zone. The consideration of the time of closing the ring, adjusted to the respective rock properties and the ground pressure has from the very beginning been an essential part of the principles of the New Austrian Tunneling Method (NATM). Rabcewicz proposed a failure mode for the deep tunnels and gave a failure mode for Tunnel excavations.

The first major thing is a flexible outer arch-or protective support-design to stabilize the structure accordingly and consists of a systematically anchored rock arch with surface protection mostly by shotcrete, possibly reinforced by additional ribs and closed by the invert.

The second means of support is an inner arch consisting of concrete and is generally not carried out before the outer arch reached “Equilibrium”. Vardar (1979), one of the main researchers with Prof Müller in Karlsruhe, explained the main features of NATM in 22 items as follows;

i. The main item of the support in underground structures is the surrounding rock beyond the excavated zone, the older method on the right of Figure 4.5 clearly shows that the load carrying unit is formed with stones, wooden pieces etc.

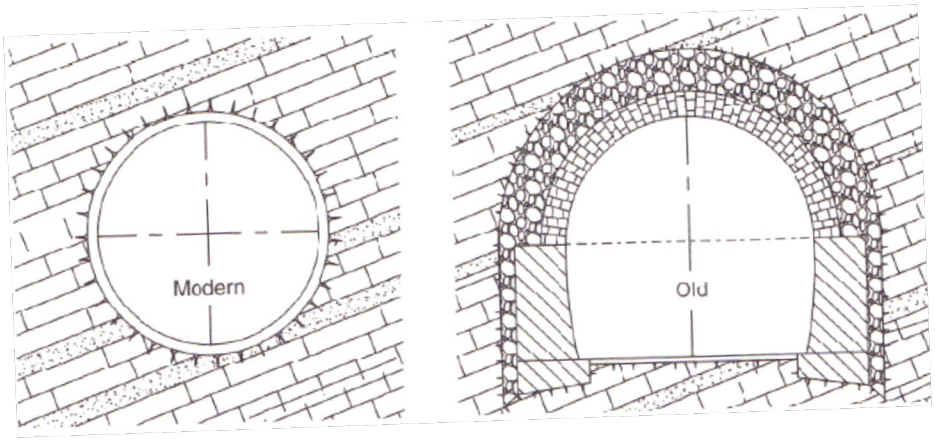

Figure 4.5. The main load carrying is the rock mass (Müller, 1978)

ii. The main principle is to prevent the strength of the rock during excavation,

iii. It is strongly advised to prevent relaxation of the rock. This would cause the decrease of the strength of the rock. Figure 4.6 b indicates that old method creates a loosened zone since the inner lining takes time for masonry construction

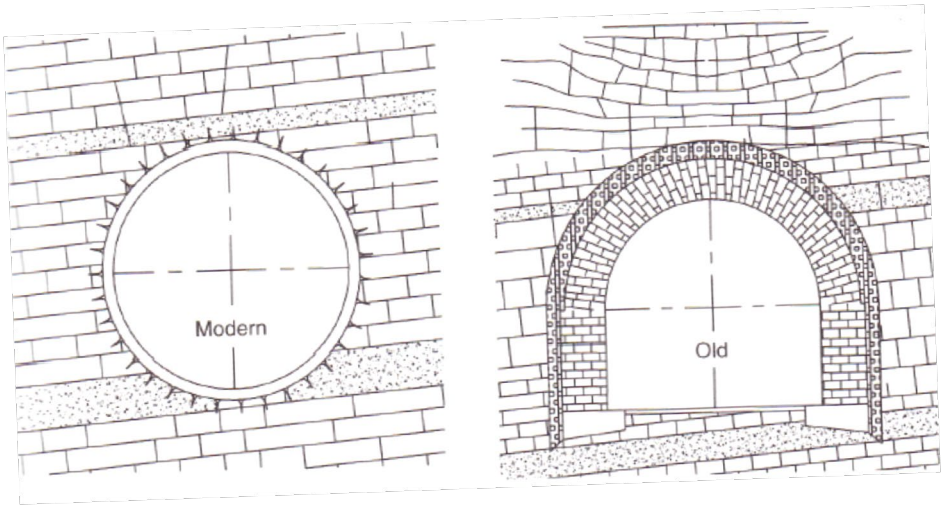

Figure 4.6. Loosening should be prevented as it reduces strength (Müller, 1978)

iv. It is preferred not to create one dimensional and two-dimensional stress environment. The strength of the rock will also be decreased by means of these two-stress environments. If one of principal stress is likely to be zero, it will fail as seen in Figure 4.7

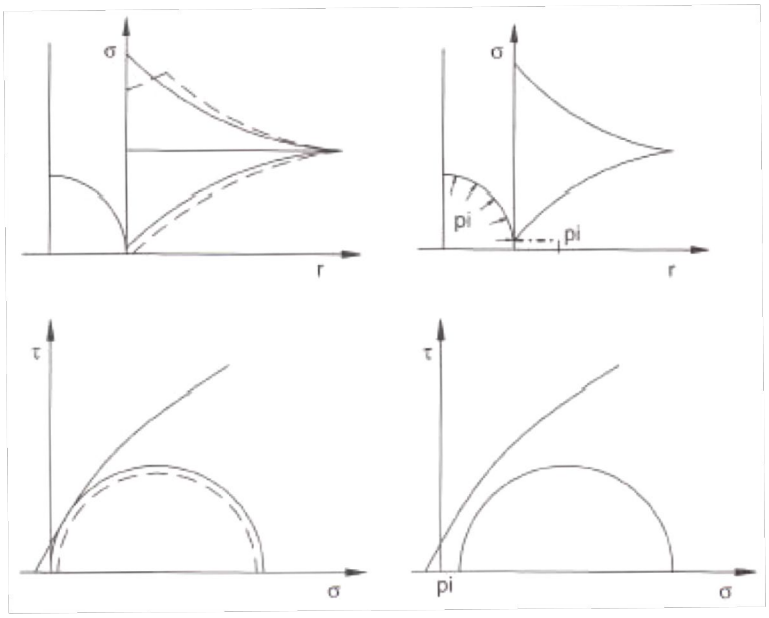

Figure 4.7. Uniaxial stress condition should be prevented (Müller, 1978)

v. The protective zone must be built without decreasing the strength of the rock. The deformations after the excavation should be controlled and governed in order to help

to create the protective zone hence the loss in strength. Success will bring safety and economy in design,

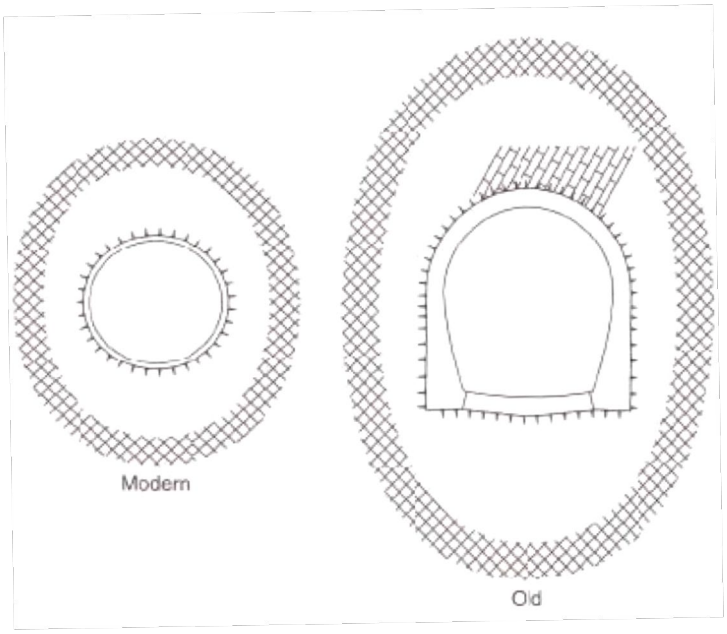

Figure 4.8. Mobilization of the protective ring without strength reduction (Müller, 1978)

vi. Reinforcement works should be done on time at required flexibility. Reinforcement works should neither start early nor ended late and the strength of the reinforcement should be neither rigid nor weak as is shown in Figure 4.9,

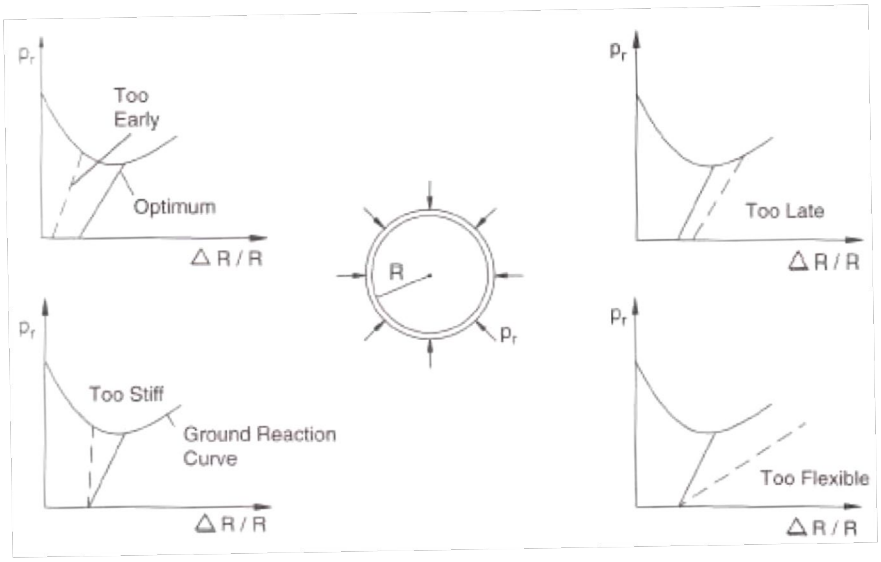

Figure 4.9. Support not to early not to late not to stiff not to flexible (Müller, 1978)

vii. The time (specific time factor) required to stay stable for rock should be calculated well (Figure 4.10),

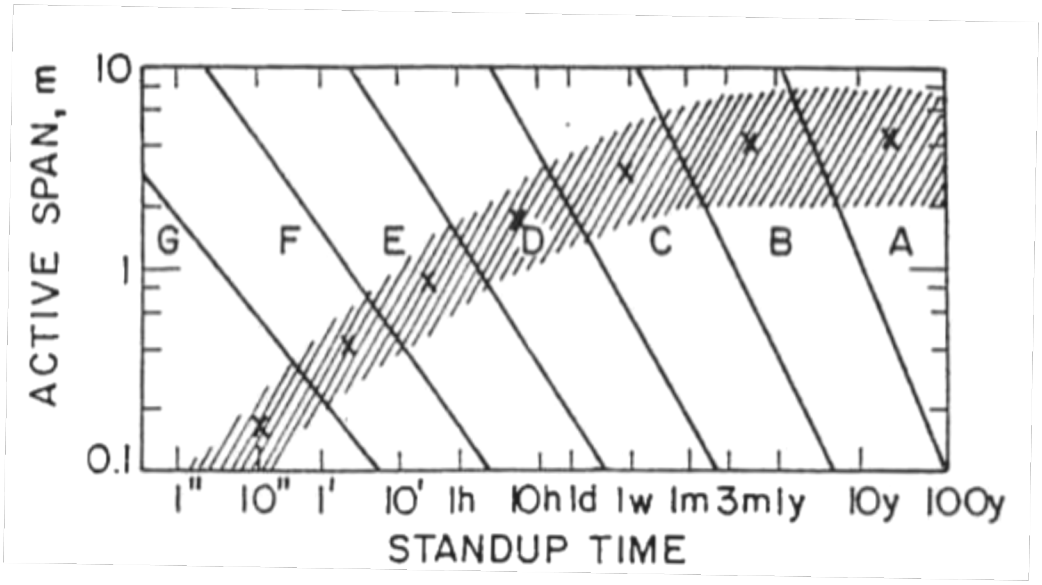

Figure 4.10. Standup time vs active span (Müller, 1978)

viii. Specific Time Factor can likely be calculated at the laboratory either can be estimated with experiments or can be determined with deformation measurements. The time without any support, deformation ratio and rock quality designations may give valuable information about this important coefficient,

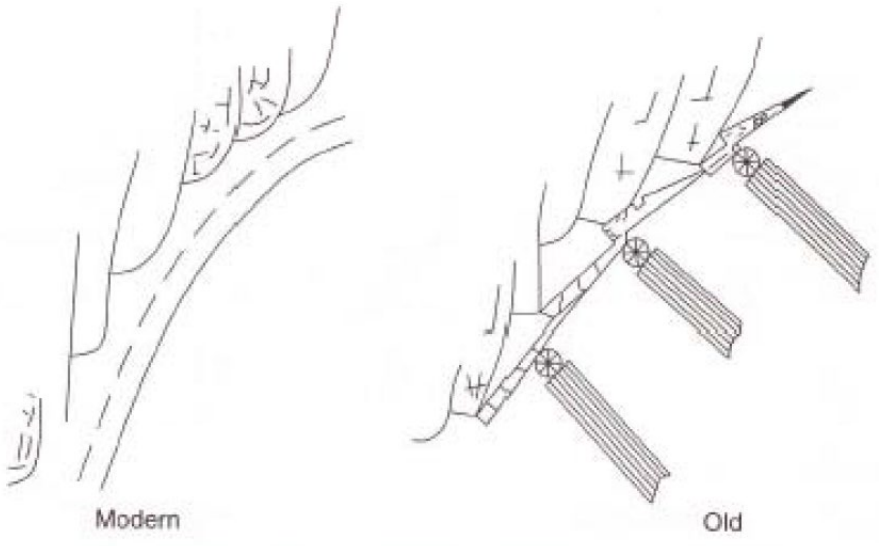

Figure 4.11. Supports should be effective overall (Müller, 1978)

ix. If big displacements and relaxations are to be expected, the strength of reinforcement has to be as distributed load and reinforcement precaution has to spread the empty surfaces. The most succeeding method is using quick set shotcrete (Figure 4.11).

x. The lining for strengthening should be as thin shells and flexible as it can bend. So, it will decrease bending moments and may prevent shear and tension cracks (Figure 4.12).

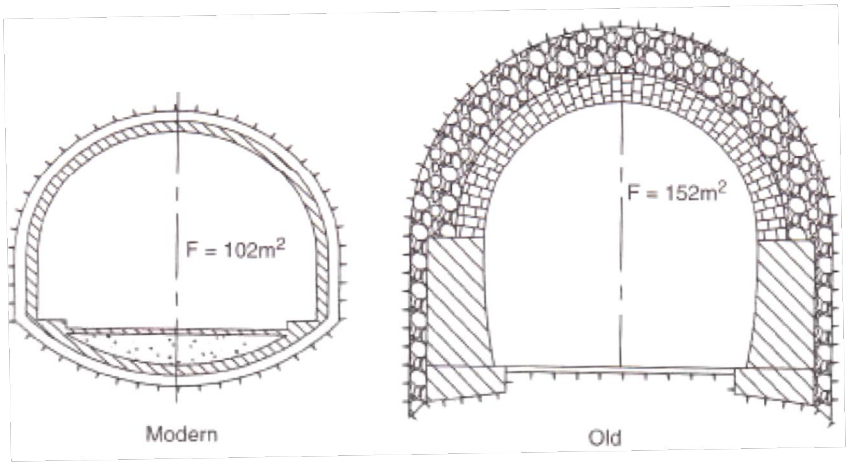

Figure 4.12 Supports should be consist of thin linings that are flexible for bending (Müller, 1978)

xi. The strengthening should be maintained with wire mesh usage and/or steel ribs-bolts hence not increasing the thickness of the shell. In order to spread the pressure on rock and to make it carry itself, anchorages can be used (Figure 4.13).

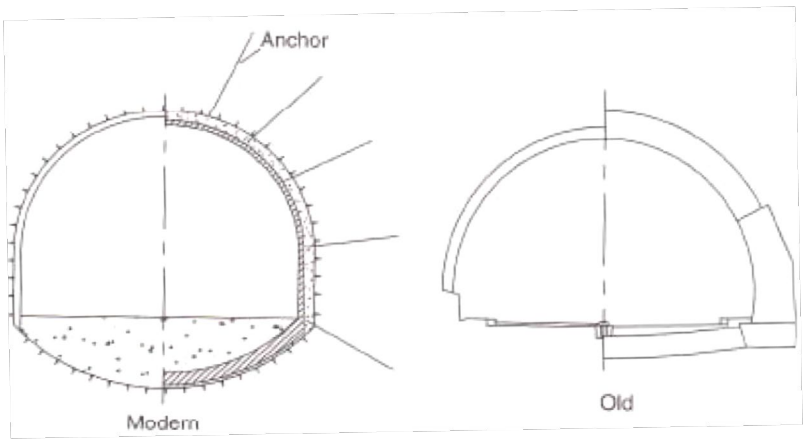

Figure 4.13. Additional support should be provided by wire mesh, steel arches and anchors not by increase of concrete liners (Müller, 1978),

xii. The time and the method of strengthening should be evaluated by means of measured displacements. The displacements and the stresses on tunnel walls and surrounding rock environment is very important since it gives brief information during execution. The initial forecasts show that the presumed project details and the real situation outputs will differ by means of new factors. So, that the underground structures have a mobility that necessitates chop and change. The step by step or round by round changing project systems should be mentioned instead of talking a singular project. The site works and studies for engineering geology and rock mechanics such as monitoring, measurements, experimentation, supervision interpretation and archiving should be done completely (Figure 4.14).

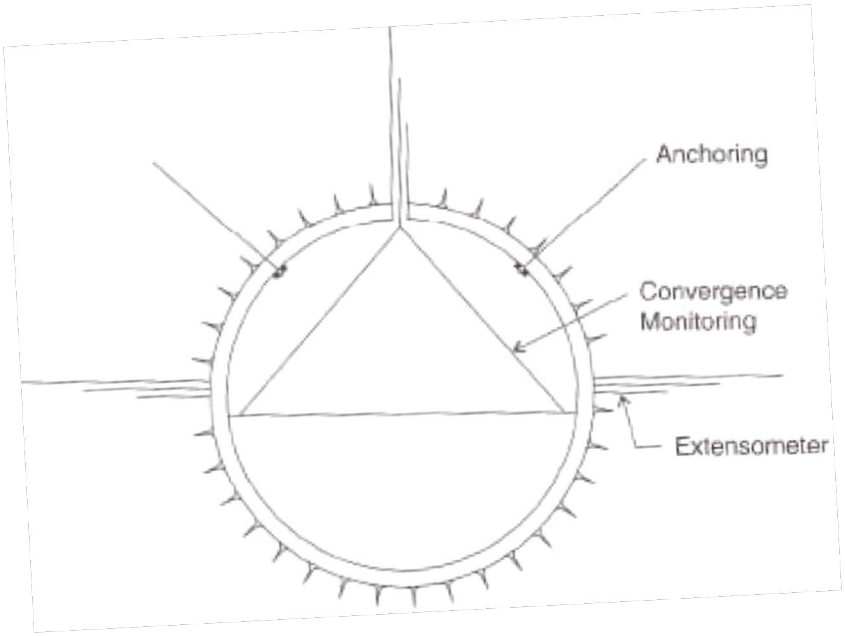

Figure 4.14. Necessary support and its timing should be adjusted according to the measuring of the displacement (Müller, 1978)

xiii. Tunnel is a ring structure that was formed by self-bearing zone and strengthening zone.

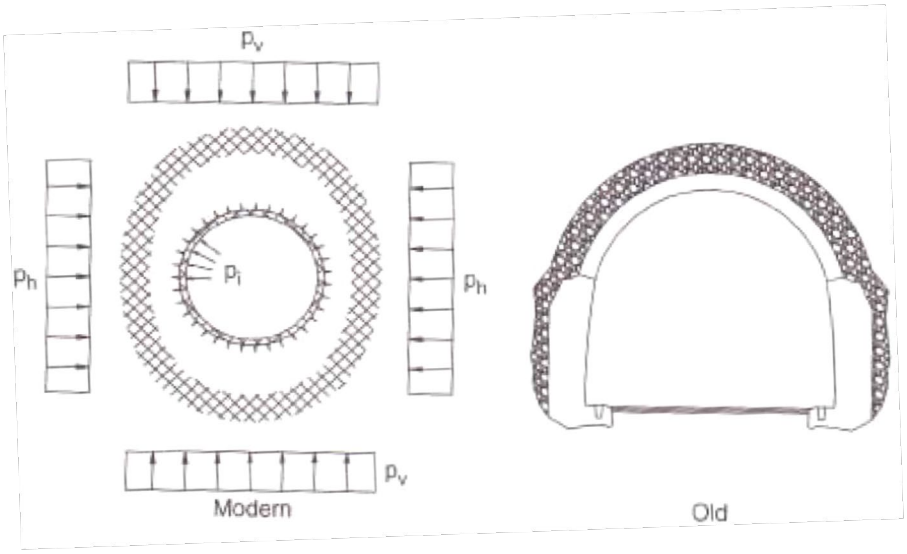

Figure 4.15. Ring structure as tunnel geometry (circular) (Müller, 1978)

xiv. The strengthening shell element should be closed ring. Arch shaped, notched or jointed ring has lower stability when compared a circular one. In this regard, kalot right and left side excavation strengthening liner should be attached as a ring to tunnel walls. This can be achieving only by sequential circular ring after full section excavation. In some cases, where the base rock is strong enough to bear the stresses, there is no need to make a circular layer (Figure 4.15).

xv. The ring should be formed as soon as possible. The behavior of the rock during secondary stress propagation is related with the shell deformations. The uncomplete ring is not a full bearing system and causes decrease in the strength of the rock with plastification of rock. Completing the ring in a short time will give prosperous results since the deformation and plastic zone formation are functions of time (Figure 4.16).

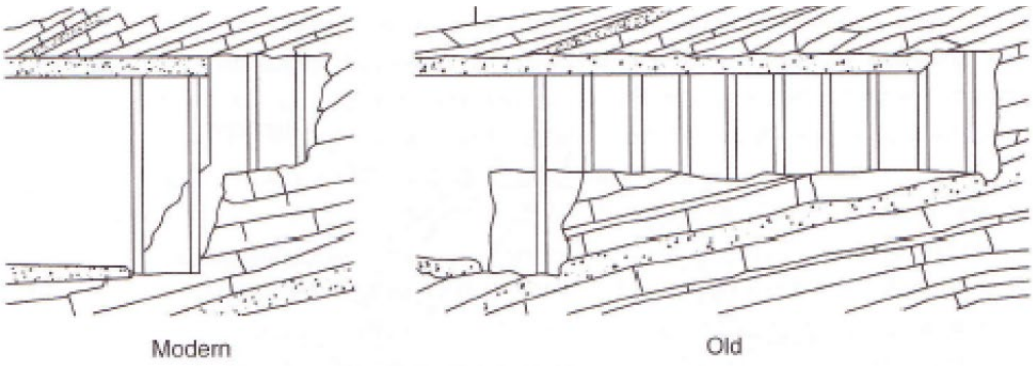

Figure 4.16. Delay will cause a change in behavior of the rock (Müller, 1978)

xvi. If we look from the stress distribution aspect, it can be said that a full excavation of the area in one part seems advantageous. In split excavations, the stress distributions changes at each step and may give harm to the rock strength. So, the mountain should be tampered as low as possible (Figure 4.17).

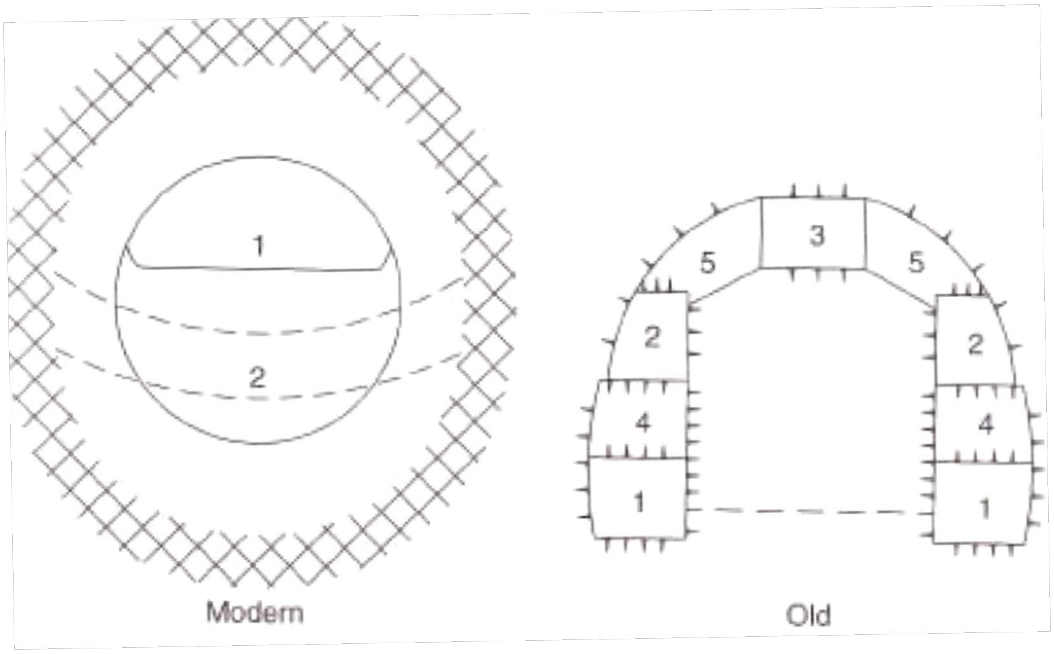

Figure 4.17. Full face heading helps to keep rock strength (Müller, 1978)

xvii. The execution type of tunnel excavations is very important since it effects the durability and safety of rock structure and directly influence the rheology of the rock. Methods may vary due to application type in organization and time. With respect to this, the advance step length, time for strengthening, closing of invert and setting of cement effects the safety of underground structures (Figure 4.18).

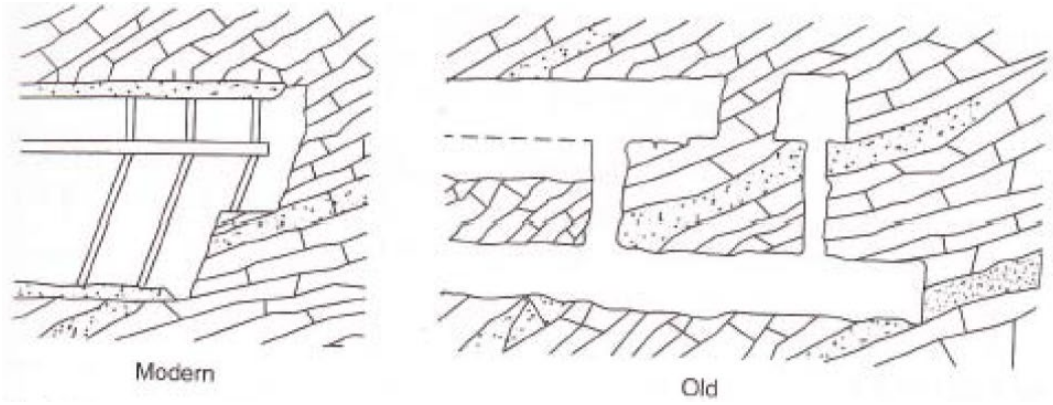

Figure 4.18. Procedure of the tunnel construction is very important (Müller, 1978)

xviii. It is suggested to avoid from sharpened corners to prevent stress localizations (Figure 4.19). This issue damages rock mass and its roughness heavily. Circular sections are to be preferred.

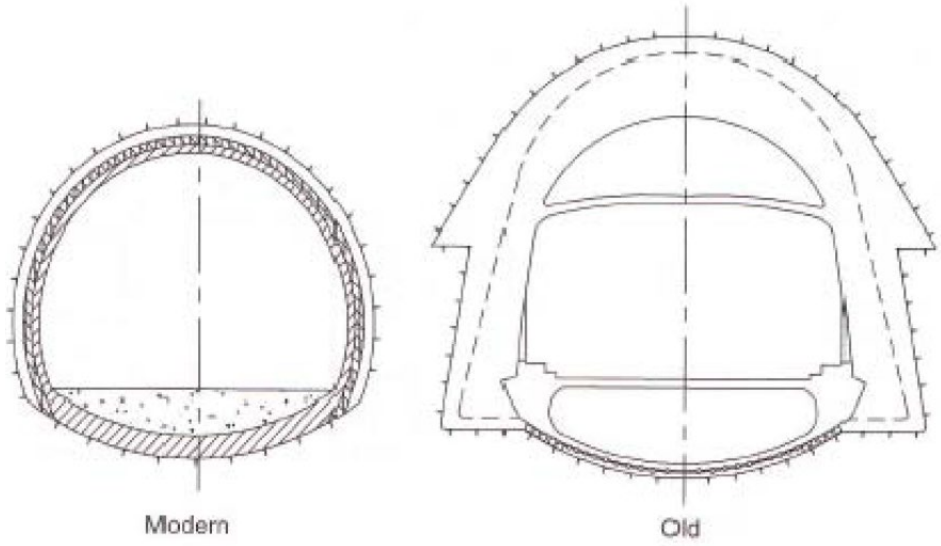

Figure 4.19. Smoothly rounded shapes help to prevent stress concentrations (Müller, 1978)

xix. If both outer (temporary) and final lining will be used, the inner lining should be as thin as possible. The interaction between liner boundary should be tight but without friction.

xx. The stability should be ensured only with temporary lining. Final lining can provide extra safety issues. Inner lining has to ensure to bear all loading and can stabilize whole rock mass when water leakage is very high. Anchorages may be used as permanent structures in this case.

xxi. Guidance and supervision measurements should be continued during execution. The knowledge of interaction system formed of rock mass and lining, the status of displacements (whether damped or continuous) is very valuable for determining the stress magnitudes and locations. The measurement systems installed in rock mass and concrete linings should be used for control of measurements.

xxii. Pore-water pressure and hydrostatic pressure acting on the support should be minimized by means of drainage filters.

5 MODEL STUDIES

This study was based on two model studies where the first part is physical models and the second half is numerical models.

5.1 Physical Model

The brief description of the experimental program is presented in the following sections. Initial tests were conducted with sugar bricks (width/length ratio 2/1) as Model Material.

i. Tests were performed on specimens of jointed block mass under unconfined conditions. The model was formed by arrangement of elemental blocks.
ii. A rock-like model material, called sugar brick, sand+oil+flour was used to prepare the jointed mass specimens.
iii. The size of the base friction table was 100 cm x 80 cm. The model material was prepared by replacing each blocks of model material in a given angle as specified. The prepared model consisted of orthogonal joint sets.
iv. The joint Set-I was continuous and inclined at an angle 0 with the horizontal. The value of 0 was varied from 0° to 90°.
v. Sandwiches of Teflon sheets smeared with silicon grease were used at the boundaries to ensure friction free end loading system.
vi. Load was applied through an endless belt rotor to give gravitational force on horizontal placed sample.
vii. The mode of failure of each model was recorded after the test.

The mechanical behavior of an underground structure in jointed rock mass has been investigated using two-dimensional model tests with equivalent model material. About 1 x 1 m models shall be constructed using special small rectangular blocks with a regular joint pattern having two orthogonal joint sets.

The main variables in the study were proposed as;

i. the joint orientation,
ii. the diameter/span of the underground opening

The characteristic deformation behavior of the rock mass for the models, following the excavation of the tunnel, is discussed. The development of "loosening zones" over the tunnel opening in all cases and their extent is aimed to be presented under different joint patterns. A relationship between the height of "loosening zones" and the joint orientation is proposed to assess the likely loading on a tunnel support for a preliminary design. Further, the main direction of loading on the tunnel support for different joint orientations is proposed to be indicated.

The influence of excavation of the tunnel opening with different sizes in jointed media shall be the main criteria in the models. This understanding shall help in predicting more accurately the development of "zones of loosening" and thereby in estimating the likely loading on the tunnel support.

5.1.1 Theory

In a base friction simulation, a gravity field is simulated by the force of friction in the model acting in the direction of friction. The force for the model tests is provided by changing the friction coefficient between the base plate and the model. The principle is to convert the profile of the research subject (i.e., the slope) into a planar model, level the plane, and move the base plate that underlies the model. The base plate is continuously moved such that the vertical direction of the original profile corresponds with the direction of motion of the base plate. The model moves with the continuous movement of the base plate. A fixed frame is arranged in the direction of motion of the base plate. A frictional force F is formed at all points of surface contact between the model and the base plate when the model is blocked by the fixed frame:

F= γm * t * μ, where; γm is the unit weight of the model material; t is the thickness of the model; and μ is the friction coefficient between the model and the sliding base plate.

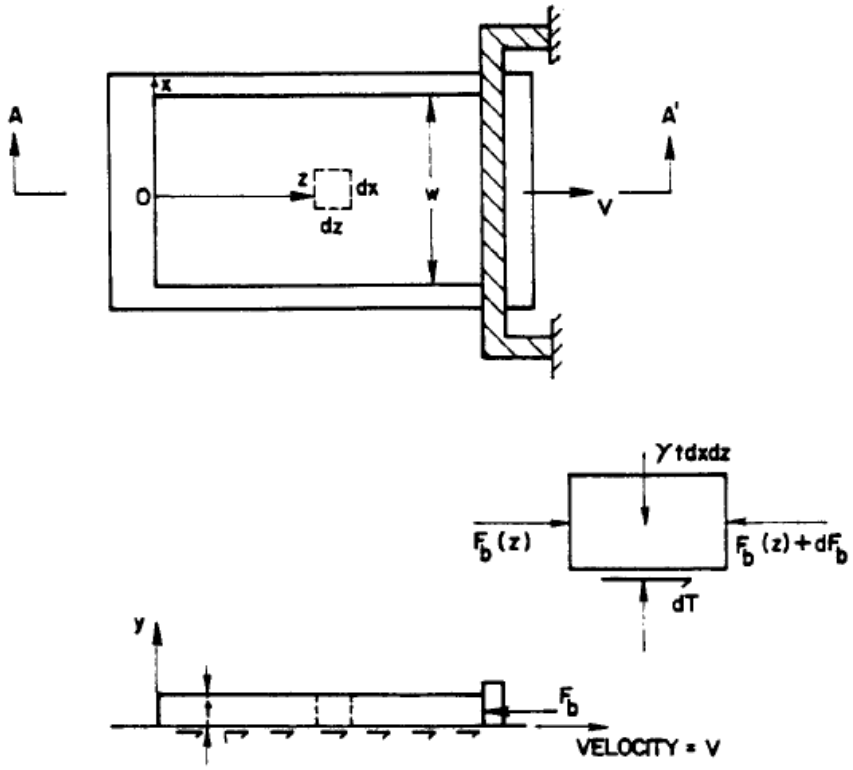

Figure 5.1. Base Friction Model apparatus plan and section (Bray, 1981)

The base friction principle is used widely to reproduce the effects of gravity in two dimensional physical models of excavations in rock. The body force of gravity is simulated by the drag of a belt along the underside of the model.

5.1.2 Model Material

The material that was decided to be used in the model should satisfy the items given below;

i. Simulation of natural material,
ii. No change of the properties as a function of time,
iii. Easy to use and recyclable,

iv. No chemical reaction,
v. Environmentally friendly and harmless to human health,
vi. Easy to find,
vii. Material properties can be controlled by varying the proportions of the components of the mixture,

In the model study sugar bricks was used in the lab works since the width length ratio was 2/1 originally. Moreover, the blocks were very well matched to defined by the bricks since the material had a dimension of 1.8 cm / 0.9 cm / 0.9 cm.

Figure 5.2. Sugar bricks geometry

Since the material is easy to find and has no chemical reaction and can be easily notched by hand, it was selected for model material.

5.1.3 Lab Works

Tests were conducted by means of model materials (sugar bricks) to illustrate the behavior of jointed rock blocks. The placement of the bricks for each case was done by hand in order to get the finest results.

Figure 5.3. Model preparation in the laboratory

A set of 49 physical model tests have been conducted simulating 7 different tunnel diameters at seven orientation of joints. These set was conducted by means of model material. The friction angle between brick were also tested by means of shear box test in the laboratory.

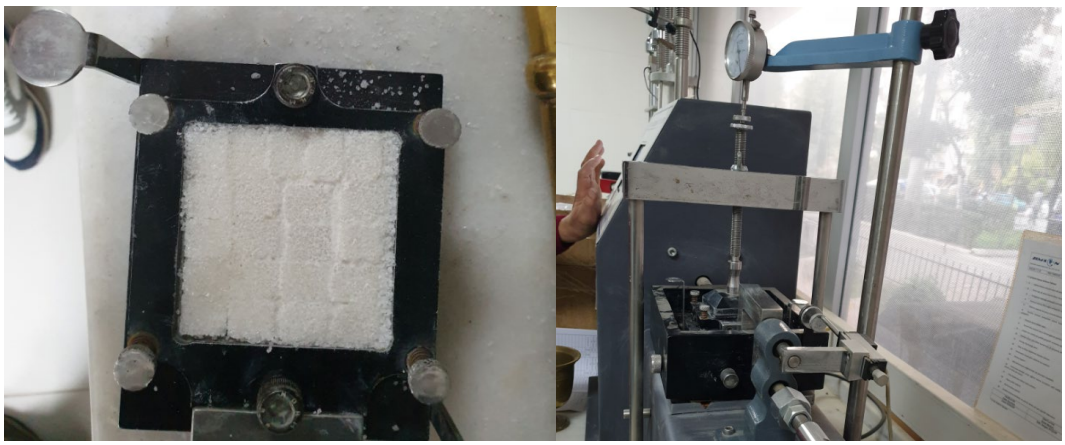

Figure 5.4. Direct shear tests for model material

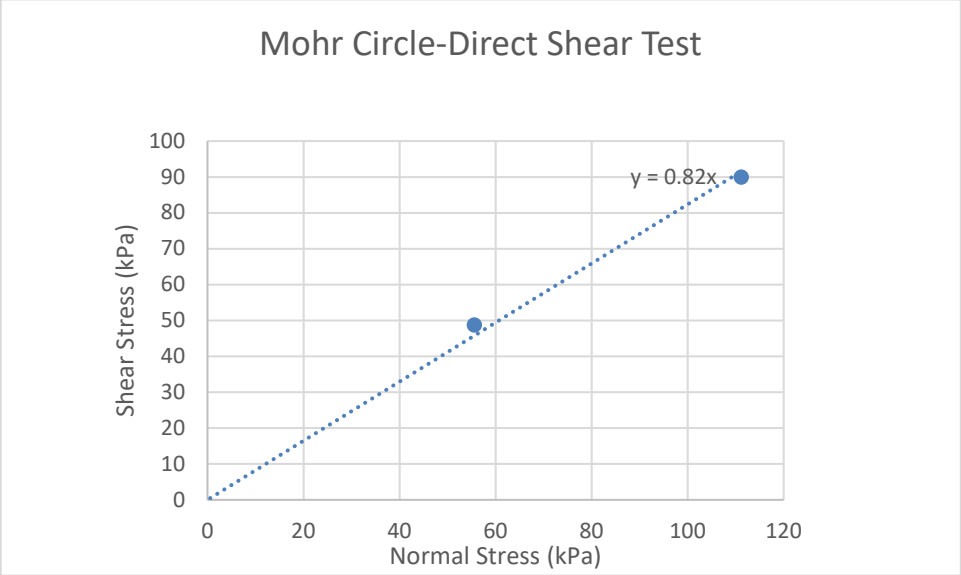

Figure 5.5. Direct shear tests for model material

The friction angle between model material blocks was also studied and direct shear tests were performed in order to get the value of friction to use in numerical models. Two tests were performed to have the trend line. The peak forces were selected in order to get the friction angles. The results as presented at Figure 5.5 gives an estimation of forty degrees at average.

One of the goals in this research is to investigate the influence of the number of joint sets on the heading of the model tunnel. Hence the diameter of the model tunnel was described as n (n=6-12) times the model material width in order to evaluate the effect of the number of joint sets. The joint pattern is proposed to have 7 different angles (with respect to horizontal) on the base friction table.

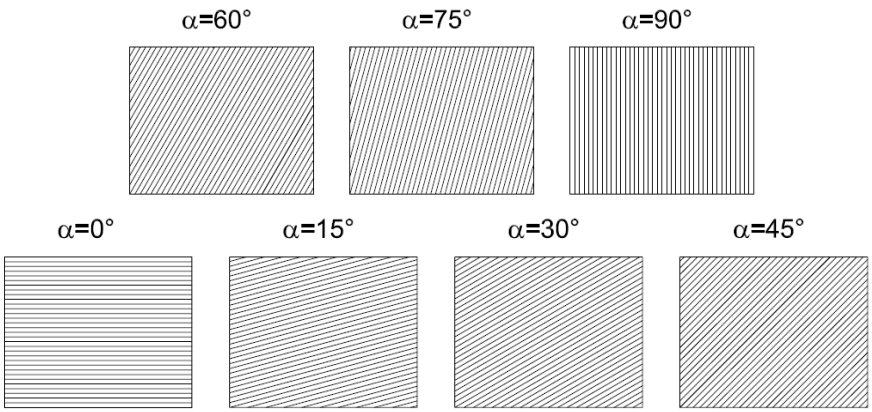

Figure 5.6. Joint patterns used in models

The existing base friction apparatus in ITU MJKM laboratories with 80 cm x 100 cm in dimensions was used for physical modelling with some adjustments. A new sliding base (PVC plastic) was prepared and the gear system was fixed.

Figure 5.7 Base Friction Table in MJKM Lab

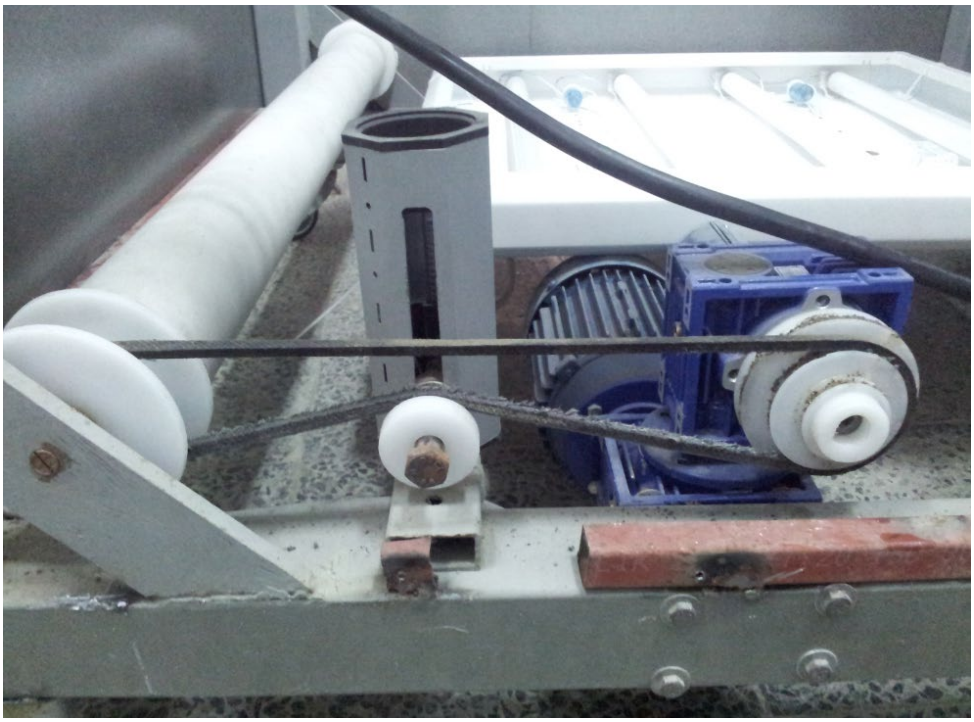

Figure 5.8 Base friction rotor and gear system

Model material was placed onto base friction table at every stage with its defined angular placement, where the tunnel shape was compiled with hand notching to its diameter. An EPS foam material that has a shape of tunnel was placed in the notched area to fulfill the requirements for initialization.

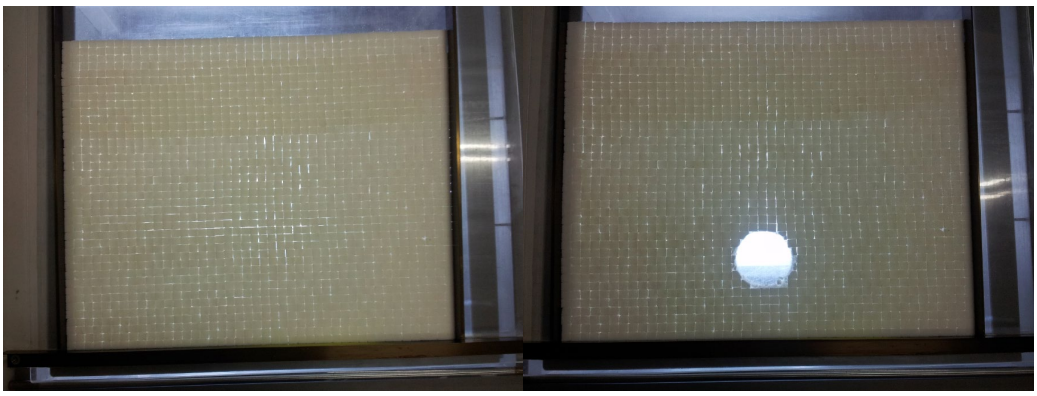

Figure 5.9 sample view from model

The invert of the tunnel structure was placed 8-10 cm from the base not to obtain a force from the bottom steel. The speed of the apparatus was selected as 0.1 cm/s where it reflects the gravitational force. Shear strength of sugar bricks were not a part of the study hence the behavior was elastic. The friction between sugar bricks and the base is enough to prevent bricks from buckling.

5.1.4 Results

Seven different diameters of tunnel with seven joint angles with respect to horizontal layering (α= 0, 15, 30, 45, 60, 75, 90 degrees) were modelled by means of base friction apparatus. The model material blocks had dimensions of 1.8 cm / 0.9 cm / 0.9 cm. Hence a 2/1 width/length ratio was used in the model. The κ factor, the proportion of interface between the top and bottom element, was selected as 1 in joint orientation. The concept of κ is explained in Figure 5.10

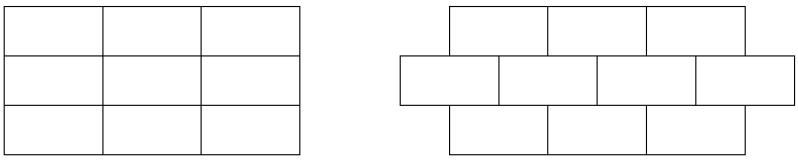

Figure 5.10. κ factor (through-going joints) =1 (a), κ factor= 0.5 (b)

The diameter of the tunnels was selected as the multiples of the width of model material block dimensions. The variation of the ratio was selected starting from six to twelve times the model material block width to be able to interpret the interaction between number of joint sets and tunnel diameter.

Table 5.1. Matrix for joint angles vs. tunnel diameter

Joint Angles (degrees)	**Tunnel Diameter**						
	D1=10.8 cm 6 joint sets	**D2=12.6 cm 7 joint sets**	**D3=14.4 cm 8 joint sets**	**D4=16.2 cm 9 joint sets**	**D5=18.0 cm 10 joint sets**	**D6=19.8 cm 11 joint sets**	**D7=21.6 cm 12 joint sets**
α1=0	A1D1	A1D2	A1D3	A1D4	A1D5	A1D6	A1D7
α2=15	A2D1	A2D2	A2D3	A2D4	A2D5	A2D6	A2D7
α3 =30	A3D1	A3D2	A3D3	A3D4	A3D5	A3D6	A3D7
α4=45	A4D1	A4D2	A4D3	A4D4	A4D5	A4D6	A4D7
α5=60	A5D1	A5D2	A5D3	A5D4	A5D5	A5D6	A5D7
α6=75	A6D1	A6D2	A6D3	A6D4	A6D5	A6D6	A6D7
α7=90	A7D1	A7D2	A7D3	A7D4	A7D5	A7D6	A7D7

.

The main goal was to determine the diameter of the influence zone after excavation before it was supported by differing the joint orientation and tunnel diameter. The variation of tunnel diameter was planned to interpret the effect of joint sets (quantity of joints at the top of head part of the tunnel) by means of the exact ratios with respect to tunnel diameter. The first set was adopted as six as a ratio of tunnel diameter to number of joint sets as seen in Figure 5.12.

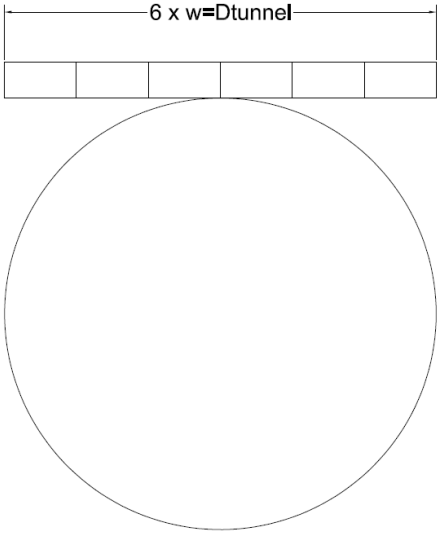

Figure 5.11. Number of through going joints at the crown

The results were interpreted so that the dimensionless ratio of influence zone diameter to tunnel diameter in the model was compared with number of joint sets. The following figures below indicates the initial and final situation of the model tests where the comparisons were made.

During test compilations, video recording and capture was done to evaluate all scenes that would come up in the models. After initialization of the gravity the eps foam was extracted from its place and base friction was rerun again to model proposed gravitational force on excavated tunnel area.

The comparison of before and after excavation screenshots was done by Guiffy software which was developed to interpret image differences due to several criteria.

Guiffy software is a commercial software and is developed for differentiation and comparison of sources in different formats. It has also capability of folder compare and file tree synchronization where it was proposed handy for this study. The functions of illumination variation filters (Heat filter, Black and White filter) were used to compare the captured photos during testing.

5.1.5 Output

First seven sets of models were with horizontal layering (a=0) where the diameter of the tunnel increases with respect to numbers of model material width (six times to 12 times of the width).

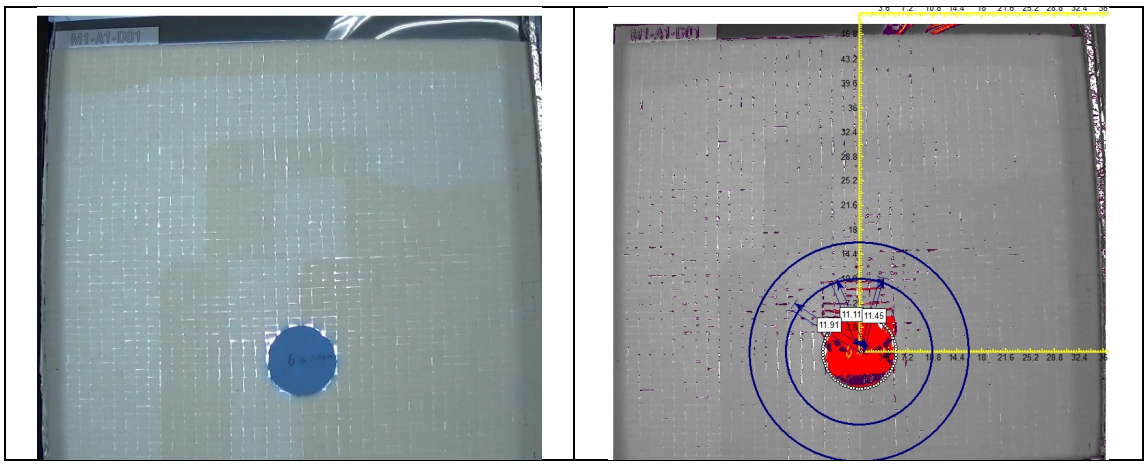

Figure 5.12. A1D01 α1 = 0° horizontal D01= Tunnel Sample diameter 01.

The first trial was with horizontal layering (α=0°) where the tunnel diameter was six times the width of the discrete model material. The comparison results indicates that the effect of tunnel hole exceeds to almost 0.9-1.1 times the diameter above the existing tunnel (Figure 5.13). The figure on the right has a scale on it with respect to diameters selected. The blue circles correspond the increase of diameter accordingly. Two or three circles were created to give a scale to interpret the influence zone diameter. Each circle represents a diameter of modelled tunnel diameter. The blue arrows were used to define the possible extension of influence zones. The heat filter of the Guiffy software was used to determine the differences before and after excavation. The first displaced zone (heat) over the excavated area was measured and taken as the influence zone as effected by excavation.

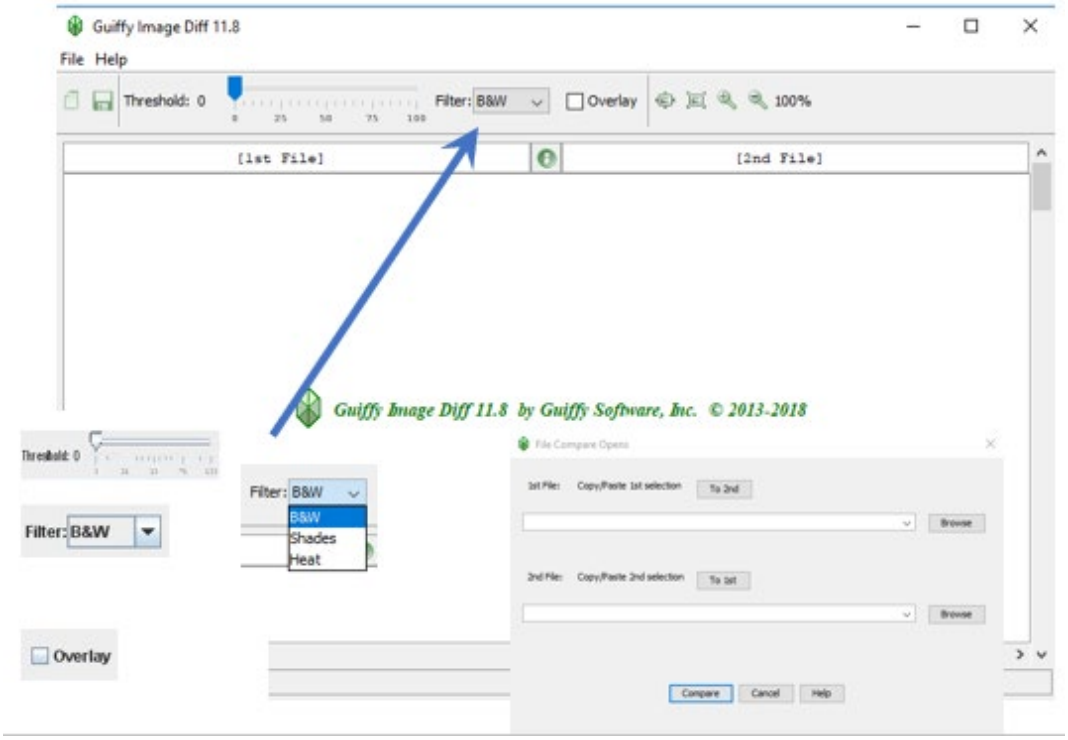

Figure 5.13. Guiffy software graphical user interface with filter options.

The Guiffy software uses three types of filter options where heat filter was used for this study (Figure 5.14). Differences can be viewed side-by-side, split horizontally, or together in a single window. Guiffy's Diff tool default compare algorithm, the Minimum Lines of Diff, is an improved version of the popular "unique anchors" algorithm.

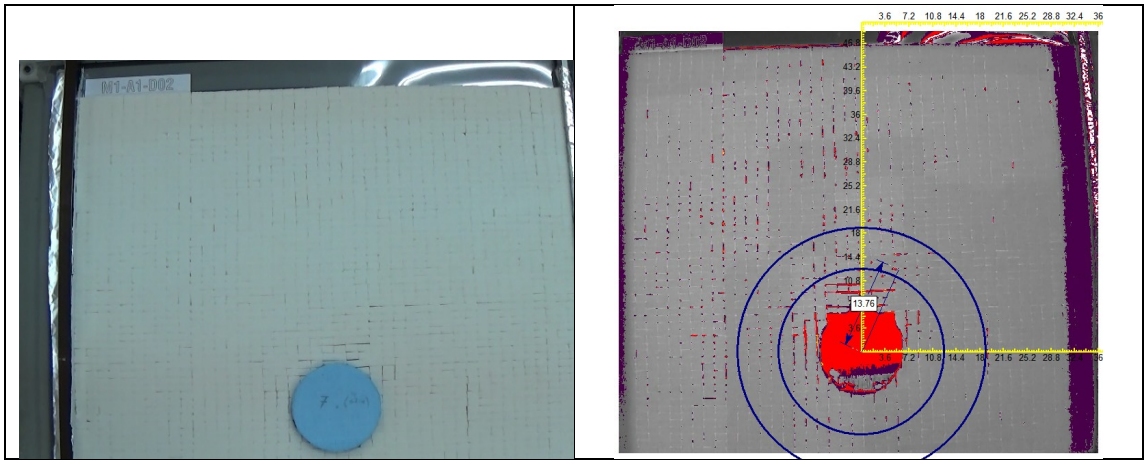

Figure 5.14. A1D02 α1 = 0° (horizontal),

The second model was also with horizontal layering (α=0°) where the tunnel diameter was enlarged to seven times the width of the discrete model material. By help of Guiffy software, the results shows us that the effect of tunnel hole exceeds to almost 1.1-1.3 diameter above the existing tunnel (Figure 5.15). The values are given in a range since the influenced zone in the crown were measured few times.

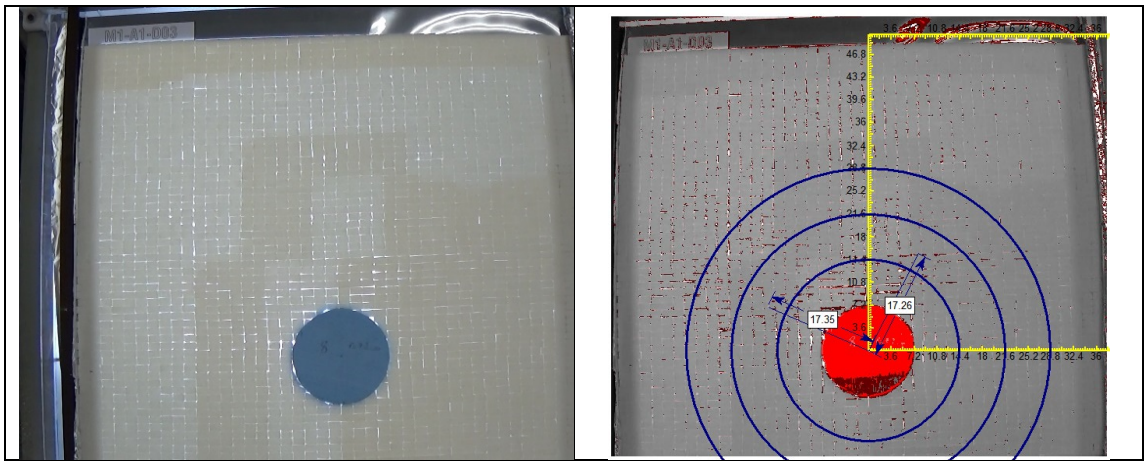

Figure 5.15. A1D03 α1 = 0° (horizontal).

The third model was also with horizontal layering (α=0°) where the tunnel diameter was enlarged to eight times the width of the discrete model material. By help of Guiffy software, the results shows us that the effect of tunnel hole exceeds to almost 1.3-1.4 diameter above the existing tunnel (Figure 5.16).

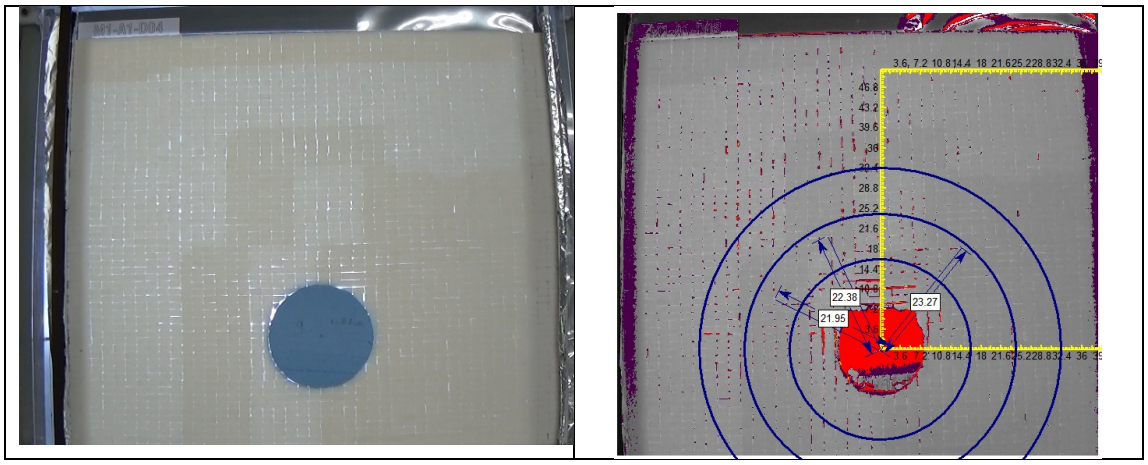

Figure 5.16. A1D04 α1 = 0° (horizontal)

The fourth model was also with horizontal layering (α=0°) where the tunnel diameter was enlarged to nine times the width of the discrete model material. By help of Guiffy software, the results shows us that the effect of tunnel hole exceeds to almost 1.5-1.8 diameter above the existing tunnel (Figure 5.17).

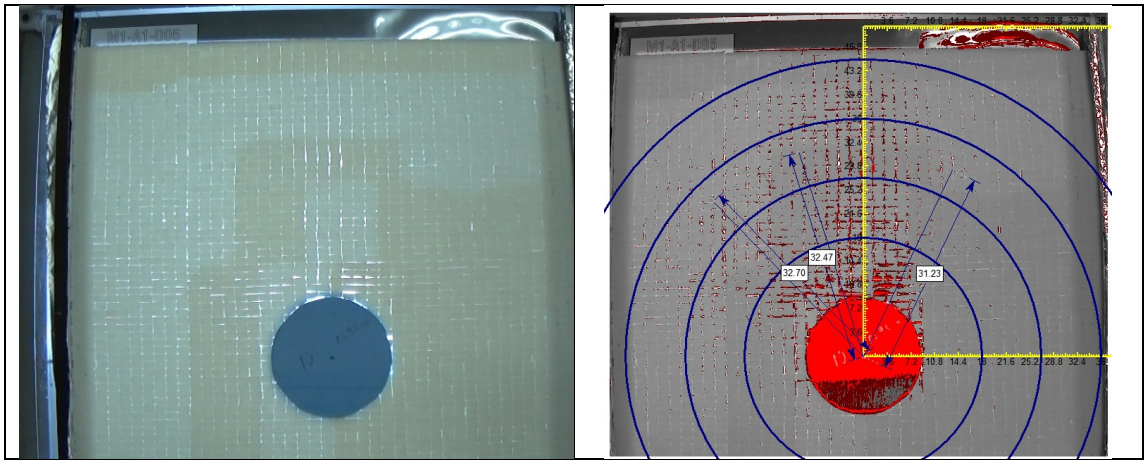

Figure 5.17. A1D05 α1 = 0° (horizontal)

The fifth model was also with horizontal layering (α=0°) where the tunnel diameter was enlarged to ten times the width of the discrete model material. By help of Guiffy software, the results shows us that the effect of tunnel hole exceeds to almost 2.3-2.5 diameter above the existing tunnel (Figure 5.18).

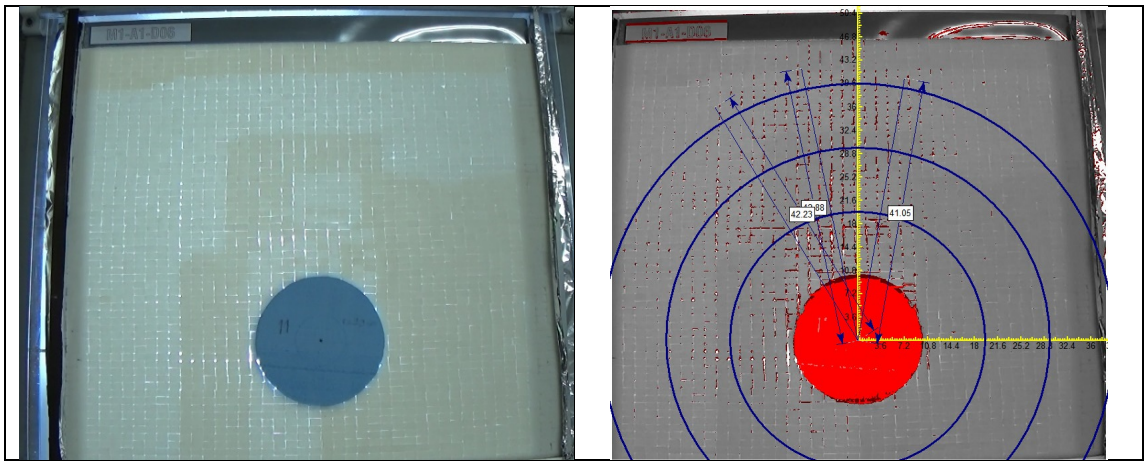

Figure 5.18. A1D06 α1 = 0° (horizontal)

The sixth model was also with horizontal layering (α=0°) where the tunnel diameter was enlarged to eleven times the width of the discrete model material. By help of Guiffy software, the results shows us that the effect of tunnel hole exceeds to almost 2.5-3.0 diameter above the existing tunnel (Figure 5.19).

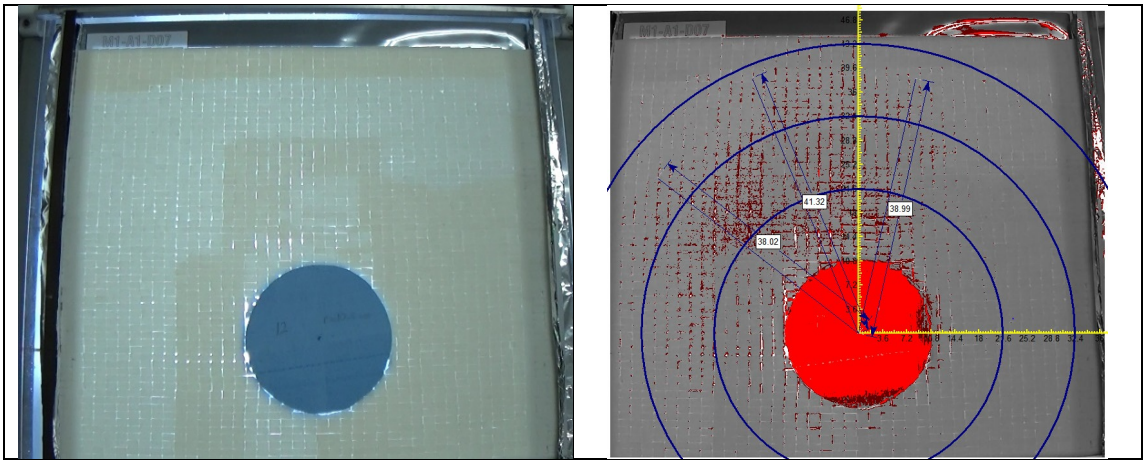

Figure 5.19. A1D06 α1 = 0° (horizontal)

The seventh model was also with horizontal layering (α=0°) where the tunnel diameter was enlarged to twelve times the width of the discrete model material. By help of guiffy software, the results shows us that the effect of tunnel hole exceeds to almost 3.1-3.3 diameter above the existing tunnel (Figure 5.20).

A brief comparison clearly indicates that; the distance of influence is extended with increasing diameter of the tunnel in same horizontal layering of rock joints.

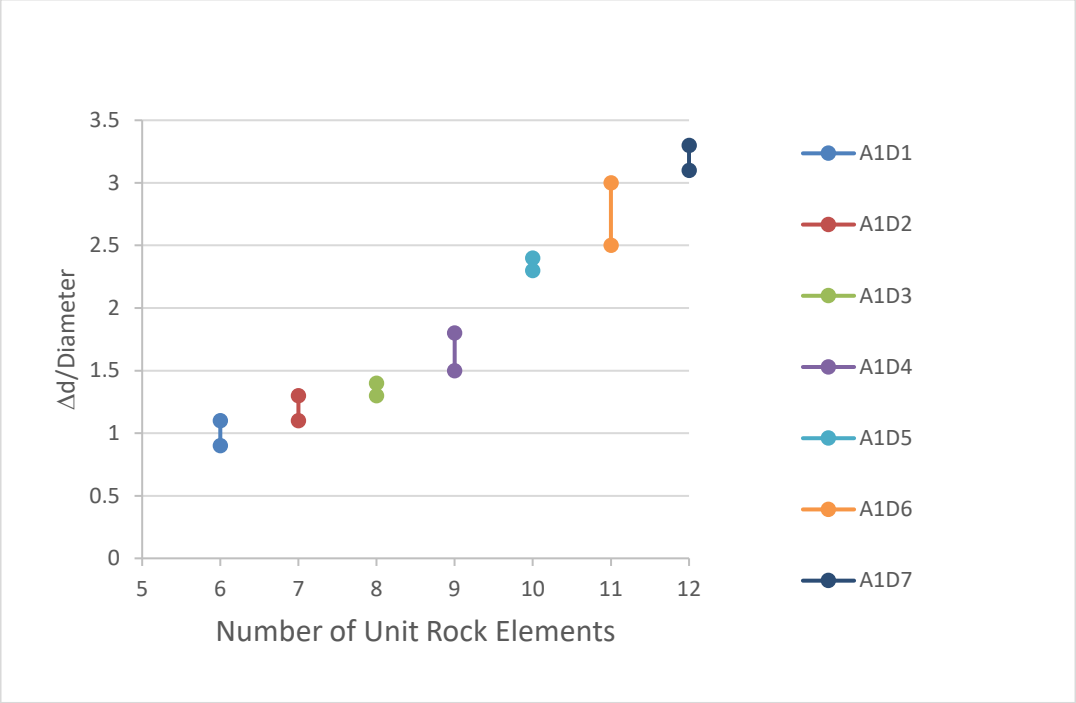

Figure 5.20. Initial evaluation of interaction of horizontal layering α=0 (7 tests)

Second seven sets of models were with 15 degrees from horizontal (α=15°) where the diameter of the tunnel increases also as in first set with respect to numbers of model material width (six times to twelve times of the width of sugar bricks (joint sets)).

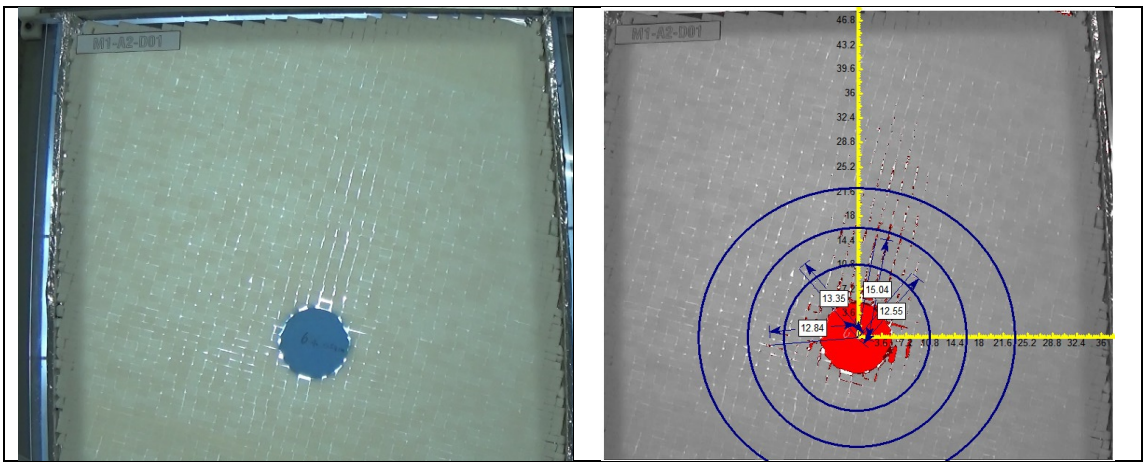

Figure 5.21. A2D01 α2 = 15° with horizontal

The eighth model was 15 degrees with horizontal (α=15°) where the tunnel diameter was enlarged to six times the width of the discrete model material. By help of Guiffy software, the results shows us that the effect of tunnel hole exceeds to almost 1.0-1.1

diameter above the existing tunnel (Figure 5.22). The main orientation of displacement for 15 degrees are found to be parallel to the joint orientation. Anisotropic orientation of influence zone with respect to horizontal bedding has come forward.

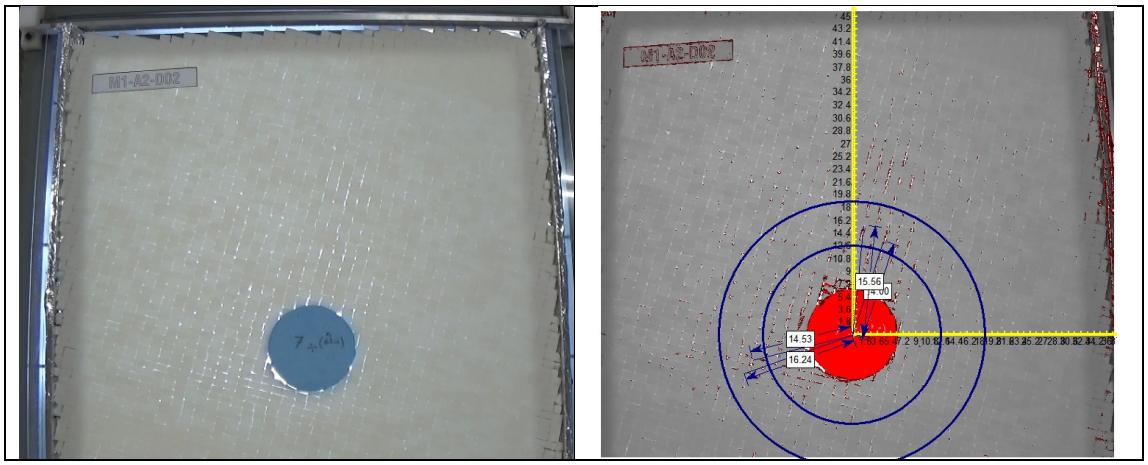

Figure 5.22. A2D02 α2 = 15° with respect to horizontal

The ninth model was 15 degrees with horizontal (α=15°) where the tunnel diameter was enlarged to seven times the width of the discrete model material. By help of Guiffy software, the results shows us that the effect of tunnel hole exceeds to almost 1.2-1.4 diameter above the existing tunnel (Figure 5.23).

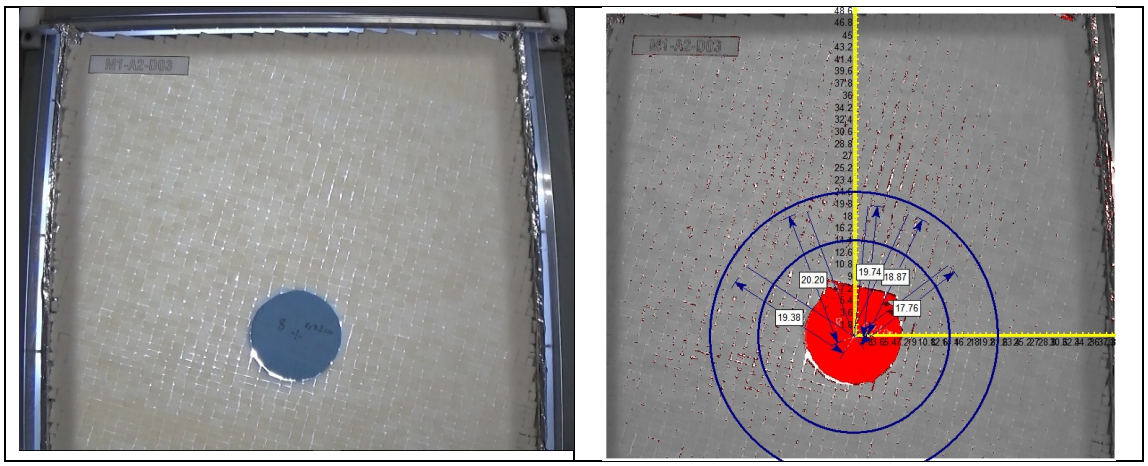

Figure 5.23. A2D03 α2 = 15° with respect to horizontal

The tenth model was 15 degrees with horizontal (α=15°) where the tunnel diameter was enlarged to eight times the width of the discrete model material. By help of Guiffy software, the results shows us that the effect of tunnel hole exceeds to almost 1.4-1.8 diameter above the existing tunnel (Figure 5.24).

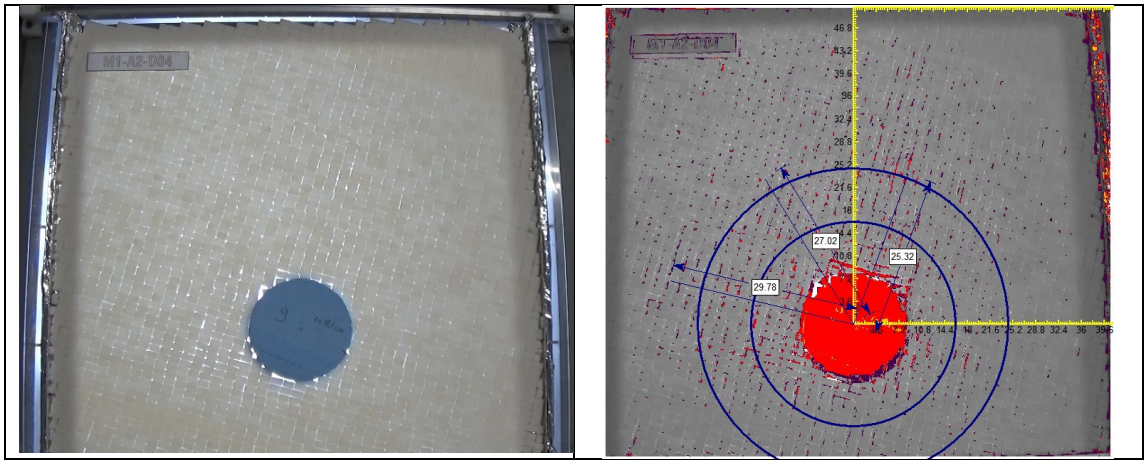

Figure 5.24. A2D04 α2 = 15° with respect to horizontal

The model#11 was 15 degrees with horizontal (α=15°) where the tunnel diameter was enlarged to nine times the width of the discrete model material. By help of Guiffy software, the results shows us that the effect of tunnel hole exceeds to almost 2.1-2.4 diameter above the existing tunnel (Figure 5.25).

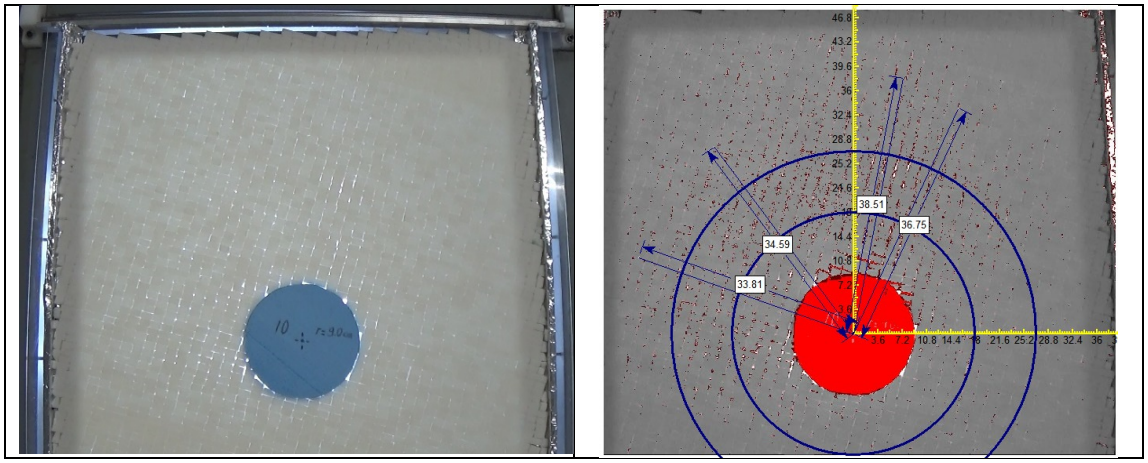

Figure 5.25. A2D05 α2 = 15° with respect to horizontal

The model#12 was 15 degrees with horizontal (α=15°) where the tunnel diameter was enlarged to ten times the width of the discrete model material. By help of Guiffy software, the results shows us that the effect of tunnel hole exceeds to almost 2.8-3.1 diameter above the existing tunnel (Figure 5.26).

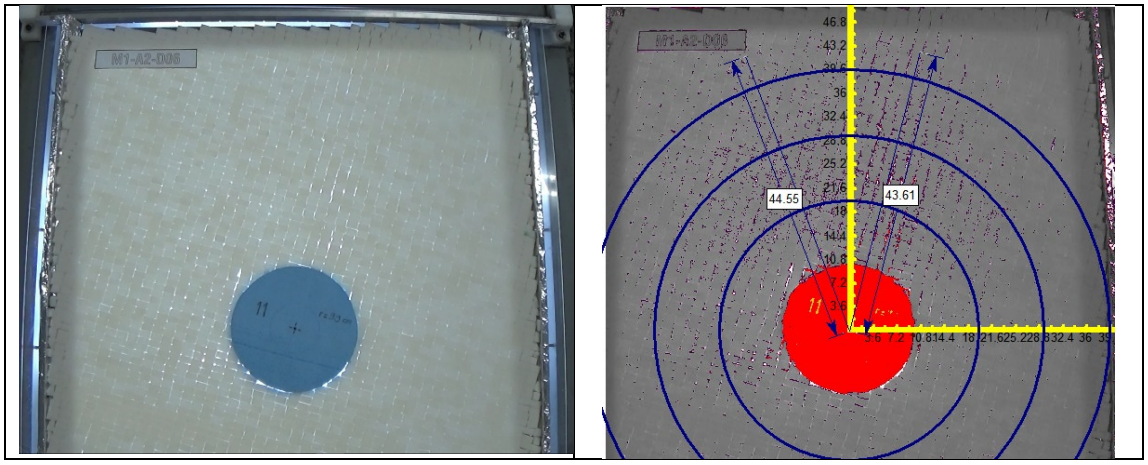

Figure 5.26. A2D06 α2 = 15° with respect to horizontal

The model#13 was 15 degrees with horizontal (α=15°) where the tunnel diameter was enlarged to eleven times the width of the discrete model material. By help of Guiffy software, the results shows us that the effect of tunnel hole exceeds to almost 3.1-3.5 diameter above the existing tunnel (Figure 5.27).

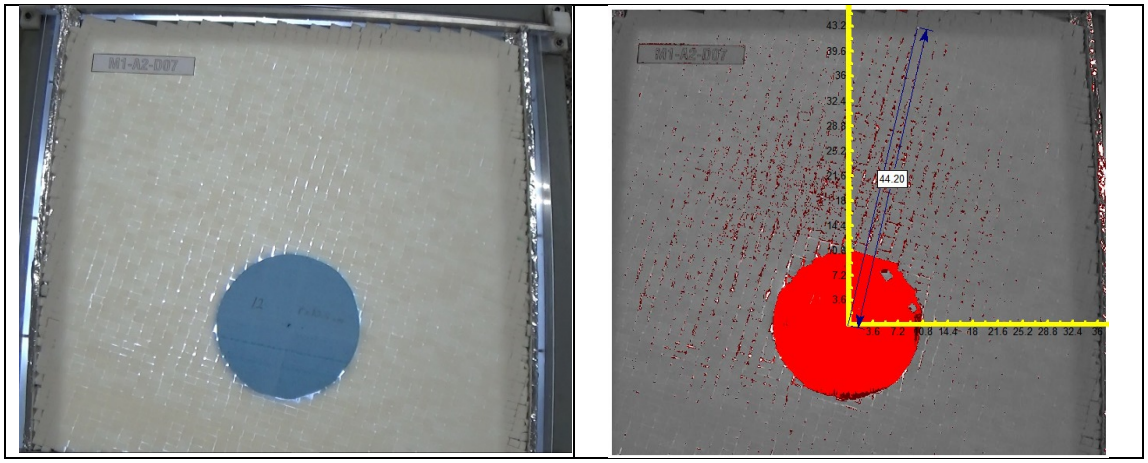

Figure 5.27. A2D07 α2 = 15° with respect to horizontal

The model#14 was 15 degrees with horizontal (α=15°) where the tunnel diameter was enlarged to twelve times the width of the discrete model material. By help of Guiffy software, the results show us that the effect of tunnel hole exceeds to almost 3.5-higher diameter above the existing tunnel where the limit is model top layer. (Figure 5.28).

The results of interaction vs the number of joint sets for second set of models with fifteen degrees are also plotted below. It seems it has almost the same form of inclination when compared to first set results.

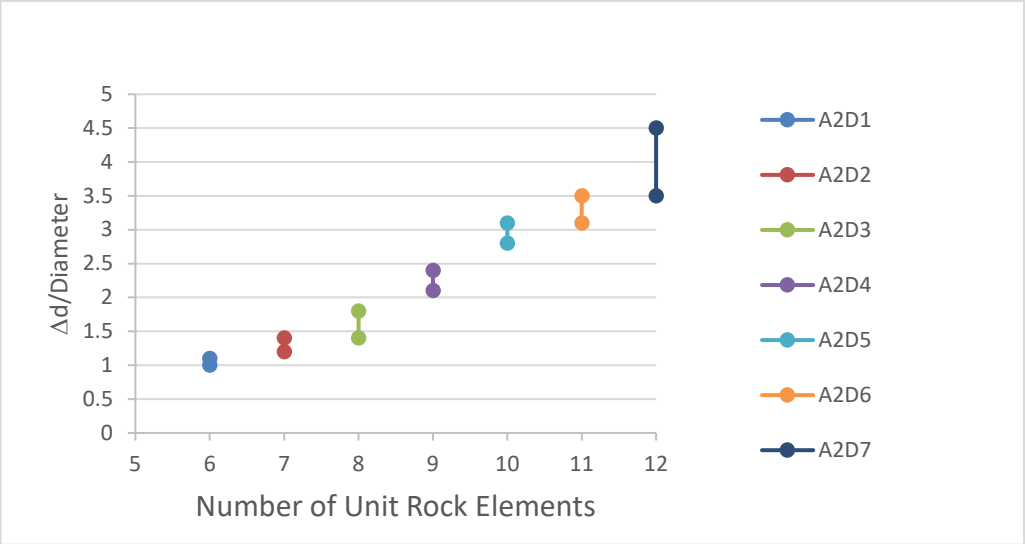

Figure 5.28. Initial evaluation of interaction of second set (α=15°) (7 tests)

Third seven sets of models were with 30 degrees from horizontal (α=30°) where the diameter of the tunnel increases also as in first set with respect to numbers of model material width (six times to 12 times of the width of bricks (joint sets))

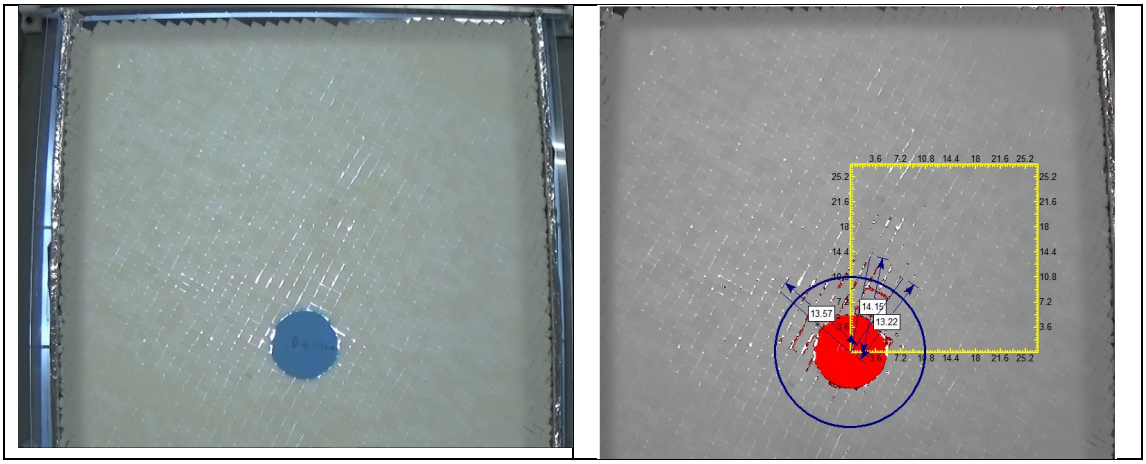

Figure 5.29. A3D01 α3 = 30° with respect to horizontal

The model#15 was 30 degrees with horizontal (α=30°) where the tunnel diameter was enlarged to six times the width of the discrete model material. By help of Guiffy software, the results shows us that the effect of tunnel hole exceeds to almost 1.1-1.3 diameter above the existing tunnel (Figure 5.30). Anisotropic orientation of influence zone with respect to horizontal bedding has come forward.

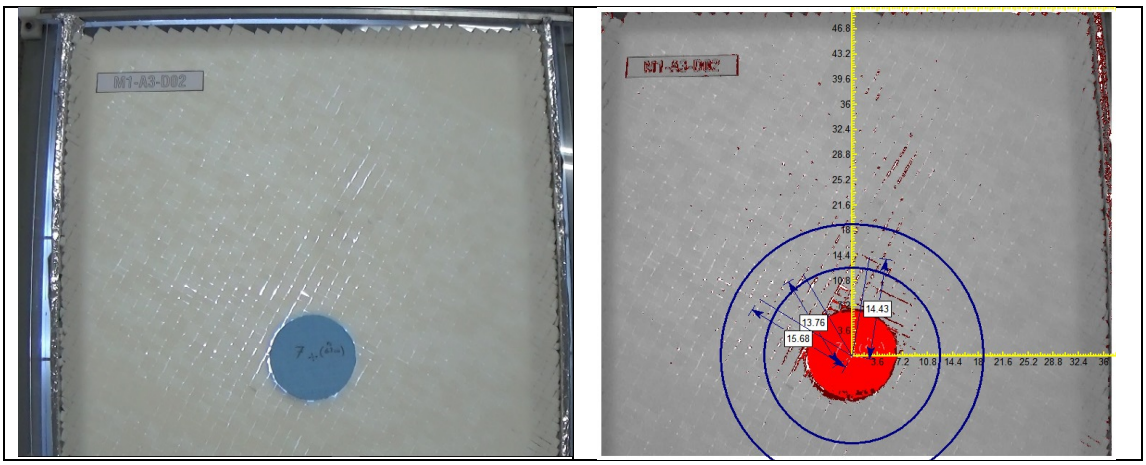

Figure 5.30. A3D02 α3 = 30° with respect to horizontal

The model#16 was 30 degrees with horizontal (α=30°) where the tunnel diameter was enlarged to seven times the width of the discrete model material. By help of Guiffy software, the results shows us that the effect of tunnel hole exceeds to almost 1.2-1.5 diameter above the existing tunnel (Figure 5.31).

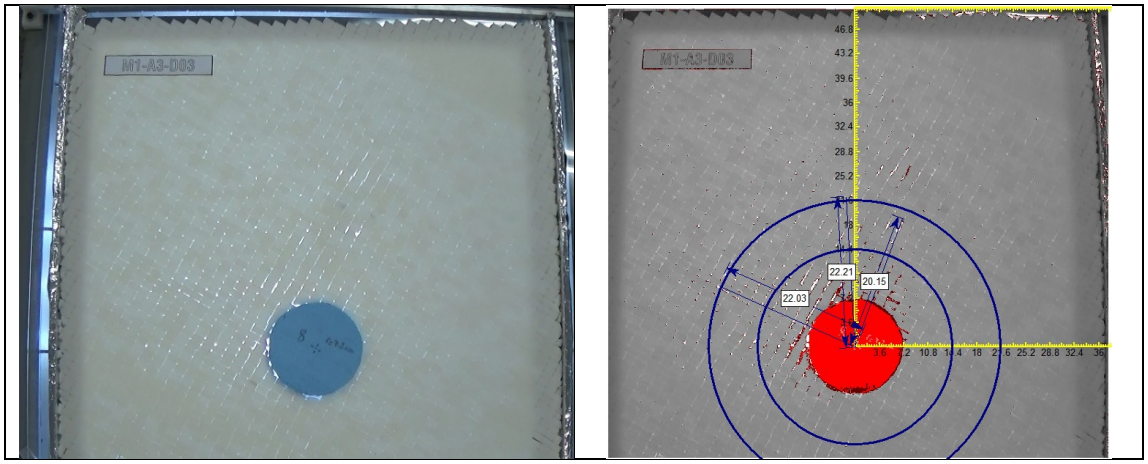

Figure 5.31. A3D03 α3 = 30° with respect to horizontal

The model#17 was 30 degrees with horizontal (α=30°) where the tunnel diameter was enlarged to eight times the width of the discrete model material. By help of Guiffy software, the results shows us that the effect of tunnel hole exceeds to almost 1.8-2.1 diameter above the existing tunnel (Figure 5.32).

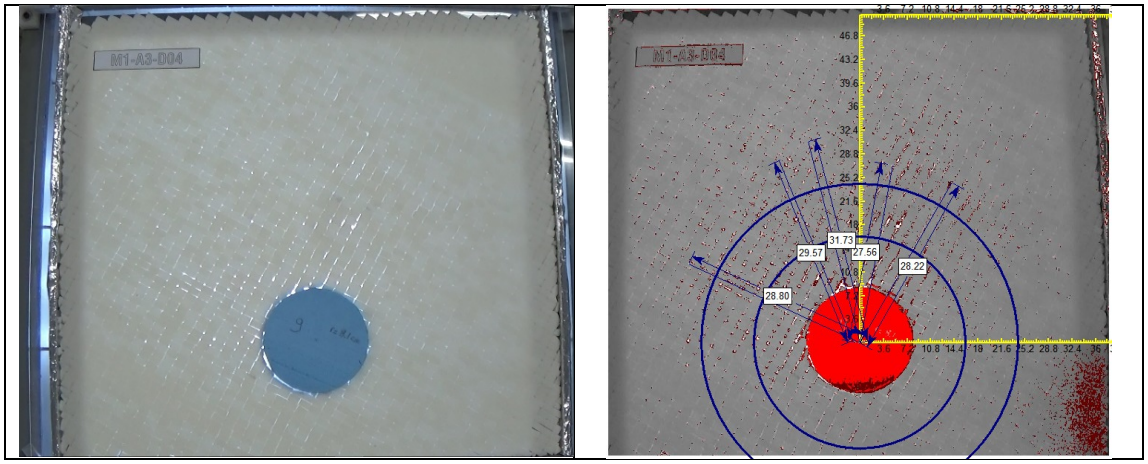

Figure 5.32. A3D04 α3 = 30° with respect to horizontal

The model#18 was 30 degrees with horizontal (α=30°) where the tunnel diameter was enlarged to nine times the width of the discrete model material. By help of Guiffy software, the results shows us that the effect of tunnel hole exceeds to almost 1.8-2.1 diameter above the existing tunnel (Figure 5.33).

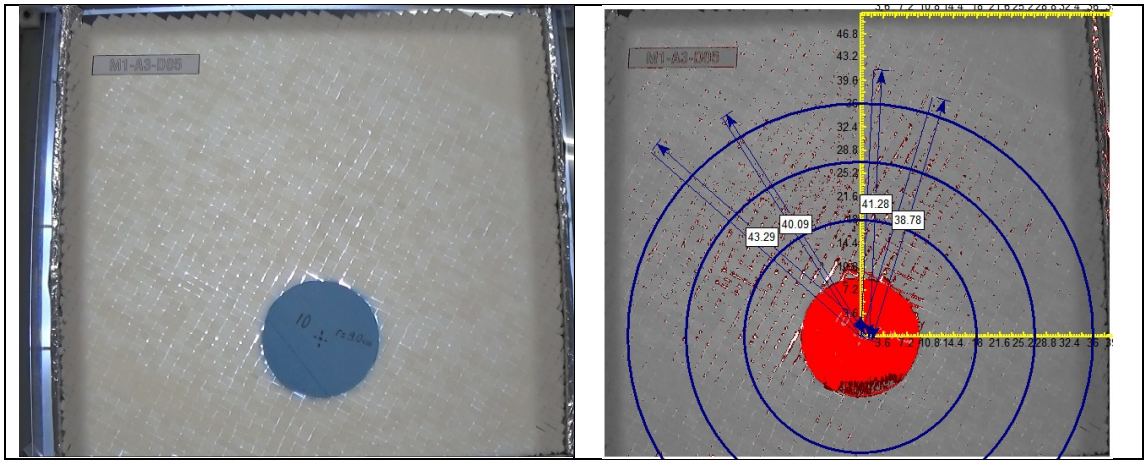

Figure 5.33. A3D05 α3 = 30° with respect to horizontal

The model#19 was 30 degrees with horizontal (α=30°) where the tunnel diameter was enlarged to ten times the width of the discrete model material. By help of Guiffy software, the results shows us that the effect of tunnel hole exceeds to almost 2.8-3.2 diameter above the existing tunnel (Figure 5.34).

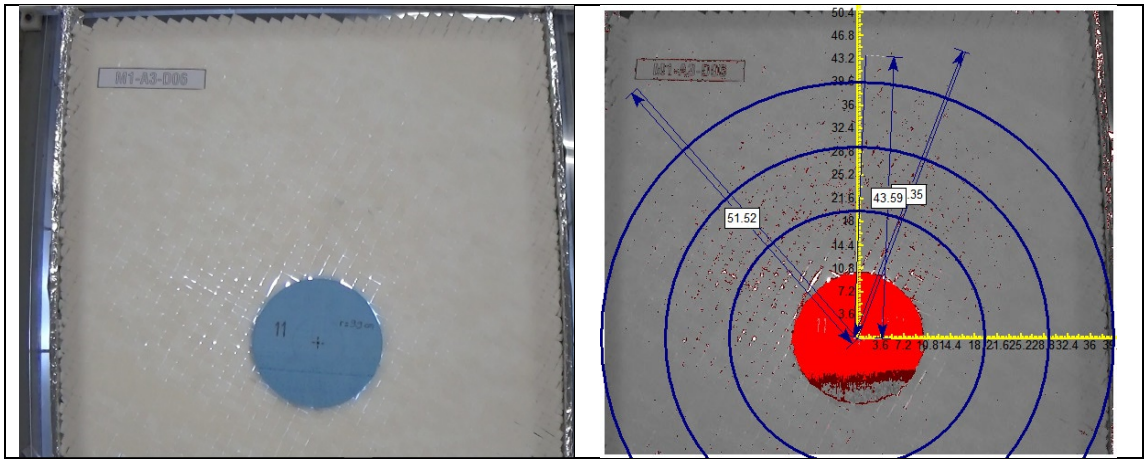

Figure 5.34. A3D06 α3 = 30° with respect to horizontal

The model#20 was 30 degrees with horizontal (α=30°) where the tunnel diameter was enlarged to eleven times the width of the discrete model material. By help of Guiffy software, the results shows us that the effect of tunnel hole exceeds to almost 3.3-3.8 diameter above the existing tunnel (Figure 5.35).

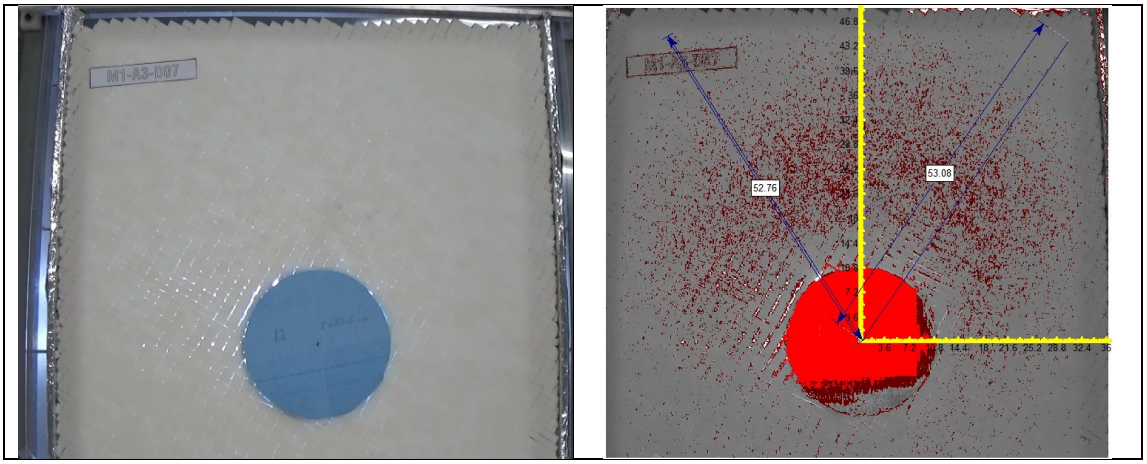

Figure 5.35. A3D07 α3 = 30° with respect to horizontal

The model#21 was 30 degrees with horizontal (α=30°) where the tunnel diameter was enlarged to twelve times the width of the discrete model material. By help of Guiffy software, the results show us that the effect of tunnel hole exceeds to almost 4.0-4.8 diameter above the existing tunnel. It was also observed that with increasing diameter (bigger one), the zone of influence also was affected tremendously (Figure 5.36).

The third set results (interaction vs the number of joint sets) with thirty degrees are also plotted below. It seems it has almost the same form of inclination when compared to first two sets results.

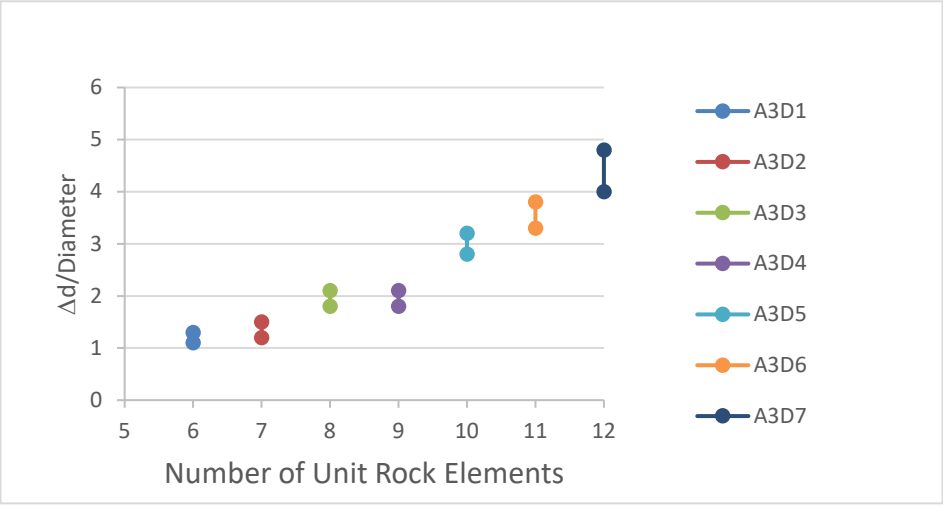

Figure 5.36. Initial evaluation of interaction of third set (α=30°) (7 tests)

Fourth seven sets of models were with discontinuities having an inclination of 45 degrees from horizontal (α=45°) where the diameter of the tunnel increases also as in first set with respect to numbers of model material width (tunnel diameter is six times to 12 times of the width of model bricks or in other words tunnel diameter is six times to 12 times the joint spacing).

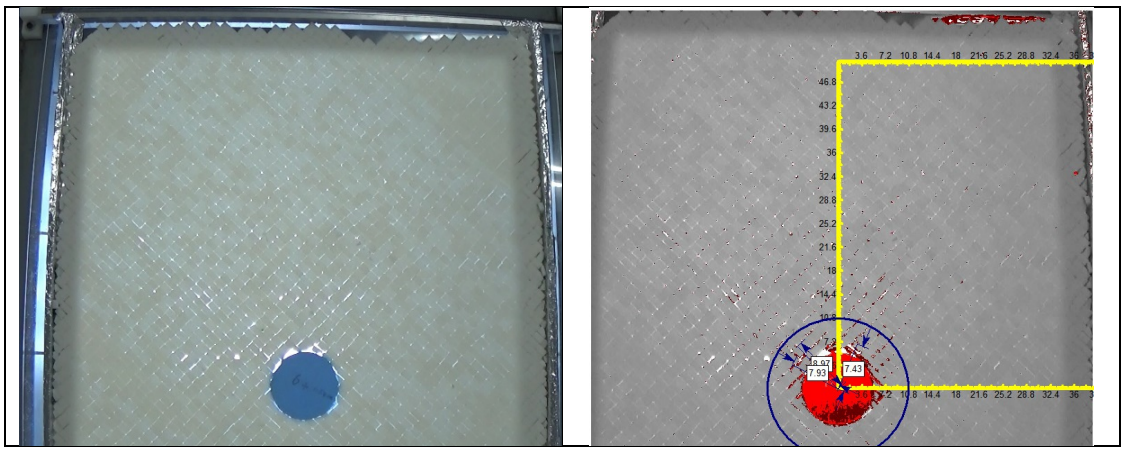

Figure 5.37. A4D01 α4 = 45° with respect to horizontal

The model#22 was 45 degrees with horizontal (α=45°) where the tunnel diameter was enlarged to six times the width of the discrete model material. The circles were created by means of illumination technique to find the influenced zone area. By help of Guiffy software, the results shows us that the effect of tunnel hole exceeds to almost 0.4-0.5 diameter above the existing tunnel (Figure 5.38). Anisotropic orientation of influence zone with respect to horizontal bedding is interpreted as symmetric in 45 degrees of orientation.

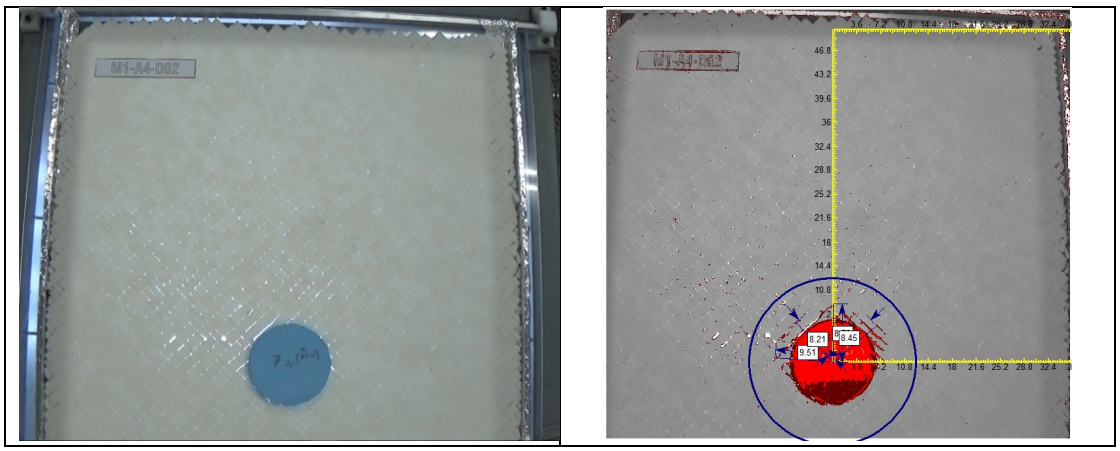

Figure 5.38. A4D02 α4 = 45° with respect to horizontal

The model#23 was 45 degrees with horizontal (α=45°) where the tunnel diameter was enlarged to seven times the width of the discrete model material. By help of Guiffy software, the results shows us that the effect of tunnel hole exceeds to almost 0.4-0.6 diameter above the existing tunnel (Figure 5.39).

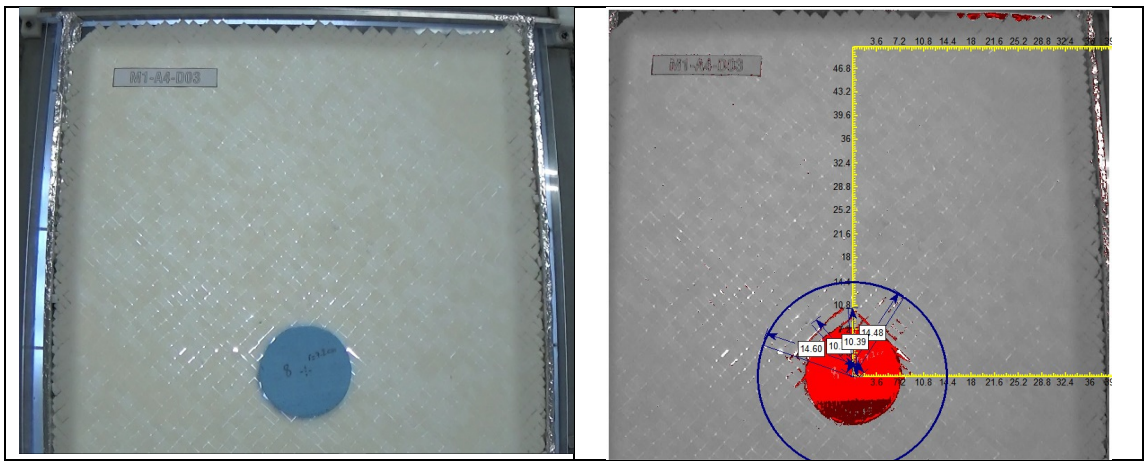

Figure 5.39. A4D03 α4 = 45° with respect to horizontal

The model#24 was 45 degrees with horizontal (α=45°) where the tunnel diameter was enlarged to eight times the width of the discrete model material. By help of Guiffy software, the results shows us that the effect of tunnel hole exceeds to almost 0.6-0.9 diameter above the existing tunnel (Figure 5.40).

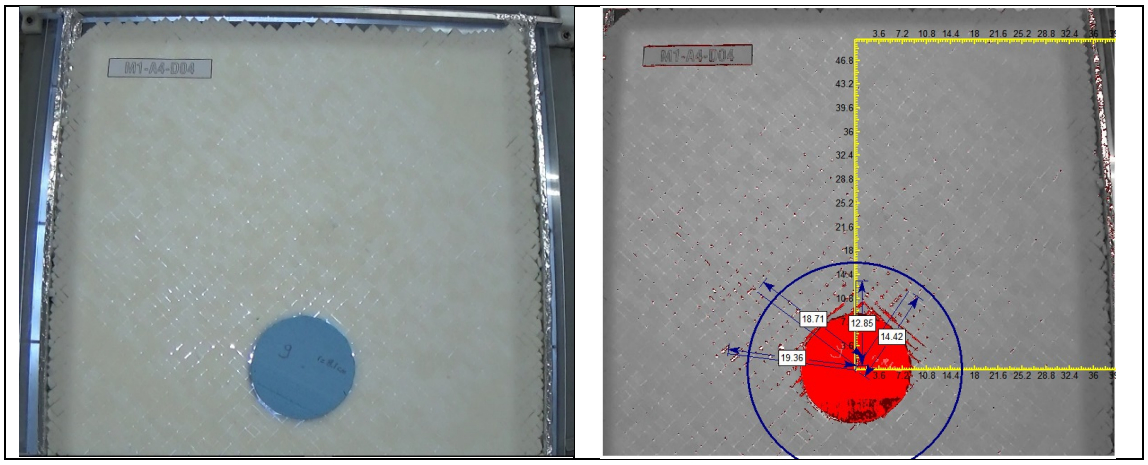

Figure 5.40. A4D04 α4 = 45° with respect to horizontal

The model#25 was 45 degrees with horizontal (α=45°) where the tunnel diameter was enlarged to nine times the width of the discrete model material. By help of Guiffy software, the results shows us that the effect of tunnel hole exceeds to almost 0.8-1.2 diameter above the existing tunnel (Figure 5.41).

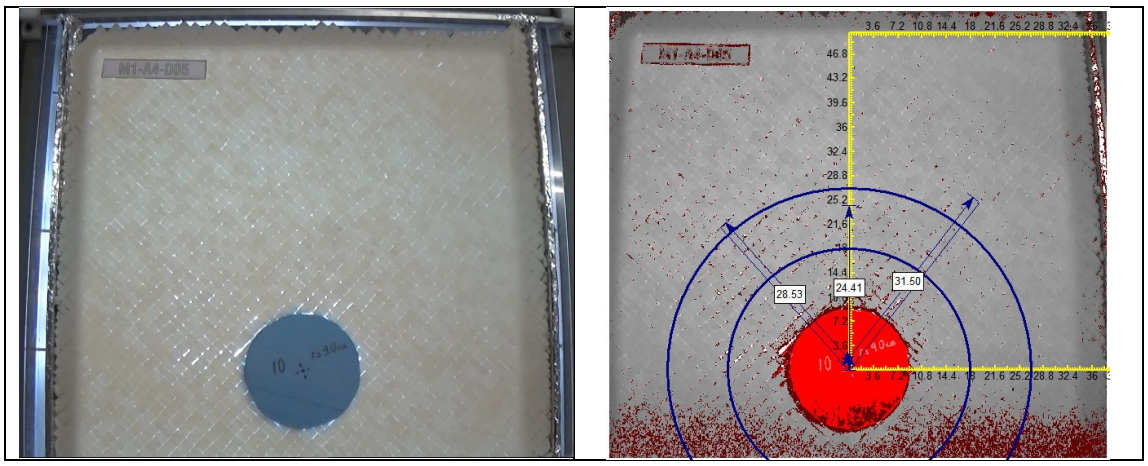

Figure 5.41. A4D05 α4 = 45° with respect to horizontal

The model#26 was 45 degrees with horizontal (α=45°) where the tunnel diameter was enlarged to ten times the width of the discrete model material. By help of Guiffy software, the results shows us that the effect of tunnel hole exceeds to almost 1.8-2.2 diameter above the existing tunnel (Figure 5.42).

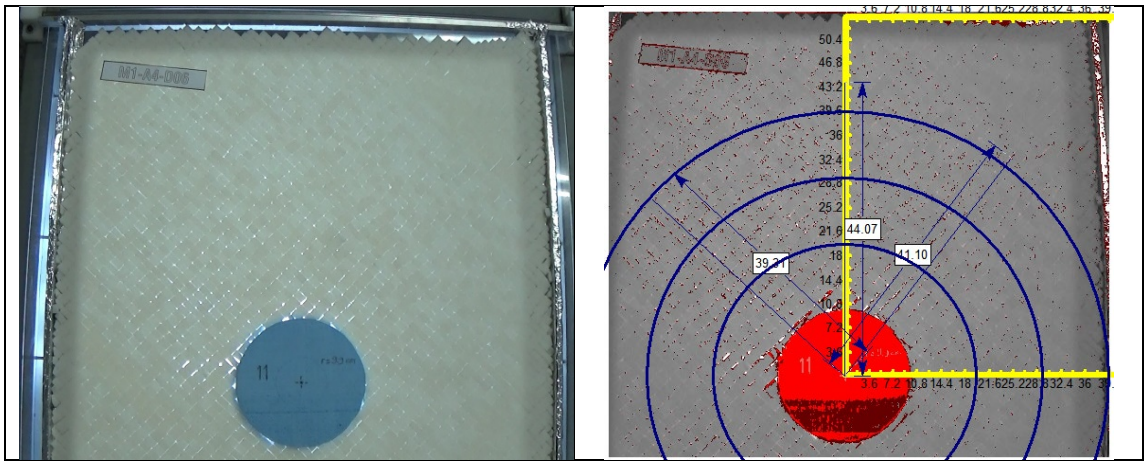

Figure 5.42. A4D06 α4 = 45° with respect to horizontal

The model#27 was 45 degrees with horizontal (α=45°) where the tunnel diameter was enlarged to eleven times the width of the discrete model material. By help of Guiffy software, the results shows us that the effect of tunnel hole exceeds to almost 2.8-3.1 diameter above the existing tunnel (Figure 5.43).

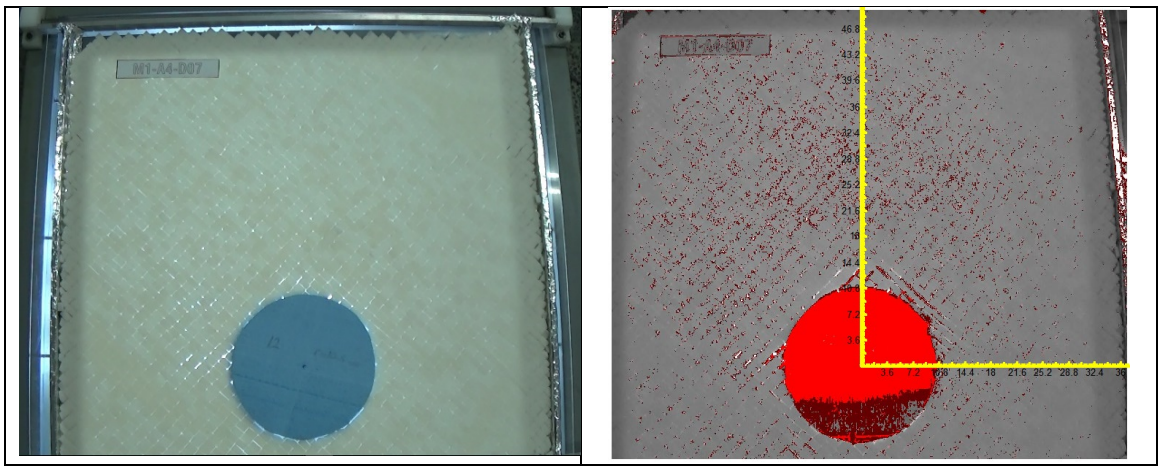

Figure 5.43. A4D07 α4 = 45° with respect to horizontal

The model#28 was 45 degrees with horizontal (α=45°) where the tunnel diameter was enlarged to twelve times the width of the discrete model material. By help of Guiffy software, the results shows us that the effect of tunnel hole exceeds to almost 3.0-4.0 diameter above the existing tunnel (Figure 5.44).

The fourth set results (interaction vs the number of joint sets) with 45 degrees are also plotted below. It seems it has almost the same form of inclination when compared to first three sets results.

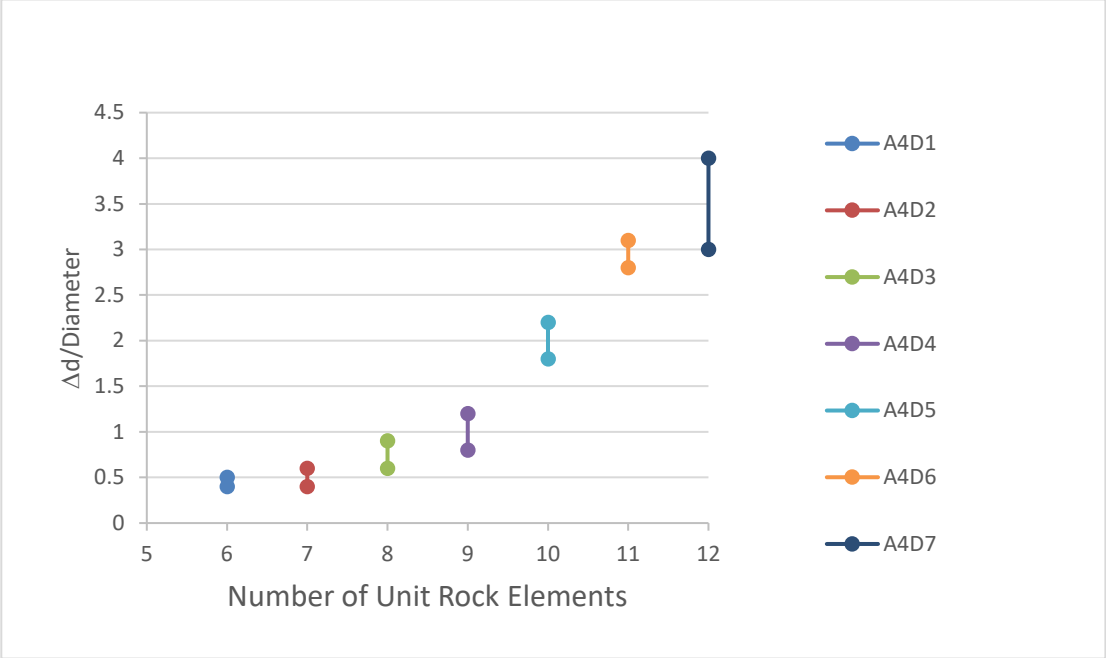

Figure 5.44. Initial evaluation of interaction of forth set (α=45°) (7 tests)

Fifth seven sets of models were with 60 degrees from horizontal (α=60°) where the diameter of the tunnel increases also as in first set with respect to numbers of model material width (six times to 12 times of the width of bricks (joint sets))

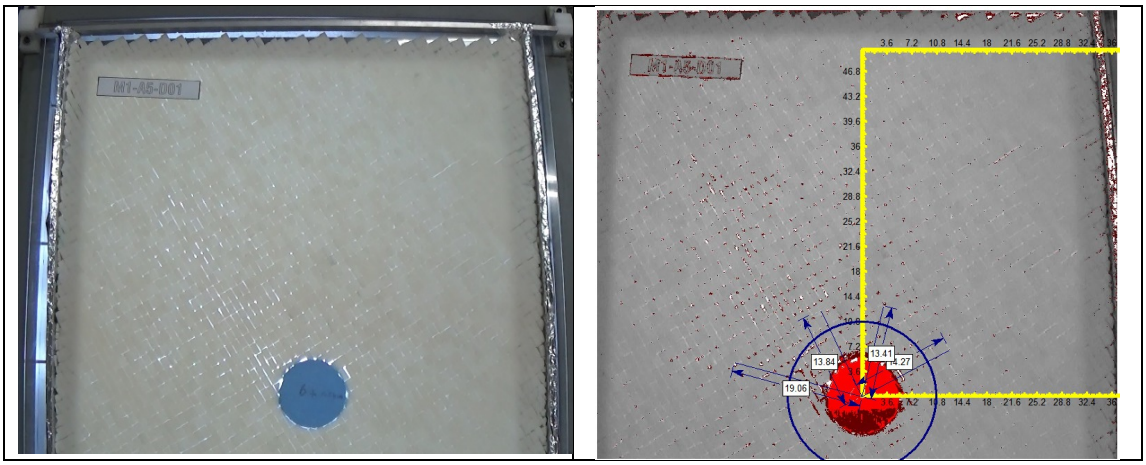

Figure 5.45. A5D01 α5 = 60° with respect to horizontal

The model#29 was 60 degrees with horizontal (α=60°) where the tunnel diameter was enlarged to six times the width of the discrete model material. By help of Guiffy software, the results shows us that the effect of tunnel hole exceeds to almost 1.3-1.9 diameter above the existing tunnel (Figure 5.46).

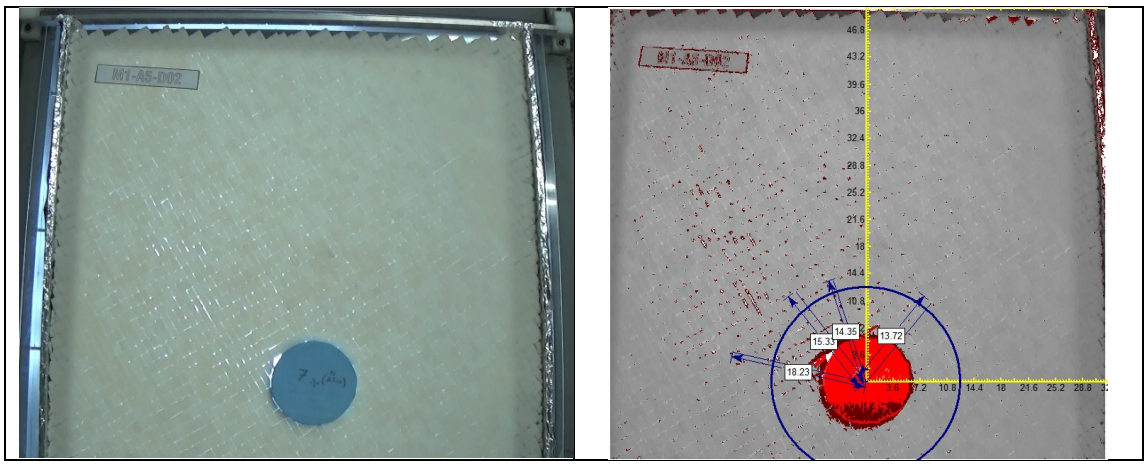

Figure 5.46. A5D02 α5 = 60° with respect to horizontal

The model#30 was 60 degrees with horizontal (α=60°) where the tunnel diameter was enlarged to seven times the width of the discrete model material. By help of Guiffy software, the results shows us that the effect of tunnel hole exceeds to almost 1.1-1.8 diameter above the existing tunnel (Figure 5.47).

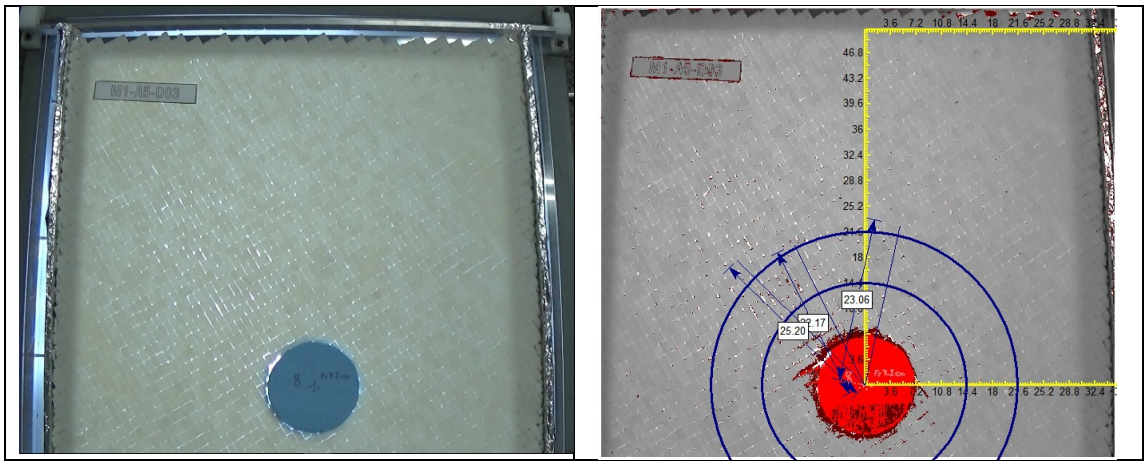

Figure 5.47 A5D03 α5 = 60° with respect to horizontal

The model#31 was 60 degrees with horizontal (α=60°) where the tunnel diameter was enlarged to eight times the width of the discrete model material. By help of Guiffy software, the results shows us that the effect of tunnel hole exceeds to almost 2.1-2.3 diameter above the existing tunnel (Figure 5.48).

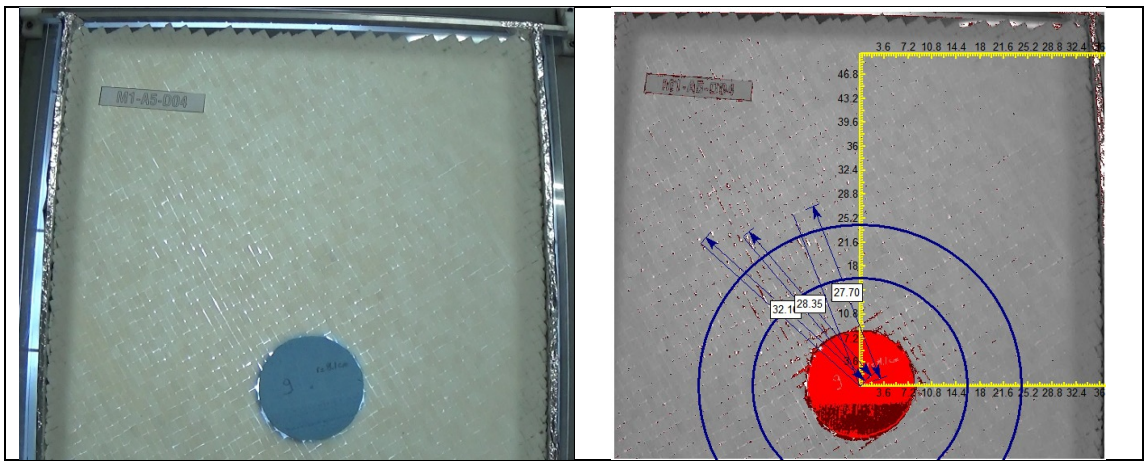

Figure 5.48 A5D04 α5 = 60° with respect to horizontal

The model#32 was 60 degrees with horizontal (α=60°) where the tunnel diameter was enlarged to eight times the width of the discrete model material. By help of Guiffy software, the results shows us that the effect of tunnel hole exceeds to almost 2.4-3.0 diameter above the existing tunnel (Figure 5.49).

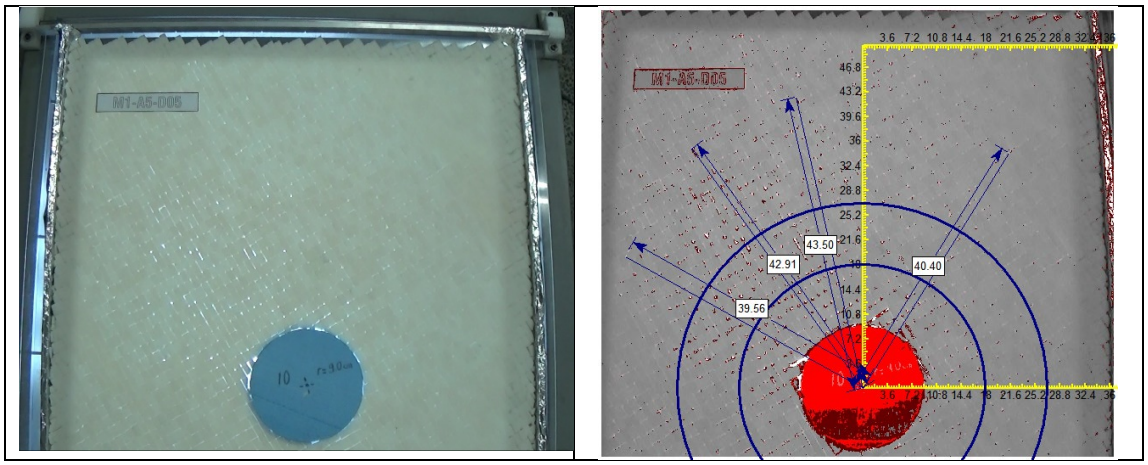

Figure 5.49. A5D05 α5 = 60° with respect to horizontal

The model#33 was 60 degrees with horizontal (s=60°) where the tunnel diameter was enlarged to eight times the width of the discrete model material. By help of Guiffy software, the results shows us that the effect of tunnel hole exceeds to almost 3.2-3.7 diameter above the existing tunnel (Figure 5.50).

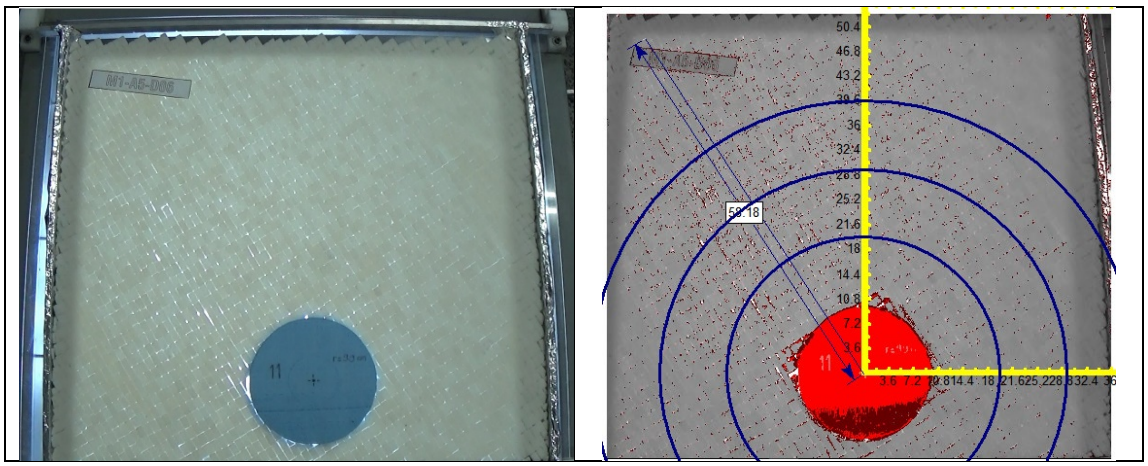

Figure 5.50. A5D06 α5 = 60° with respect to horizontal

The model#34 was 60 degrees with horizontal (α=60°) where the tunnel diameter was enlarged to eight times the width of the discrete model material. By help of Guiffy software, the results shows us that the effect of tunnel hole exceeds to almost 4.5-4.8 diameter above the existing tunnel (Figure 5.51).

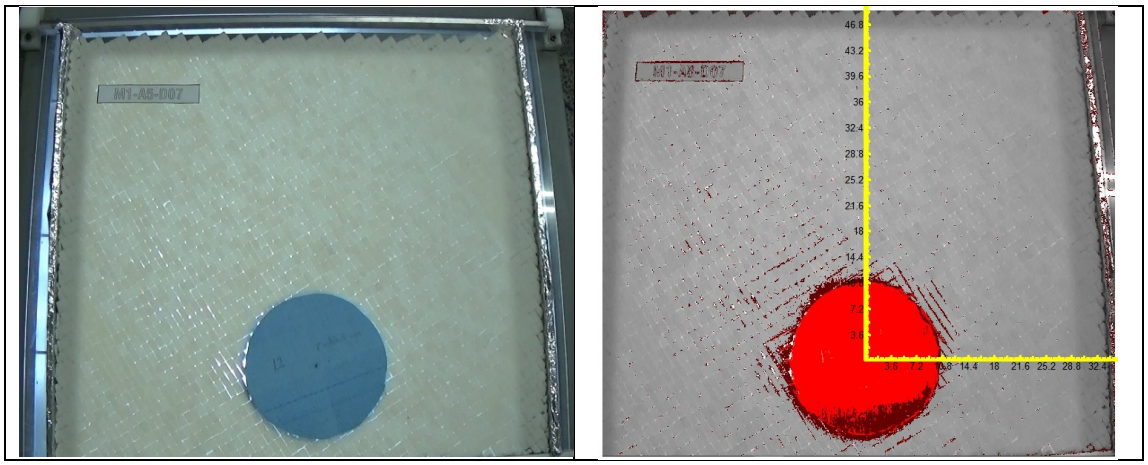

Figure 5.51. A5D07 α5 = 60° with respect to horizontal

The model#35 was 60 degrees with horizontal (α=60°) where the tunnel diameter was enlarged to eight times the width of the discrete model material. By help of Guiffy software, the results shows us that the effect of tunnel hole exceeds to almost 2.1-2.3 diameter above the existing tunnel (Figure 5.52).

The fifth set results (interaction vs the number of joint sets) with 60 degrees are also plotted below. Like other sets, it seems it has almost the same form of inclination when compared to first four sets results. Model#35 was taken out of the graph because of an undefined failure observation in model.

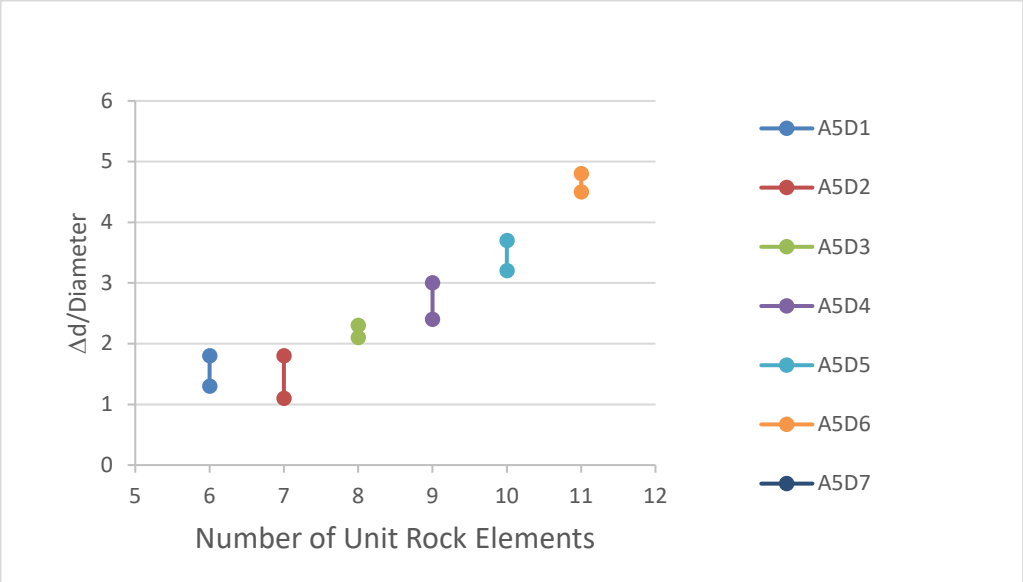

Figure 5.52. Initial evaluation of interaction of fifth set (α=60°) (7 tests)

Sixth seven sets of models were with 75 degrees from horizontal (α=75°) where the diameter of the tunnel increases also as in first set with respect to numbers of model material width (six times to 12 times of the width of bricks (joint sets))

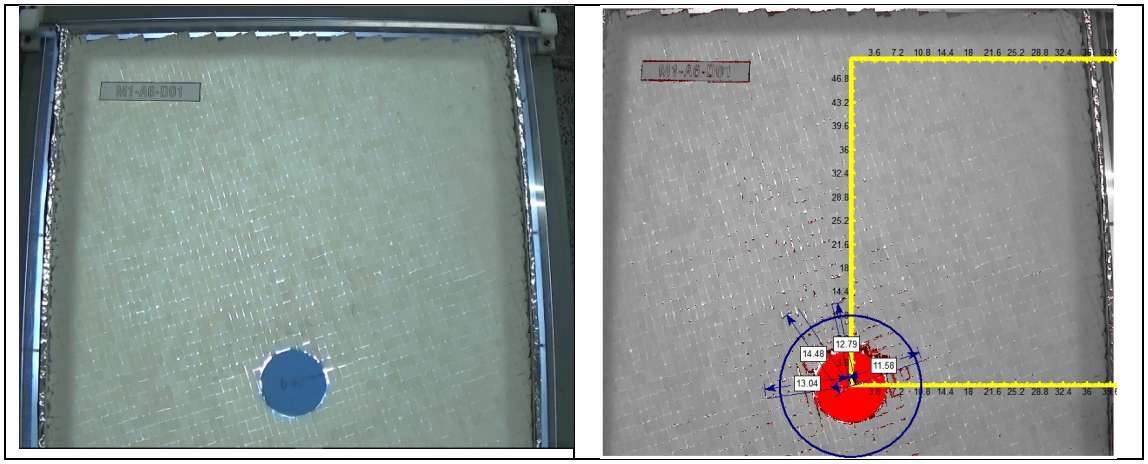

Figure 5.53. A6D01 α6 = 75° with respect to horizontal

The model#36 was 75 degrees with horizontal (α=75°) where the tunnel diameter was enlarged to six times the width of the discrete model material. By help of Guiffy software, the results shows us that the effect of tunnel hole exceeds to almost 1.0-1.3 diameter above the existing tunnel (Figure 5.54).

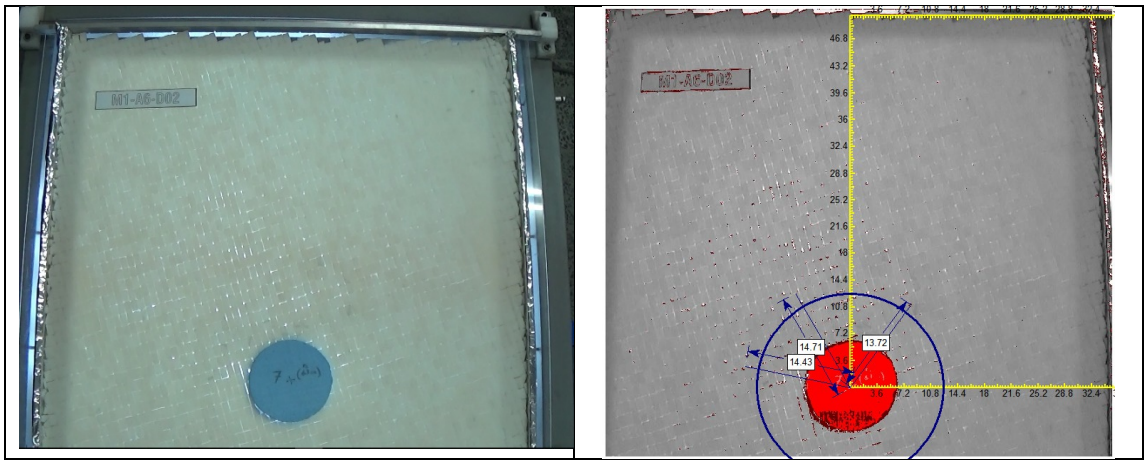

Figure 5.54. A6D02 α6 = 75° with respect to horizontal

The model#37 was 75 degrees with horizontal (α=75°) where the tunnel diameter was enlarged to seven times the width of the discrete model material. By help of Guiffy software, the results shows us that the effect of tunnel hole exceeds to almost 1.1-1.4 diameter above the existing tunnel (Figure 5.55).

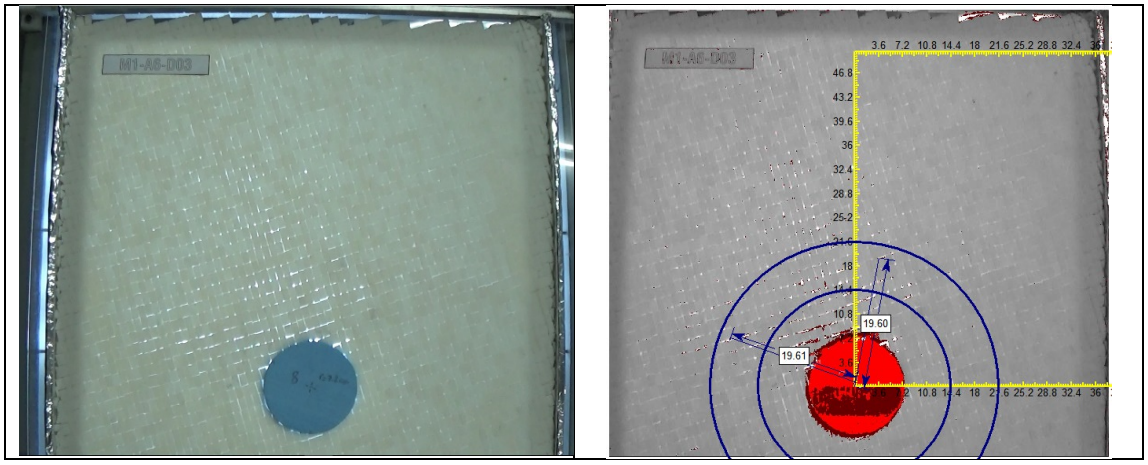

Figure 5.55. A6D03 α6 = 75° with respect to horizontal

The model#36 was 75 degrees with horizontal (α=75°) where the tunnel diameter was enlarged to eight times the width of the discrete model material. By help of Guiffy software, the results shows us that the effect of tunnel hole exceeds to almost 1.6-1.8 diameter above the existing tunnel (Figure 5.56).

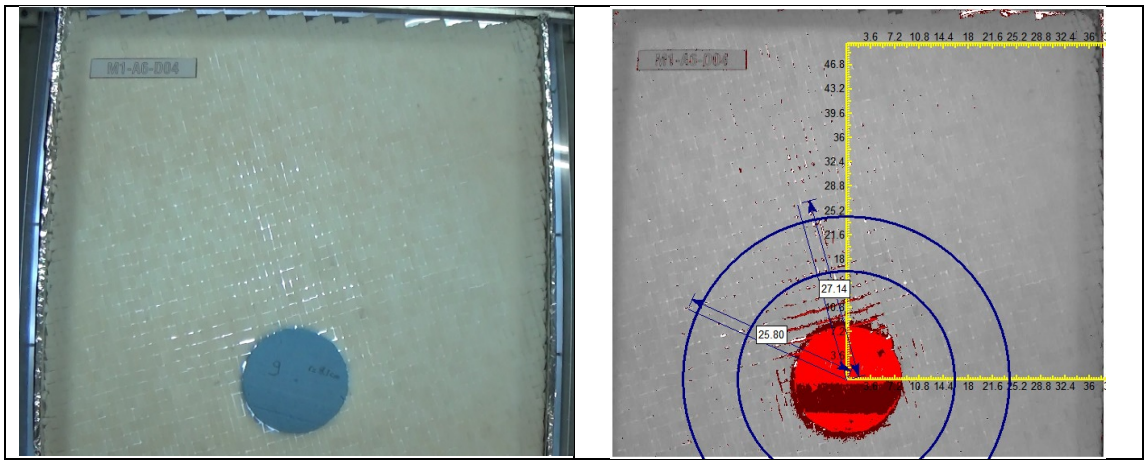

Figure 5.56. A6D04 α6 = 75° with respect to horizontal

The model#39 was 75 degrees with horizontal (α=75°) where the tunnel diameter was enlarged to nine times the width of the discrete model material. By help of Guiffy software, the results shows us that the effect of tunnel hole exceeds to almost 2.1-2.3 diameter above the existing tunnel (Figure 5.57).

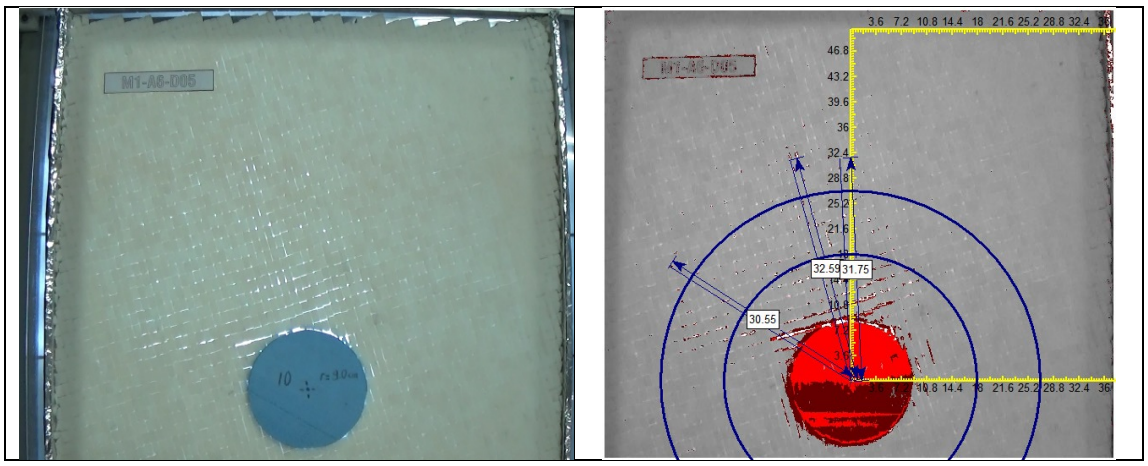

Figure 5.57. A6D05 α6 = 75° with respect to horizontal

The model#40 was 75 degrees with horizontal (α=75°) where the tunnel diameter was enlarged to ten times the width of the discrete model material. By help of Guiffy software, the results shows us that the effect of tunnel hole exceeds to almost 2.3-2.6 diameter above the existing tunnel (Figure 5.58).

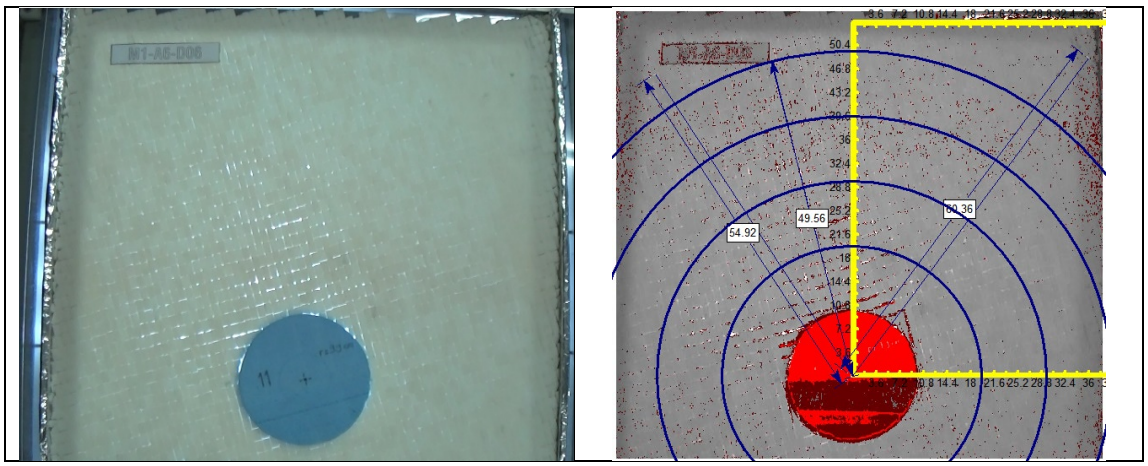

Figure 5.58. A6D06 α6 = 75° with respect to horizontal

The model#41 was 75 degrees with horizontal (α=75°) where the tunnel diameter was enlarged to eleven times the width of the discrete model material. By help of Guiffy software, the results shows us that the effect of tunnel hole exceeds to almost 3.9-4.0 diameter above the existing tunnel (Figure 5.59).

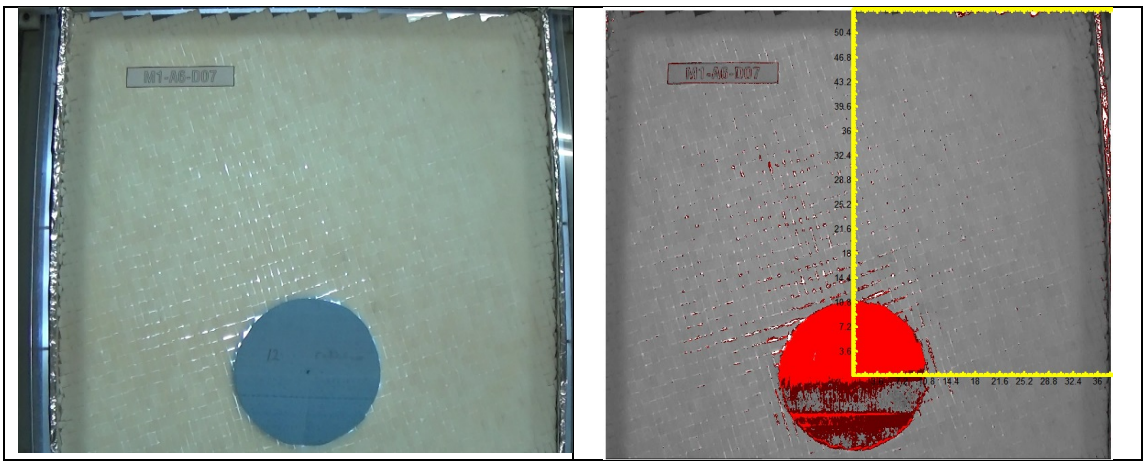

Figure 5.59. A6D07 α6 = 75° with respect to horizontal

The model#42 was 75 degrees with horizontal (α=75°) where the tunnel diameter was enlarged to twelve times the width of the discrete model material. By help of Guiffy software, the results shows us that the effect of tunnel hole exceeds to almost 1.6-1.8 diameter above the existing tunnel (Figure 5.60).

The sixth set results (interaction vs the number of joint sets) with 75 degrees are also given below. Compared to first five sets results it seems it has almost the same form of inclination except last model.

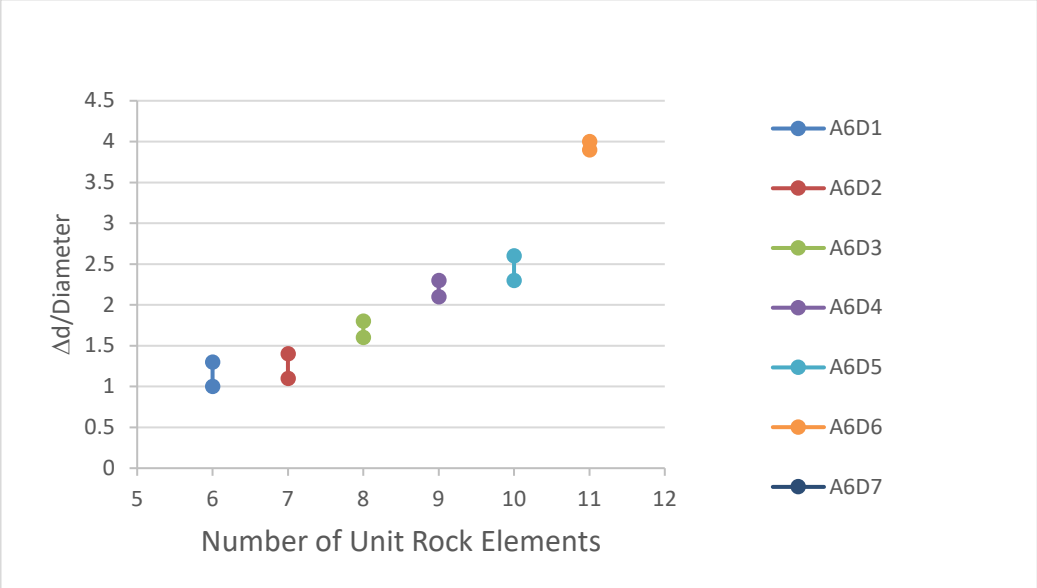

Figure 5.60. Initial evaluation of interaction of sixth set (α=75°) (7 tests)

Seventh seven sets of models were with 90 degrees from horizontal (α=90°) where the diameter of the tunnel increases also as in first set with respect to numbers of model material width (six times to 12 times of the width of bricks (joint sets))

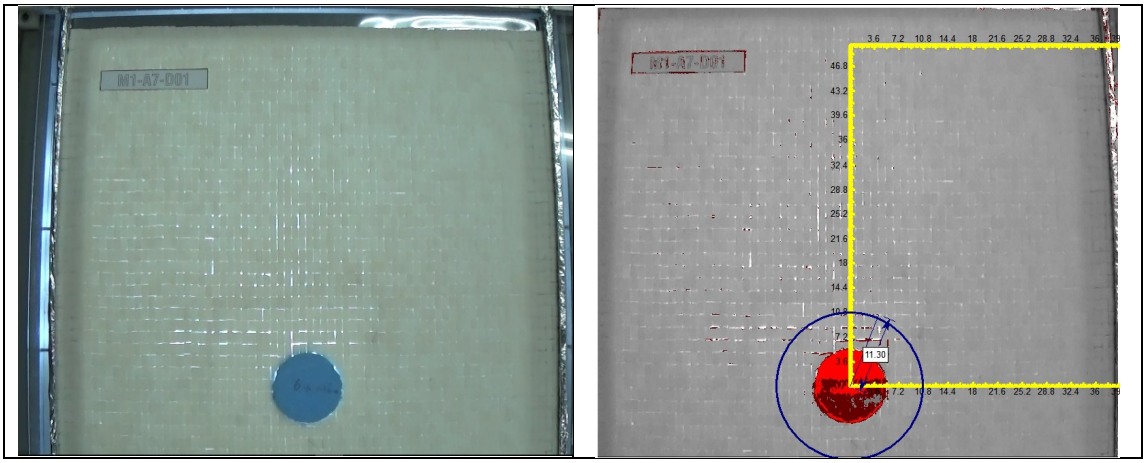

Figure 5.61. A7D01 α7 = 90° with respect to horizontal

The model#43 was 90 degrees with horizontal (α=90°) where the tunnel diameter was enlarged to six times the width of the discrete model material. By help of Guiffy software, the results shows us that the effect of tunnel hole exceeds to almost 0.8-1.1 diameter above the existing tunnel (Figure 5.62).

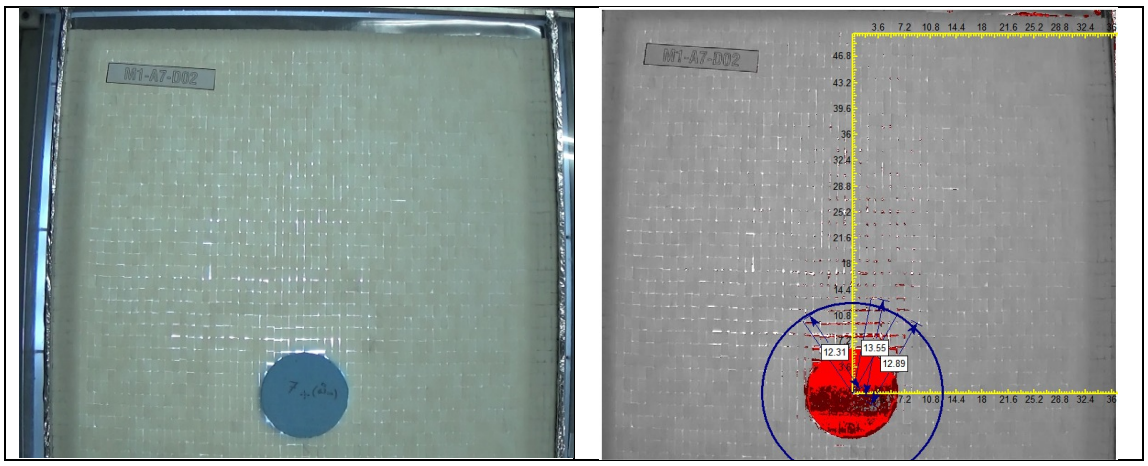

Figure 5.62. A7D02 α7 = 90° with respect to horizontal

The model#44 was 90 degrees with horizontal (α=90°) where the tunnel diameter was enlarged to seven times the width of the discrete model material. By help of Guiffy software, the results shows us that the effect of tunnel hole exceeds to almost 0.9-1.2 diameter above the existing tunnel (Figure 5.63).

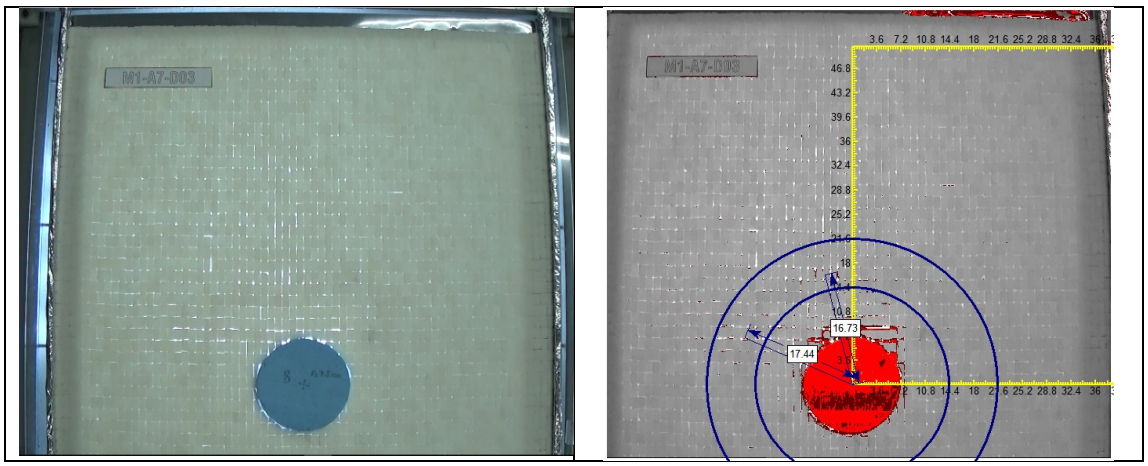

Figure 5.63. A7D03 α7 = 90° with respect to horizontal

The model#45 was 90 degrees with horizontal (α=90°) where the tunnel diameter was enlarged to eight times the width of the discrete model material. By help of Guiffy software, the results shows us that the effect of tunnel hole exceeds to almost 1.2-1.4 diameter above the existing tunnel (Figure 5.64).

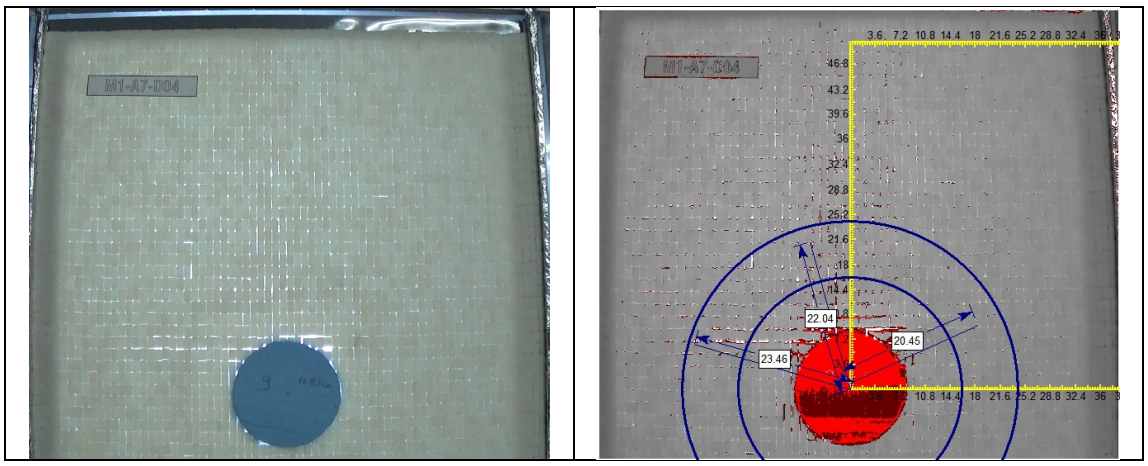

Figure 5.64. A7D04 α= 90° with respect to horizontal

The model#46 was 90 degrees with horizontal (α=90°) where the tunnel diameter was enlarged to nine times the width of the discrete model material. By help of Guiffy software, the results shows us that the effect of tunnel hole exceeds to almost 1.4-1.8 diameter above the existing tunnel (Figure 5.65).

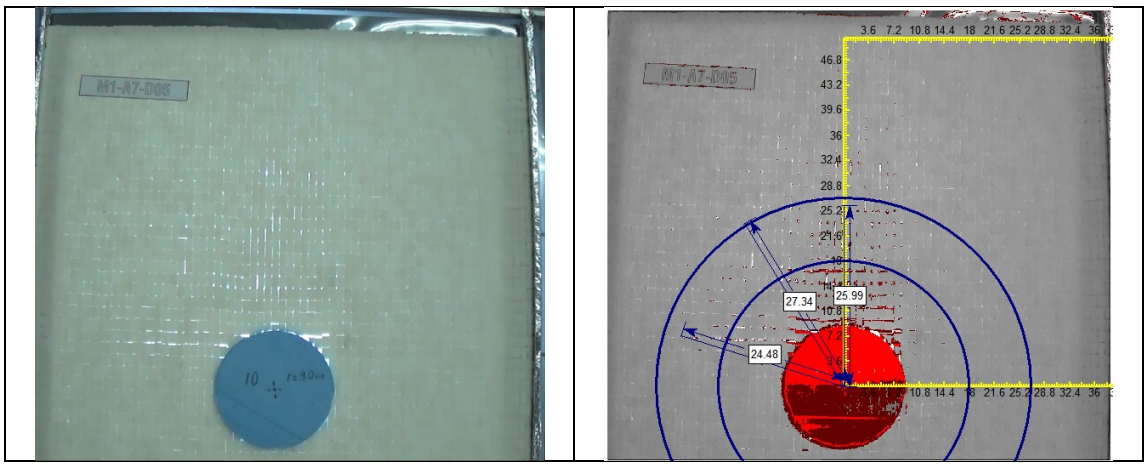

Figure 5.65. A7D05 α7 = 90° with respect to horizontal

The model#47 was 90 degrees with horizontal (α=90°) where the tunnel diameter was enlarged to ten times the width of the discrete model material. By help of Guiffy software, the results shows us that the effect of tunnel hole exceeds to almost 1.6-2.0 diameter above the existing tunnel (Figure 5.64).

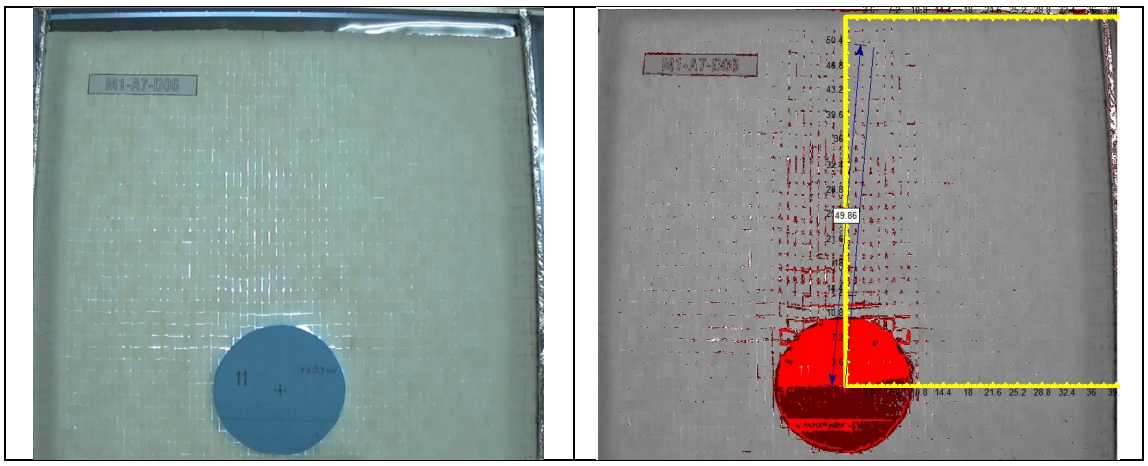

Figure 5.66. A7D06 α7 = 90° with respect to horizontal

The model#48 was 90 degrees with horizontal (α=90°) where the tunnel diameter was enlarged to eleven times the width of the discrete model material. By help of Guiffy software, the results shows us that the effect of tunnel hole exceeds to almost 2.5-2.8 diameter above the existing tunnel (Figure 5.67).

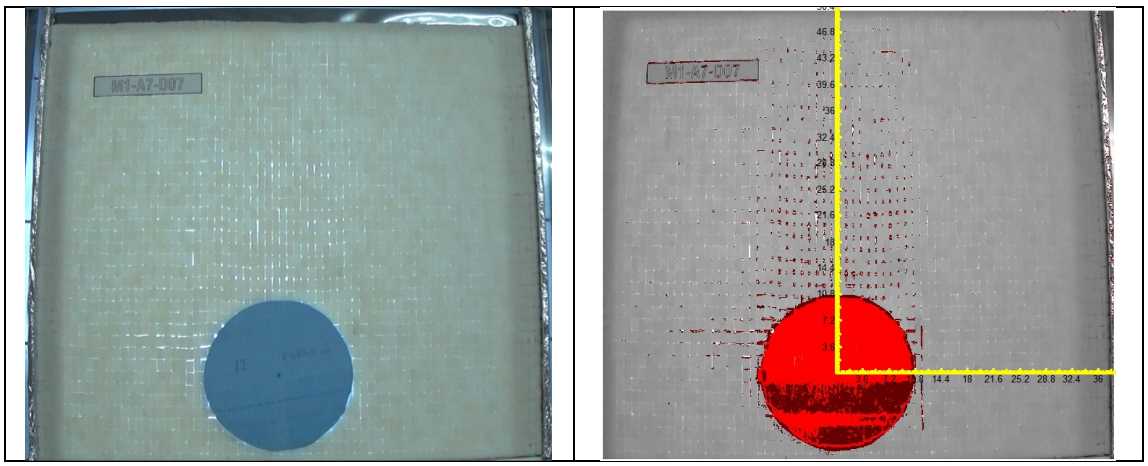

Figure 5.67. A7D07 α7 = 90° with respect to horizontal

The model#49 was 90 degrees with horizontal (α=90°) where the tunnel diameter was enlarged to twelve times the width of the discrete model material. By help of Guiffy software, the results shows us that the effect of tunnel hole exceeds to almost 2.5-3.2 (ground surface limit) diameter above the existing tunnel (Figure 5.68).

The last (seventh) set results (interaction vs the number of joint sets) with 90 degrees are also given below. It can be seen that with increasing number of unit rock elements at heading, the influence zone also exceeds with a nonlinear (exponential) function. This shall be evaluated in Part 6 Results.

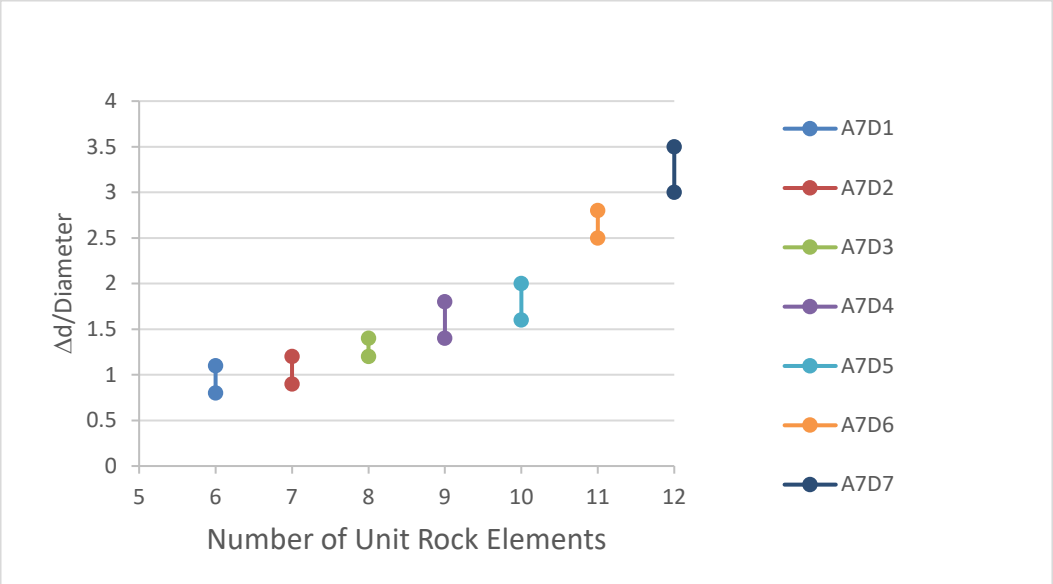

Figure 5.68. Initial evaluation of interaction of seventh set (α=90°) (7 tests)

The brief results are given as a graph in Figure 5.70 for all orientation angles. The graph indicates that sixty degrees of dip angles have the biggest effect on the influence zone with same number of joint systems at tunnel crown area.

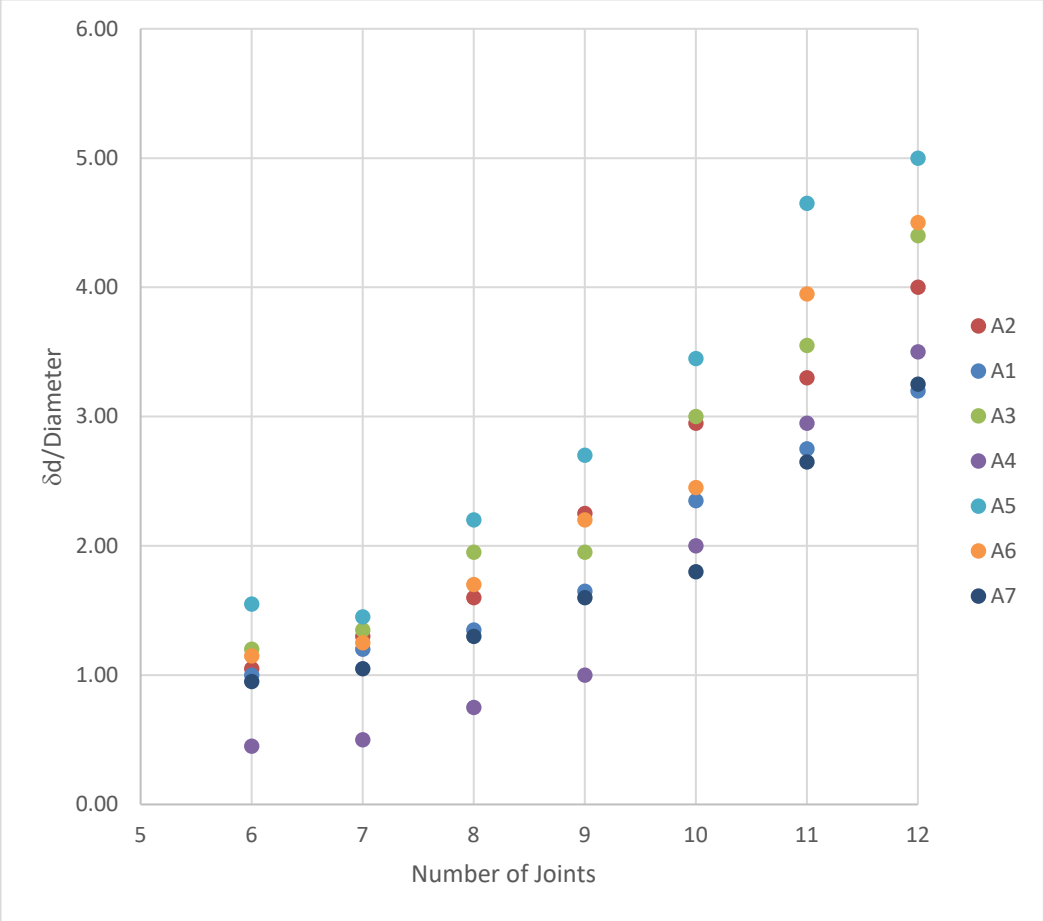

Figure 5.69. total results with respect to orientation angles

5.2. Numerical Models

The results of the physical models have been calibrated by 2D Finite Element Analysis Software by Rocscience RS2 in two-dimensional plane strain conditions. The software allows user to define three different joints in different angles. These joints are names as ubiquitous joint sets in the software.

Parallel deterministic joint model was selected with two joint sets same as applied in physical modelling. The material was accepted as elastic since the model material was selected to be elastic during tests.

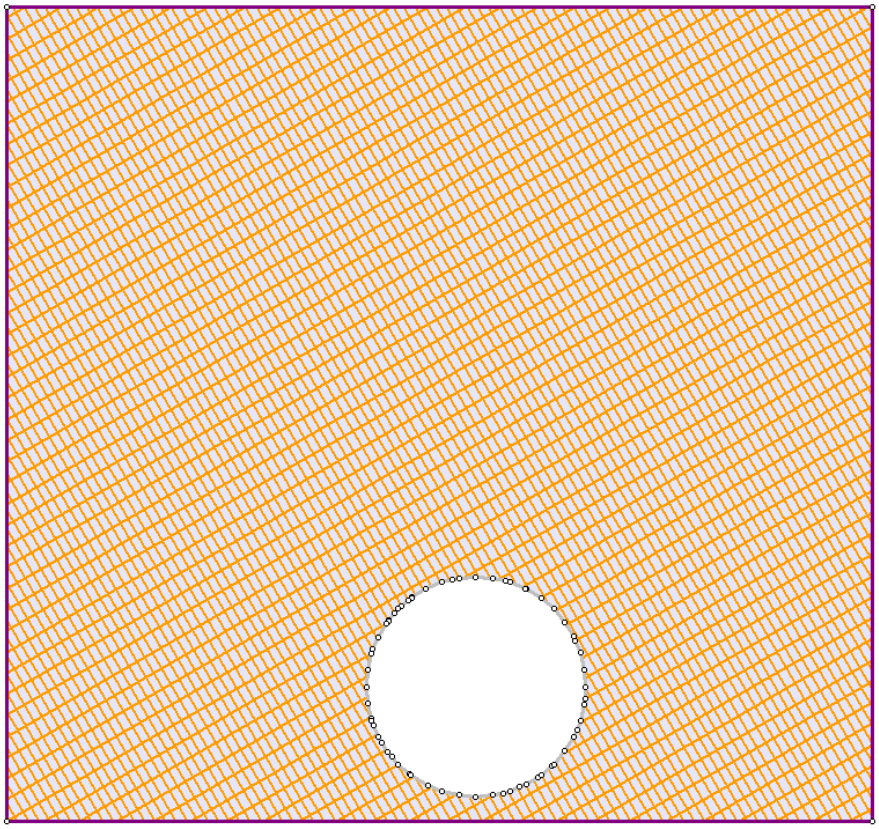

Figure 5.70. Sample joint orientation used in Phase2 software

Forty-nine models (7 diameters with seven different joint dip angles) were prepared in the software. The peak friction angle was taken as forty degrees (which represents friction angle of sugar bricks as tested with direct shear test) in Mohr Coulomb slip criterion. 1.8 x 0.9 m joint geometry was used as in the physical models where the diameter of the tunnel also increased with parallel to physical model. Diameter of tunnel structure was selected to represent minimum 6 number of joints as minimum where it was expanded to a 12 joint jets at the crown. That concludes a tunnel diameter starting from 10.6 m to 21.6 m

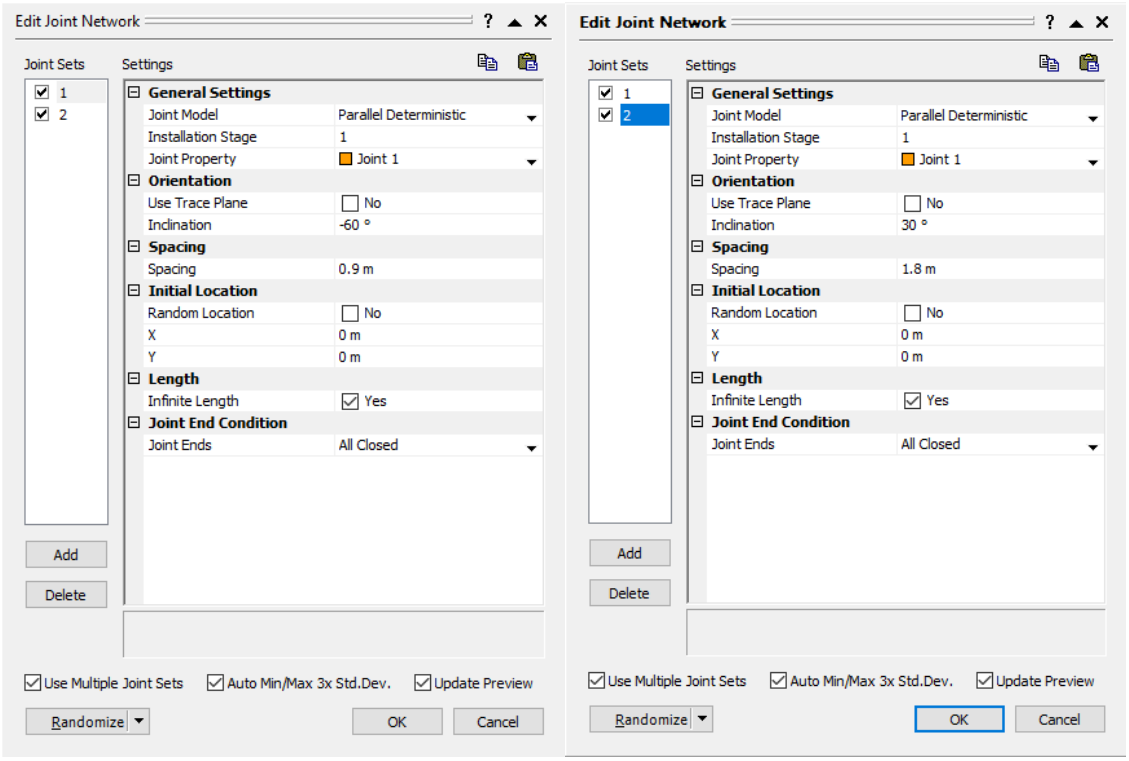

Figure 5.71. Input for joint geometry

The result of strains was not used in evaluation since the main idea was to build a dimensionless ratio for the influence zone for tunneling. Influence zone were considered to be at the edges of strength factor 1.0 and evaluated accordingly. The post behavior of physical models is used for the influence zone where it coincides almost with numerical model studies. Furthermore, the strength reduction factor of joints is evaluated that critical factor of safety was taken around “1” unity for joint movements. It must be noted that in some cases (especially in bigger diameters) the model boundaries needed to be extended.

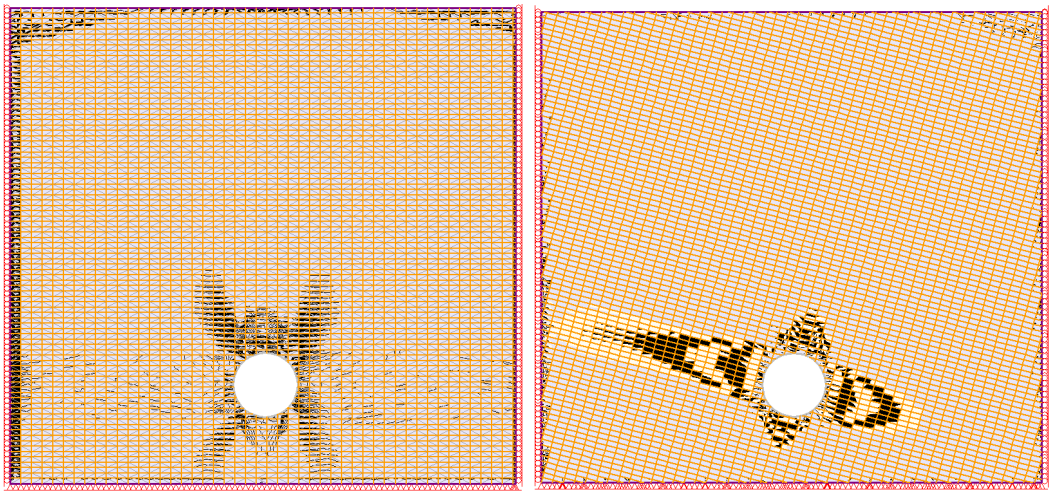

Figure 5.72. D1A1 and D1A2 strength factors FS<1.1

It is observed from Figure 5.73 that the angle of anisotropy effects the tunnel zone unsymmetrically. This behavior is almost parallel to the physical models.

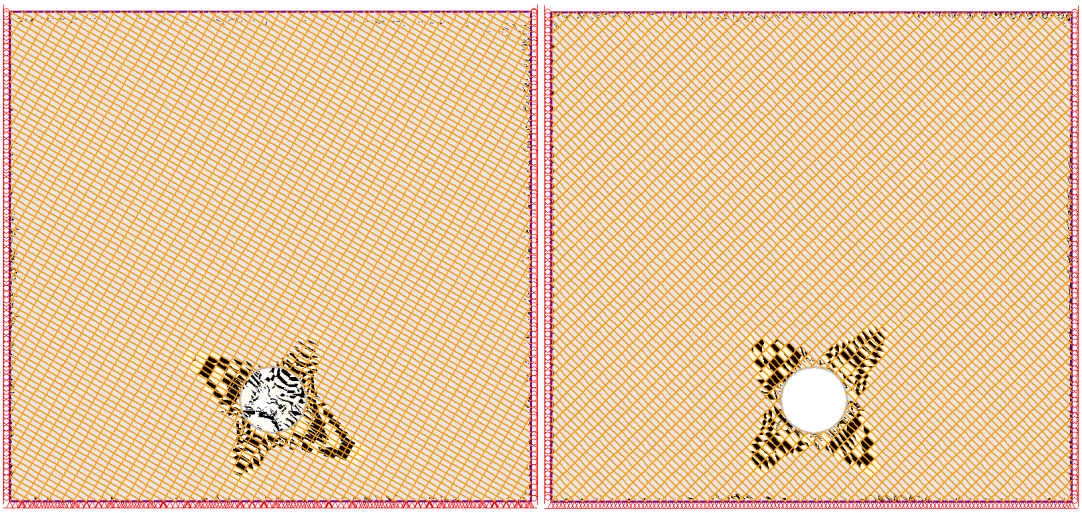

Figure 5.73. D1A3 and D1A4 strength factors FS<1.1

Figure 5.74 is 30 and 45 degrees where also same type of unsymmetrical behavior flashed. It is also observed that 45 degrees have the minimum effected zone

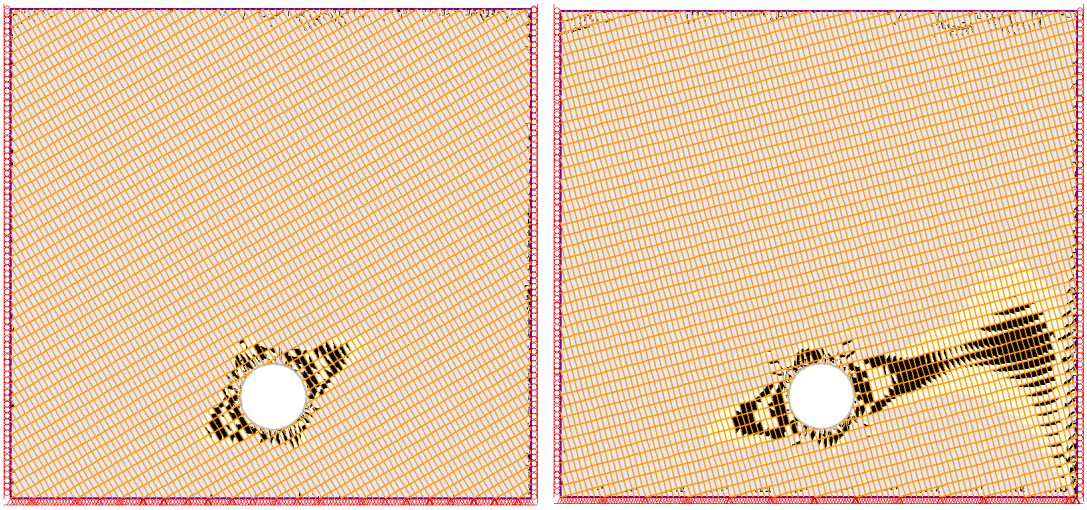

Figure 5.74. D1A5 and D1A6 strength factors FS<1.1

Figure 5.75 and Figure 5.76 are for 60, 75 and 90 degrees for horizontal layering (α= 0 degrees)

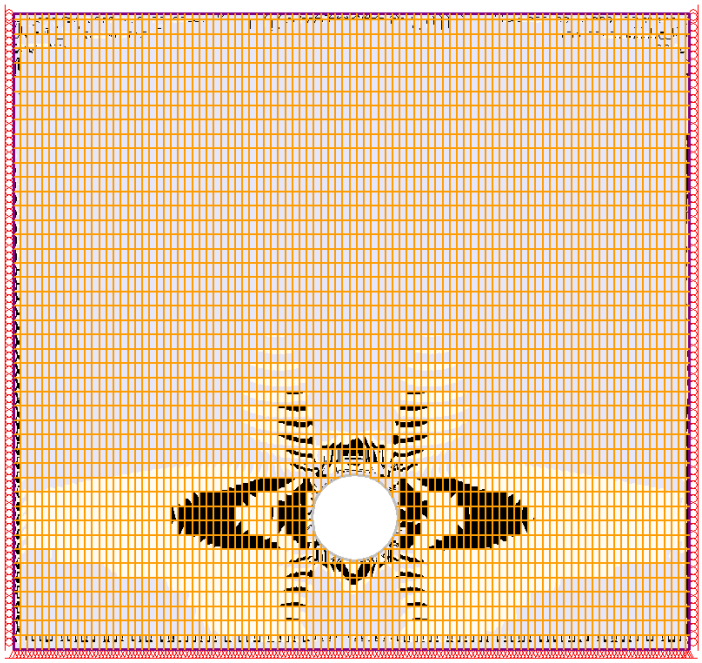

Figure 5.75. D1A7 strength factors FS<1.1

It is concluded that the results from D1A1 to D7A7 have a limited influence area where 45 degrees seems the tightest zone around it.

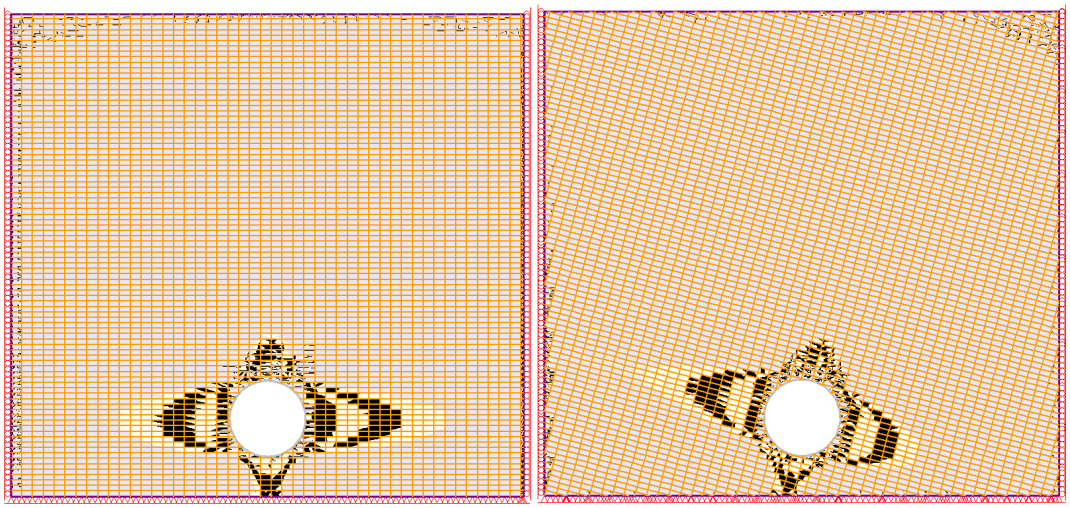

Figure 5.76. D2A1 and D2A2 strength factors FS<1.1

Second set of numerical analysis were run for bigger diameter (Diameter 2) and same type of anisotropy was also observed (Figure 5.77 & Figure 5.78).

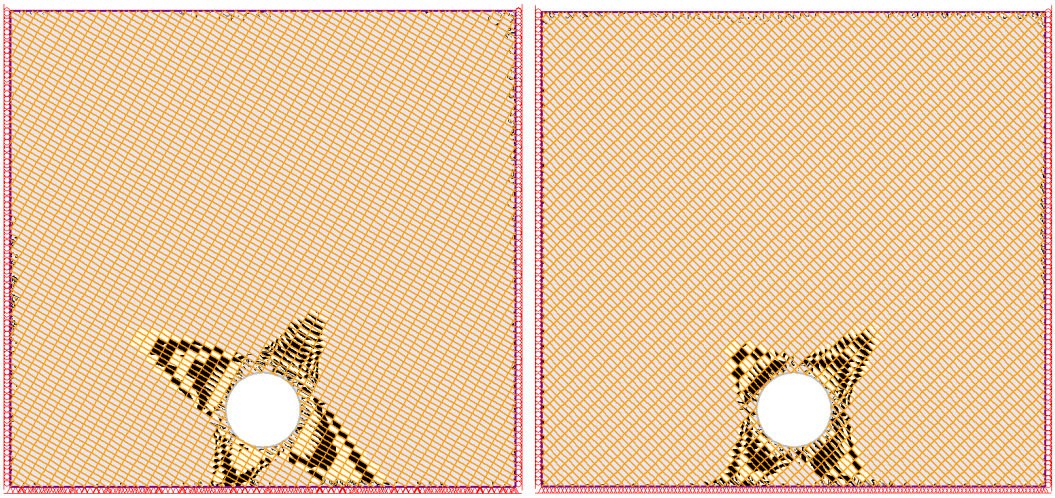

Figure 5.77. D2A3 and D2A4 strength factors FS<1.1

The boundary zone of the tunnel with respect to model seems effective in adjacent areas where the upper part has the same type of trend compared to first set of diameter models.

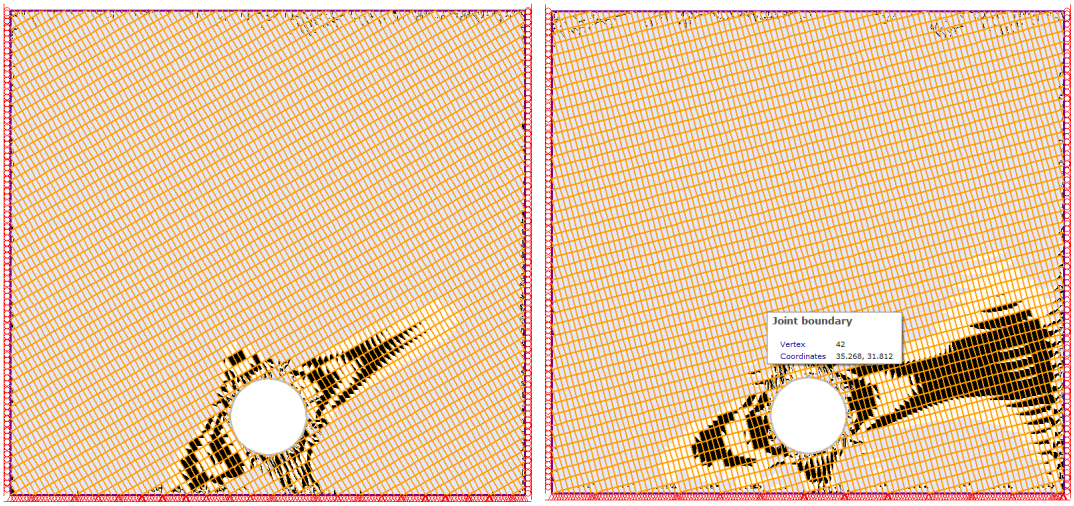

Figure 5.78. D2A5 and D2A6 strength factors FS<1.1

Joint orientation angle of 60 degrees interpreted a big zone of influence where 75 degrees also have numerical constraints compared to sixty degrees (Figure 5.79).

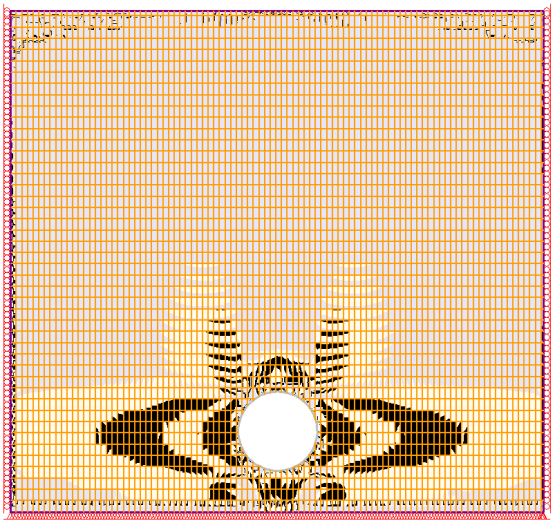

Figure 5.79. D2A7 strength factors FS<1.1

The ninety degrees angle of orientation has some interesting outputs where the numerical model stress state can affect the results (Figure 5.80).

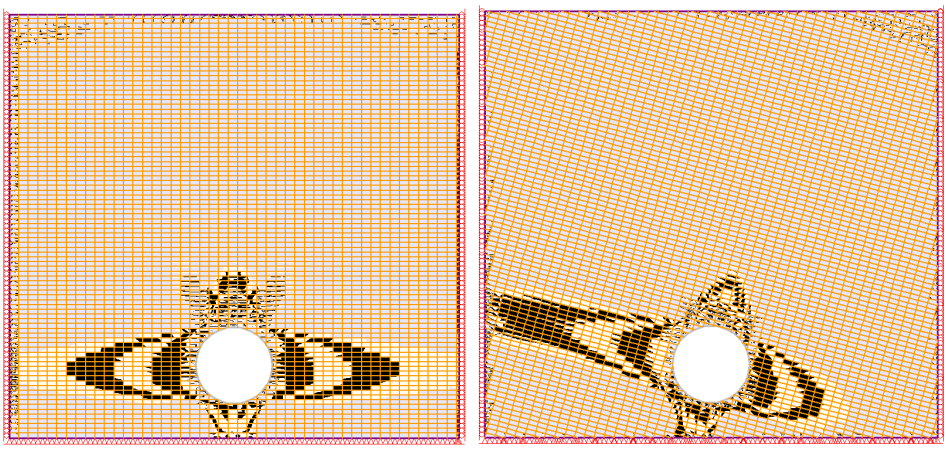

Figure 5.80. D3A1 and D3A2 strength factors FS<1.1

With increasing diameter (dia#3) the influence zones are growing faster compared to smaller diameters (Figure 5.81).

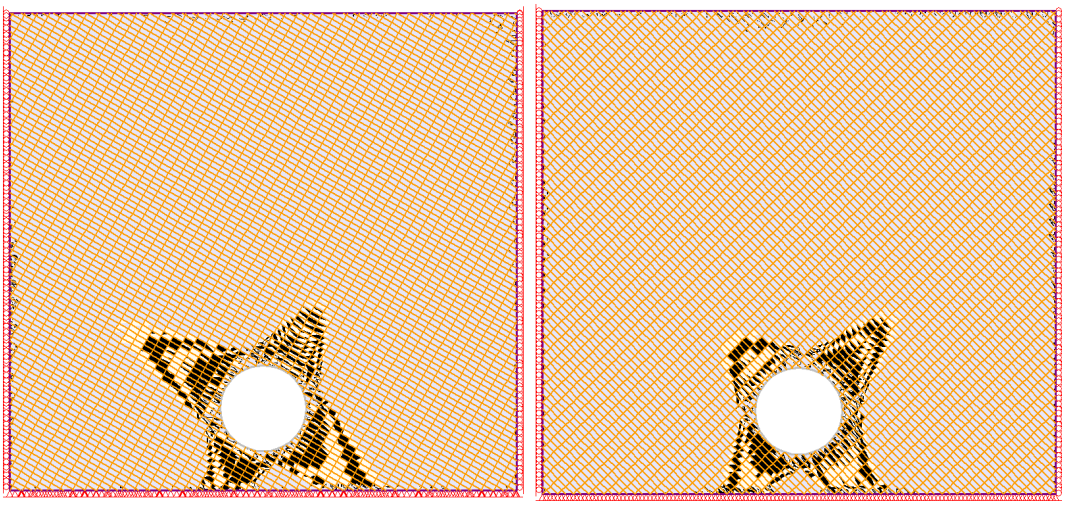

Figure 5.81. D3A3 and D3A4 strength factors FS<1.1

Forty-five degrees of joint orientation seems again the lowest affected zone (Figure 5.82).

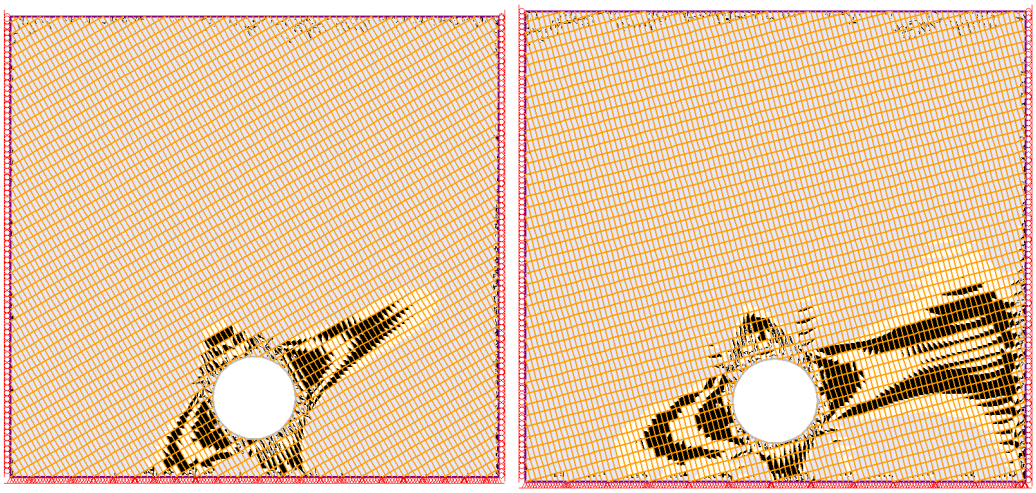

Figure 5.82 D3A5. and D3A6 strength factors FS<1.1

75 degrees of joint orientation have a different behavior when compared to other inclinations (Figure 5.83).

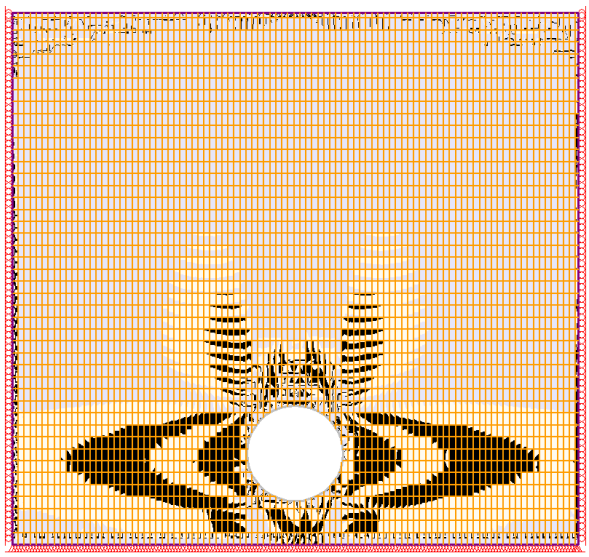

Figure 5.83. D3A7 strength factors FS<1.1

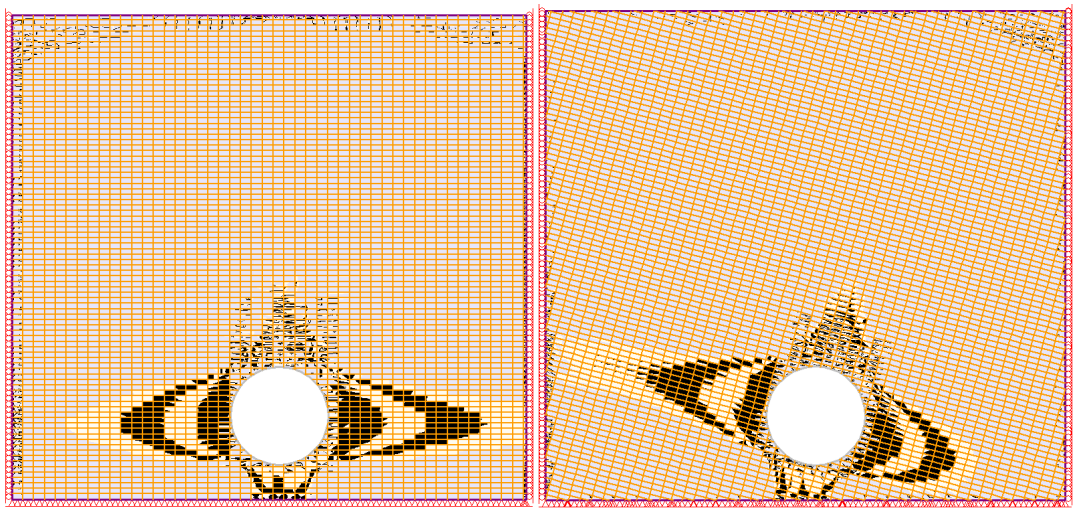

Figure 5.84. D4A1 and D4A2 strength factors FS<1.1

Diameter#4 tunnel has been a bit more effected in numerical analysis (Figure 5.84 & Figure 5.85)

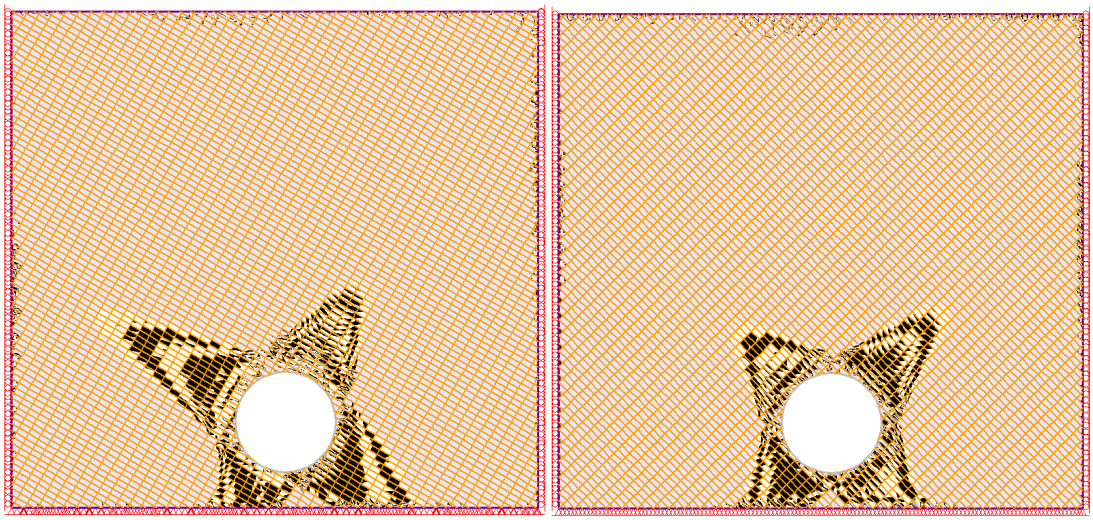

Figure 5.85. D4A3 and D4A4 strength factors FS<1.1

Almost in all cases 45 degrees orientations have the least affected areas as seen in figure on the right (Figure 5.86)

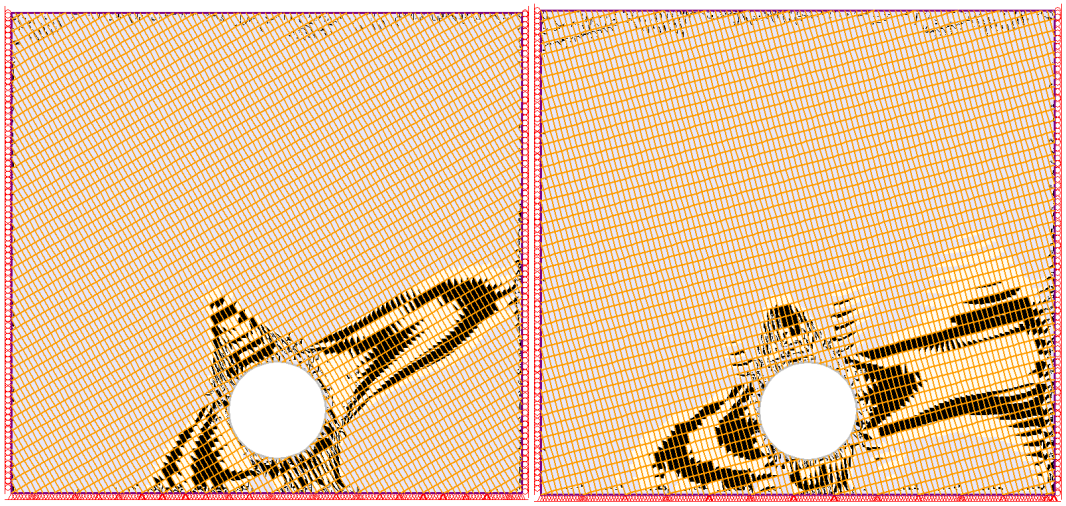

Figure 5.86. D4A5 and D4A6 strength factors FS<1.1

Sixty degrees of joint orientation are resulted in high affected zone where the boundary conditions seem unfair to seventy-five degrees of orientation (Figure 5.87)

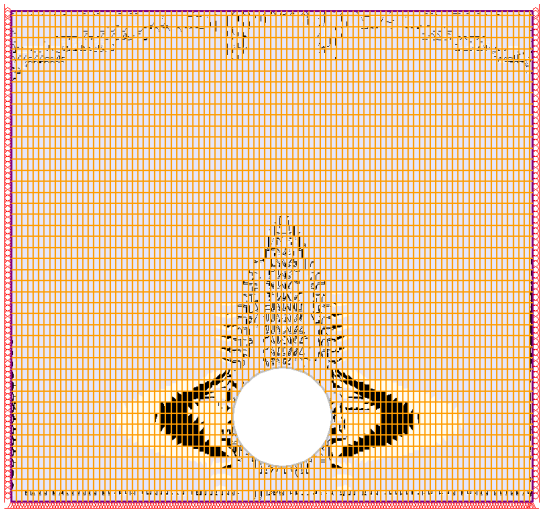

Figure 5.87. D4A7 strength factors FS<1.1

The behavior of upper part of the tunnel seems clearly in increasing diameters in horizontal bedding (Figure 5.88)

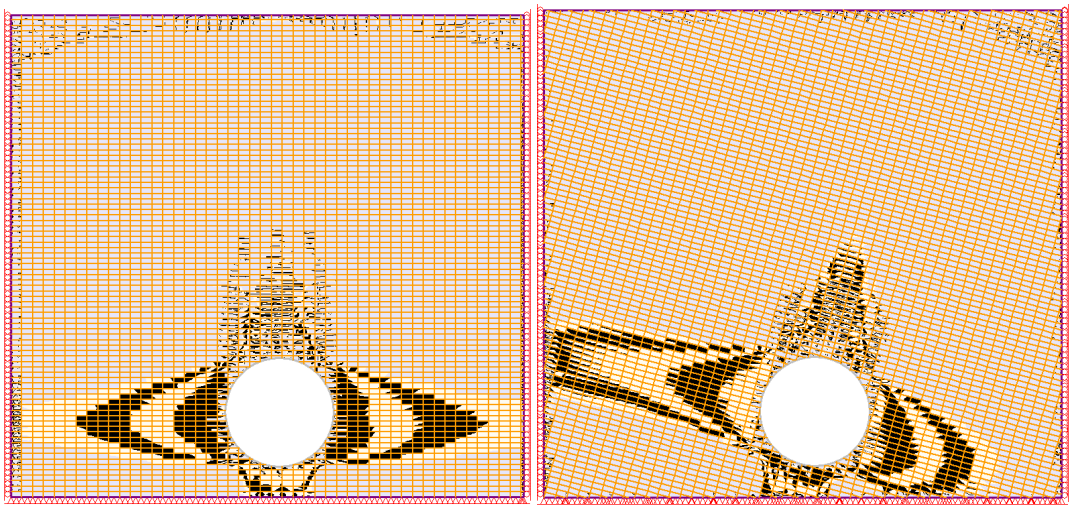

Figure 5.88. D5A1 and D5A2 strength factors FS<1.1

The effect of the increasing diameter reaches to the boundary conditions since it is affected also with orientation of joints (Figure 5.89).

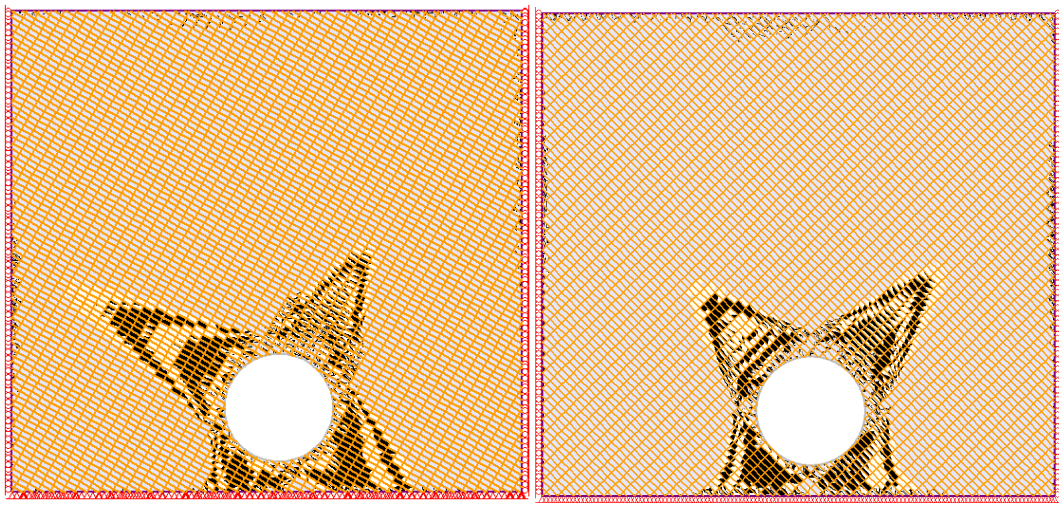

Figure 5.89. D5A3 and D5A4 strength factors FS<1.1

Forty-five degrees of join orientation has same behavior where the effect has been widened by means of tunnel diameter increase (Figure 5.90)

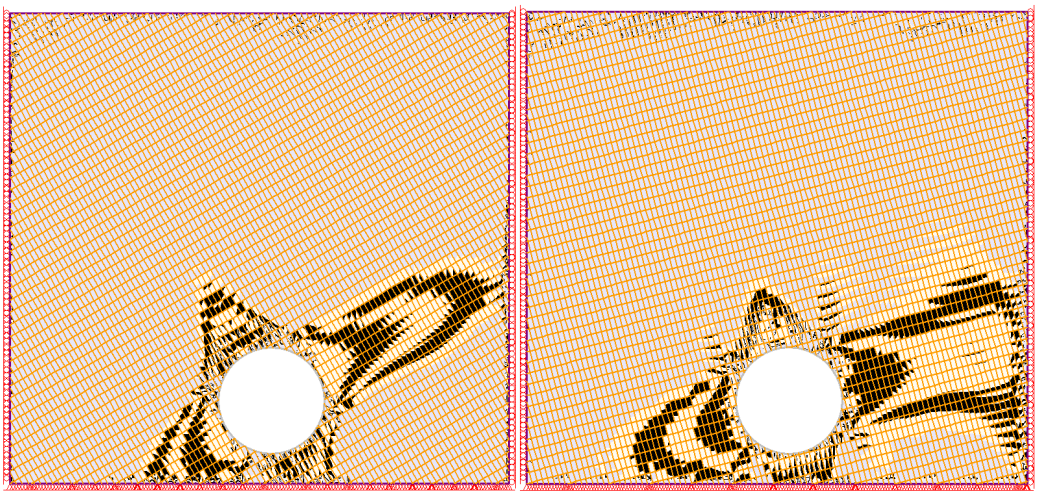

Figure 5.90. D5A5 and D5A6 strength factors FS<1.1

Same type of behavior in sixty- and seventy-five-degrees orientations. The effect can be seen more clearly (Figure 5.91).

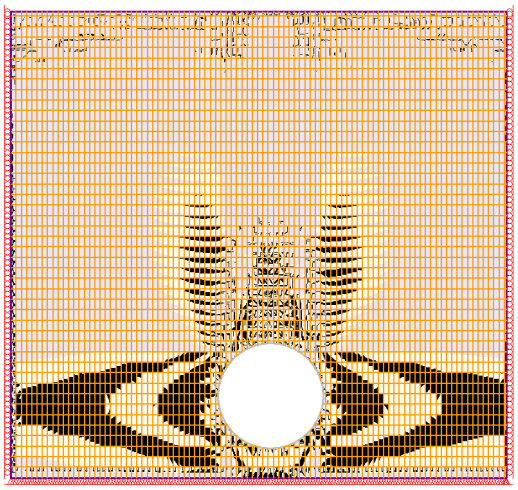

Figure 5.91. D5A7 strength factors FS<1.1

The tremendous increase of ninety degrees influence zone can be evaluated from Figure 5.92

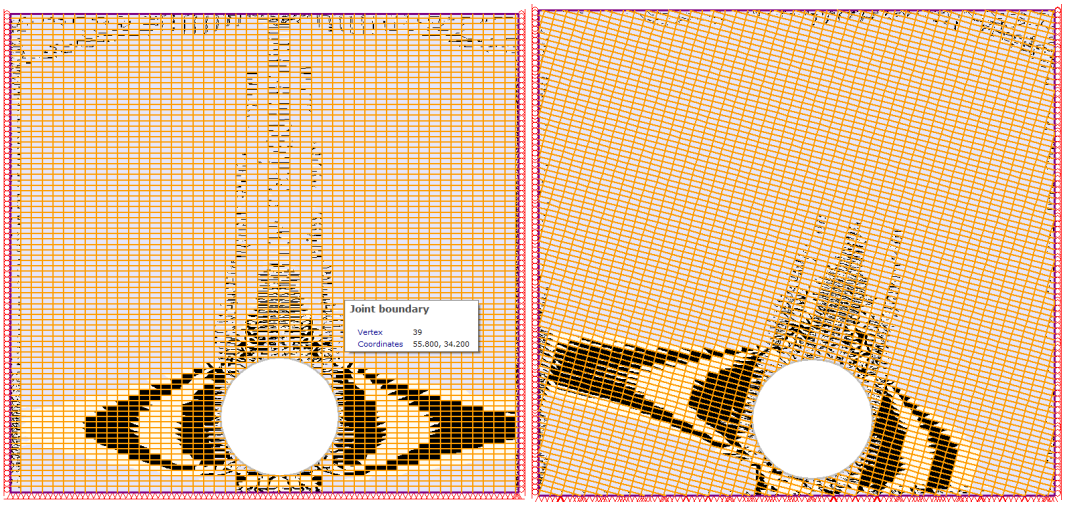

Figure 5.92. D6A1 and D6A2 strength factors FS<1.1

It is clearly observed that the influence zone almost reaches to the boundaries with increasing diameter (diameter#6) (Figure 5.93).

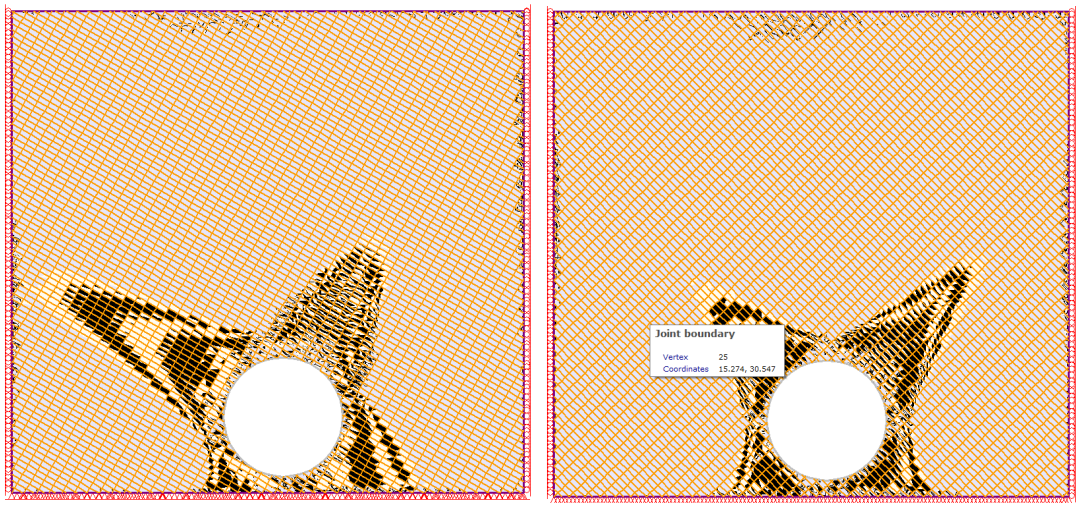

Figure 5.93. D6A3 and D6A4 strength factors FS<1.1

Even in big diameters forty-five degrees have the least affected area (Figure 5.94).

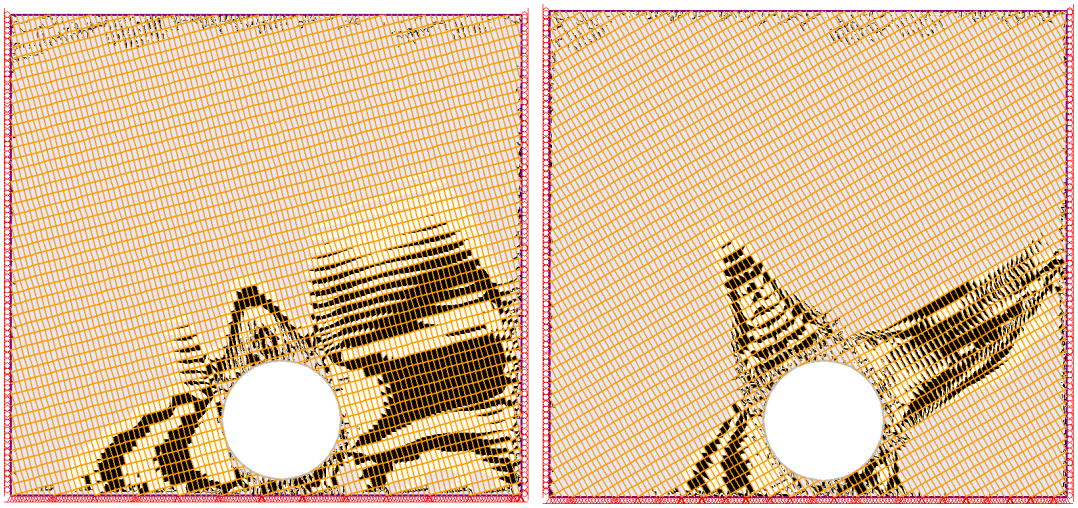

Figure 5.94. D6A5 and D6A6 strength factors FS<1.1

The influence of sixty and seventy-five degrees can be clearly seen from Figure 5.95.

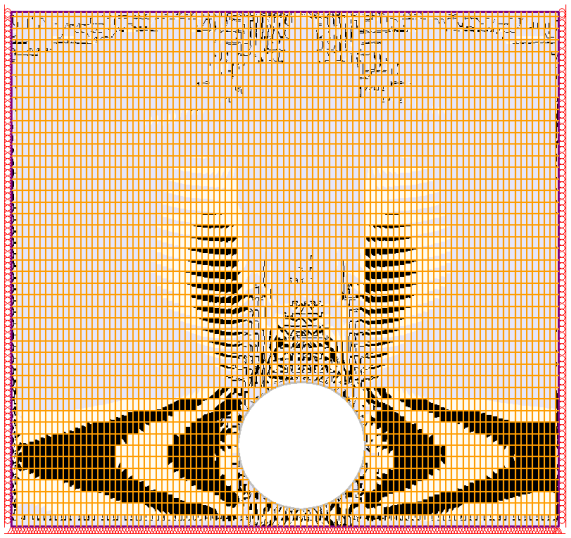

Figure 5.95. D6A7 strength factors FS<1.1

Ninety degrees of orientation is also affected by diameter increase (Figure 5.96)

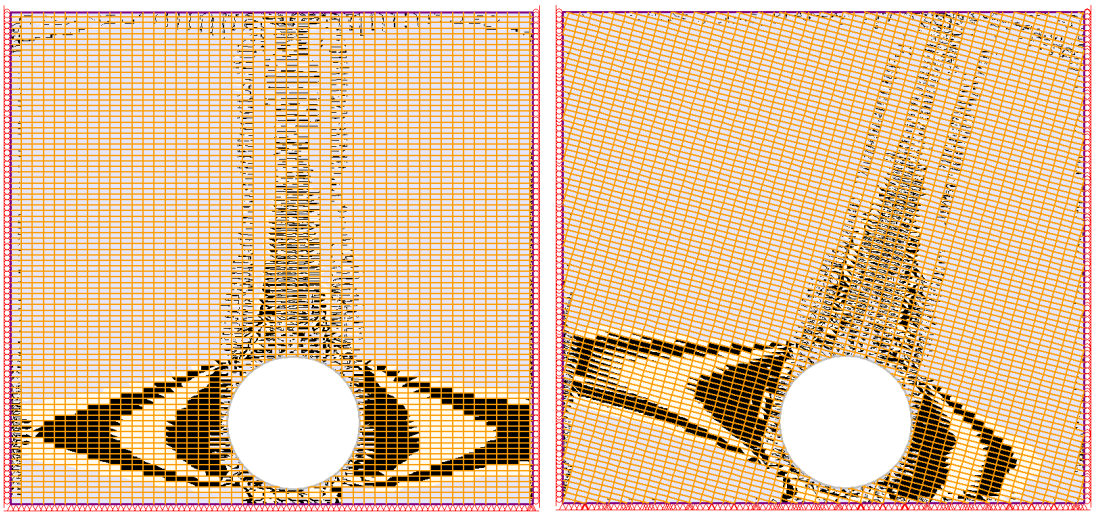

Figure 5.96. D7A1 and D7A2 strength factors FS<1.1

The influence of the biggest diameter is clearly seen even for horizontal orientation. (Figure 5.97).

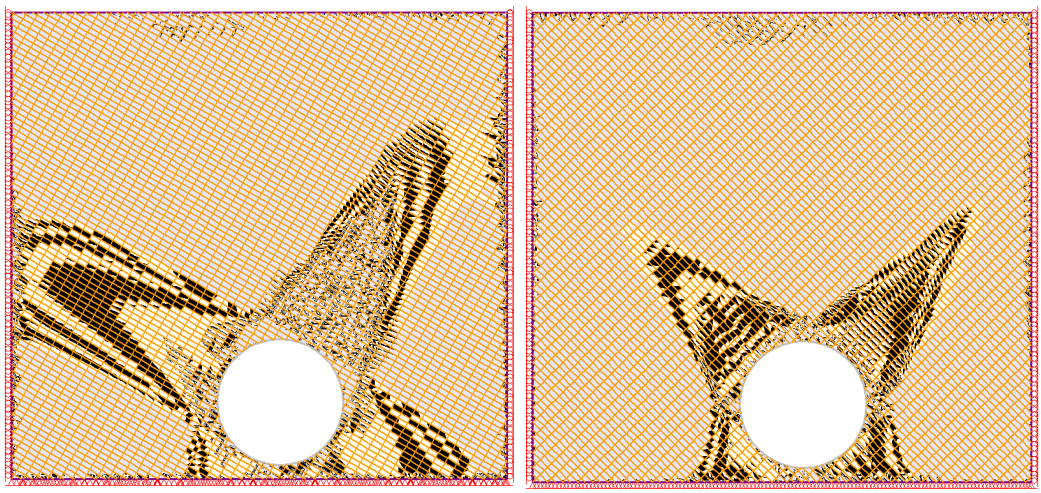

Figure 5.97. D7A3 and D7A4 strength factors FS<1.1

Forty-five degrees has the lowest even in the biggest diameter model (Figure 5.98)

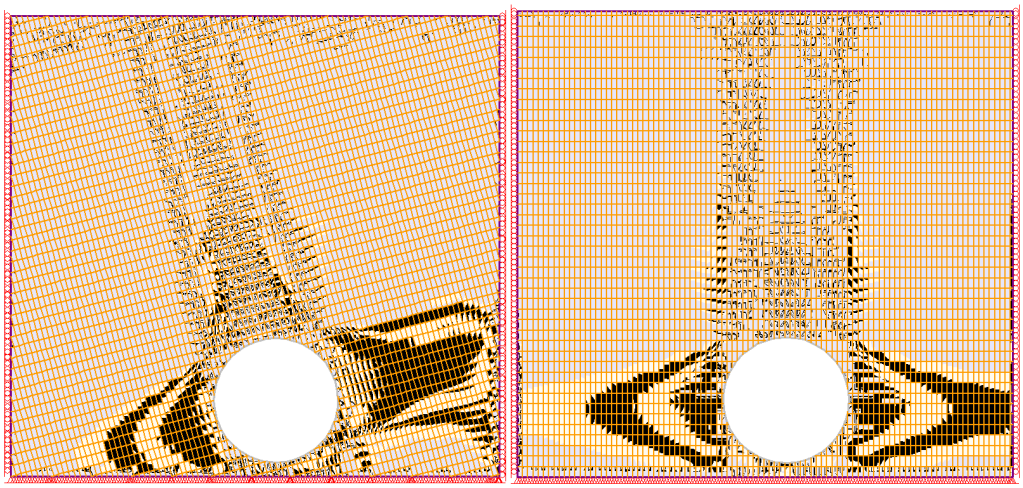

Figure 5.98. D7A6 and D7A7 strength factors FS<1.1

As can be seen from Figure 5.99, the influence zone reaches to its limits and cause a big failure zone that exceeds the upper boundaries.

6 RESULTS

The influenced zone diameters obtained from the overlay difference reports by means of Guiffy software were divided to tunnel diameters at each time to get the dimensionless ratio δd/D (D= Tunnel diameter) as defined in Figure 6.1. Afterwards, these ratios were plotted against the number of unit rock model element and an exponential distribution was achieved. The plots are given below with its standard deviation and best exponential function on it.

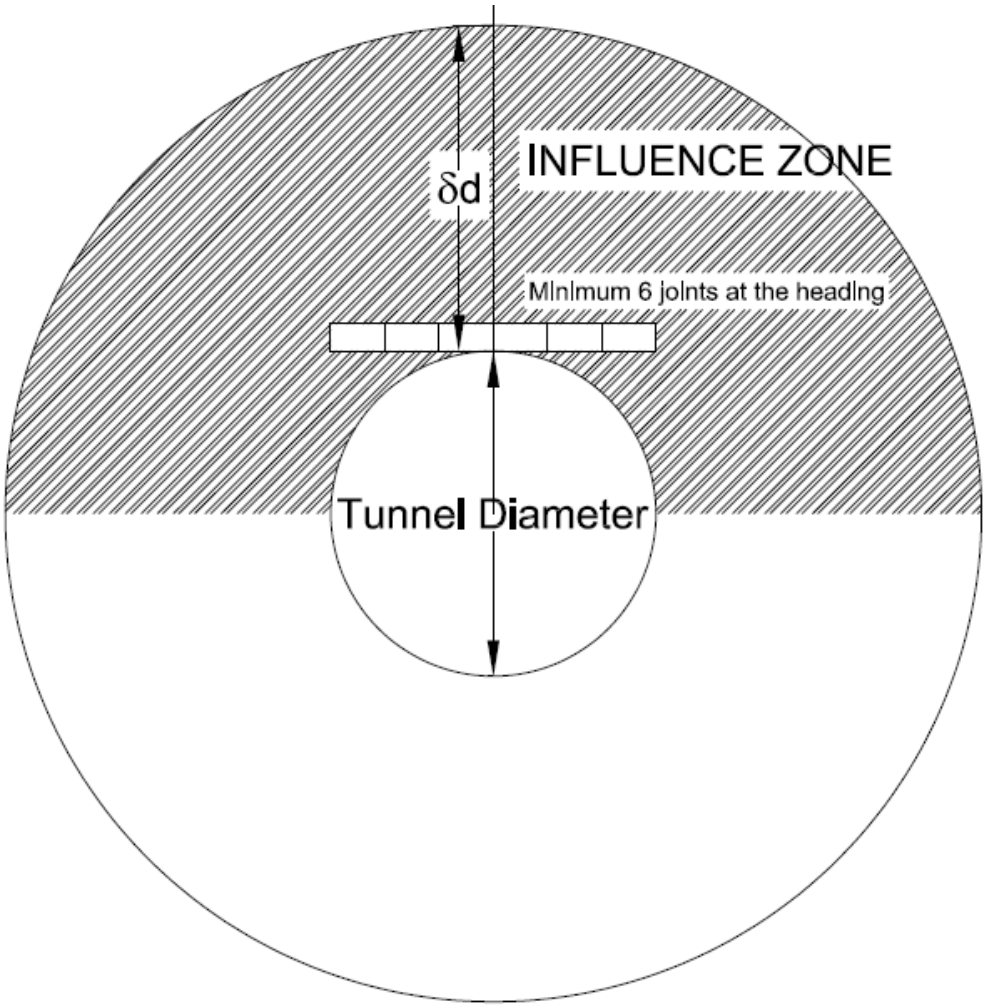

Figure 6.1. Influence zone definition

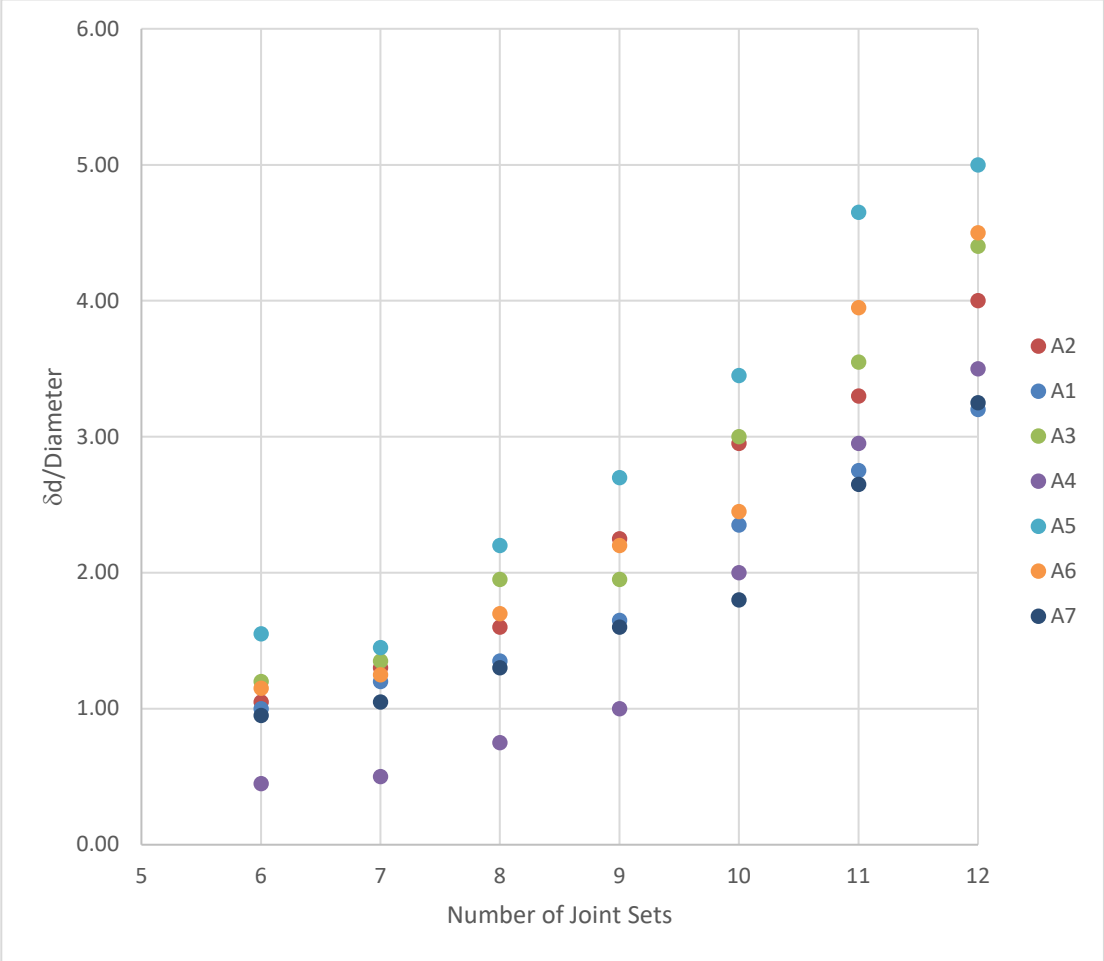

Figure 6.2. Plot of number of joint sets with respect to dip angles

From the results given in Figure 6.2 we can see that for some discontinuity directions the behavior are more effected from anisotropy. As shown in the Figure 6.2, 60 degrees of anisotropy has the most influence in the interaction where 30 degrees has the second most effective. As can be seen from the same figure, the least effective angle of discontinuity is 45. The interlocking stresses due to roofing effect arises at 45 degrees. With increasing the number of joints at the heading (orthogonal to the joint orientation) the influence zone is expanding.

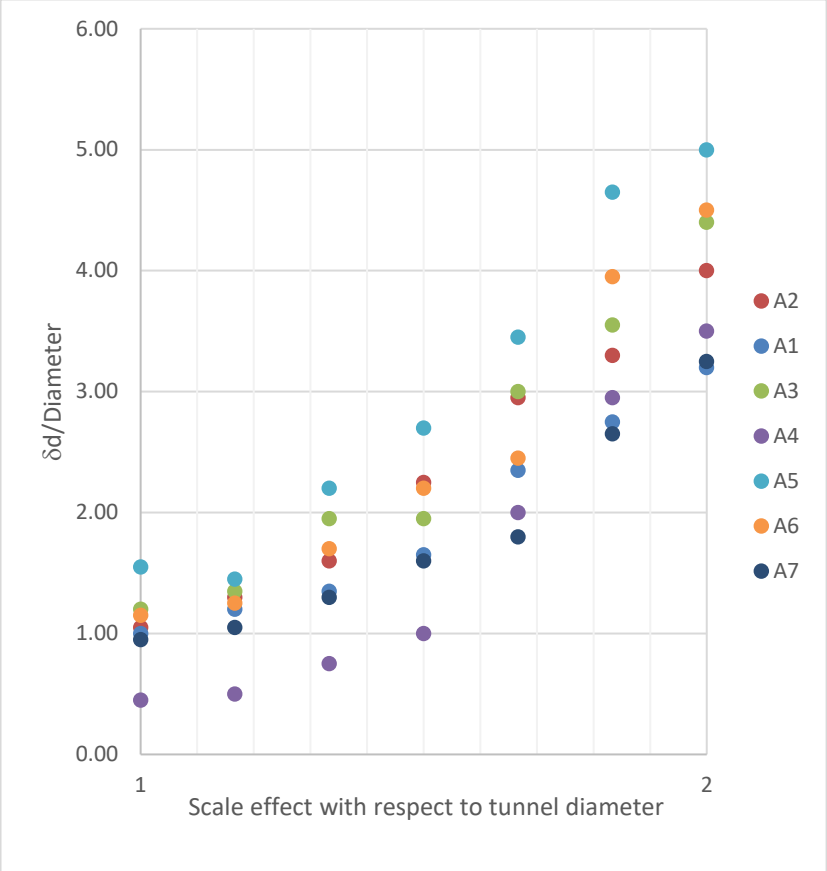

Figure 6.3. Plot of # of joint sets with respect to dip angles

The x ordinate of Figure 6.3 interprets the scale effect with respect to tunnel diameter. The outcome from this graph can be explained as; if the tunnel diameter increases even to twice of its original diameter, the influence zone shall be raised exponentially where it may be really unfeasible to be treated. The same result can be interpreted as follows as well: when the spacing between discontinuities get very small, the solution gets difficult.

The following graph clearly indicates that 60 degrees of anisotropy in κ=1 (system with through-going joints) situation has the most effective angle in any number of joint sets whereas the dimensionless ratio which may be called as interference zone coefficient is affected by number of joint sets.

Figure 6.4 is the summary of results that show that if the diameter of the tunnel increases, the interference zone also increases. To understand the nature of the trend of the

relation between the diameter and interference zone Figures 6.5 to 6.11 have been given. As can be seen from these figures as the relation is of exponential nature.

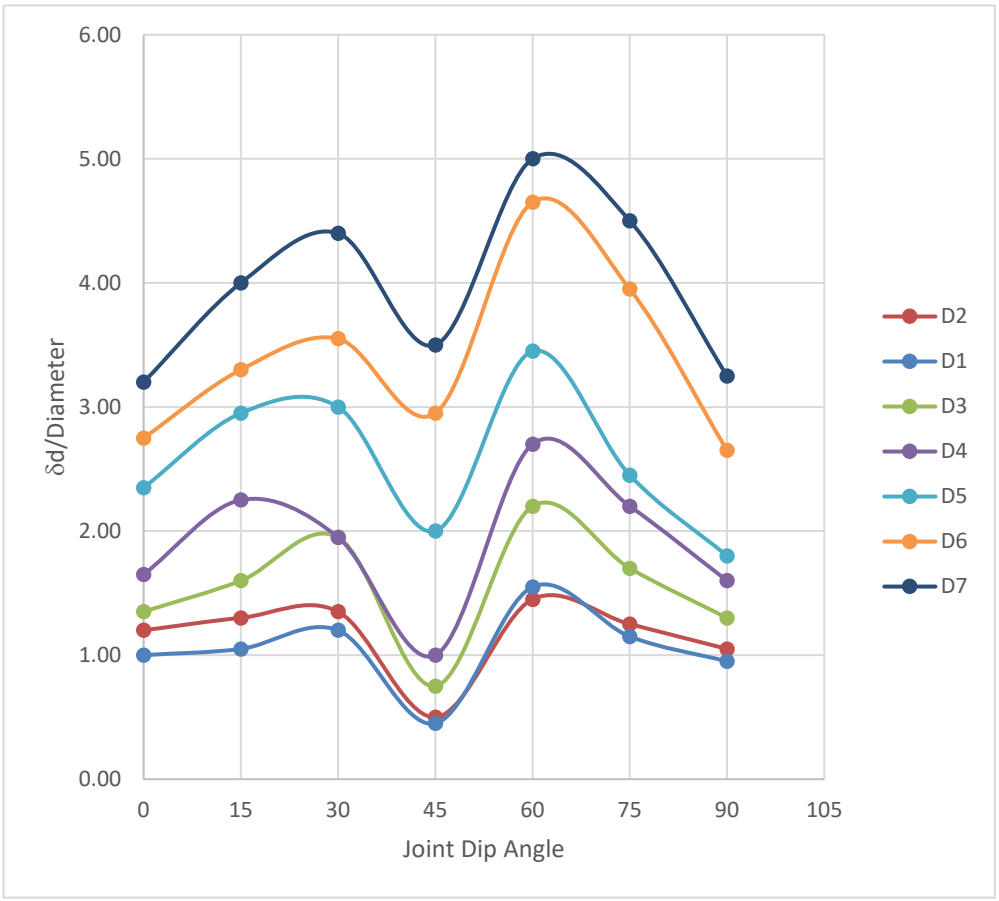

Figure 6.4. General graph of interference coefficient vs Joint dip angle with diameters

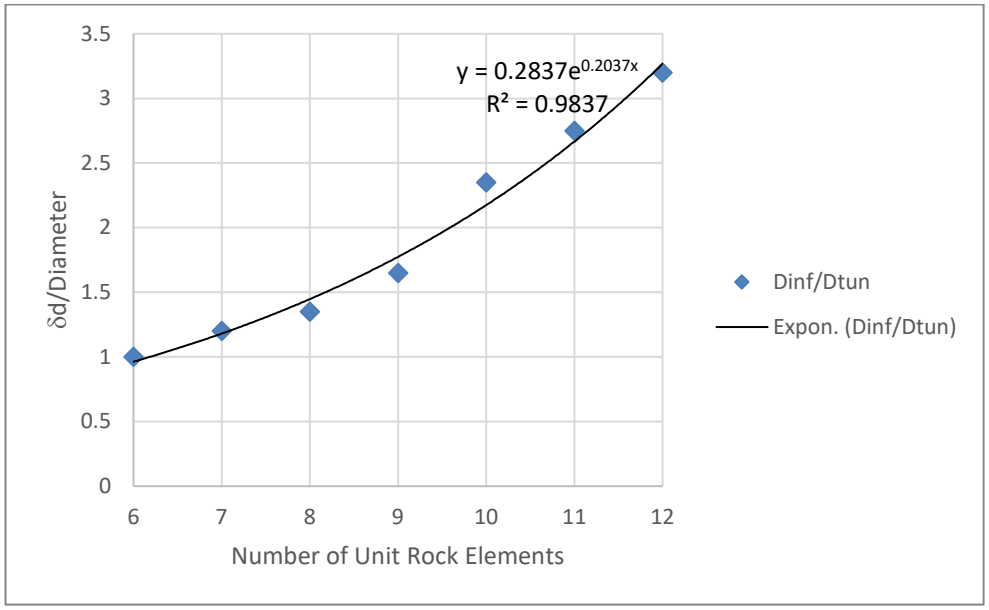

Figure 6.5. Plot of influence diameter with Joint Dip Angle = 0 degrees

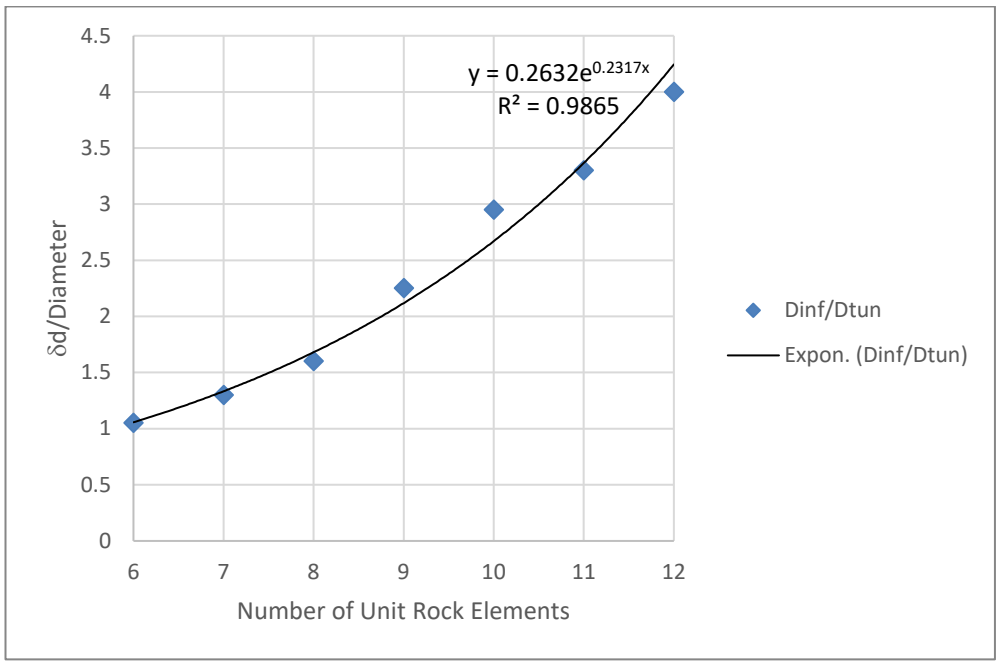

Figure 6.6. Plot of influence diameter with Joint Dip Angle = 15 degrees

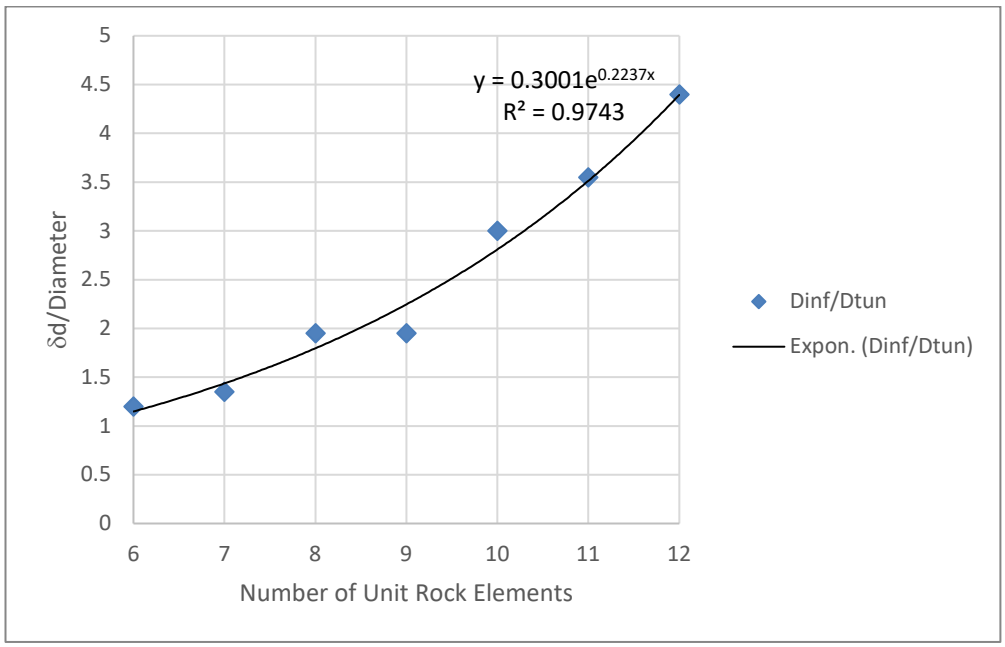

Figure 6.7. Plot of influence diameter with Joint Dip Angle = 30 degrees

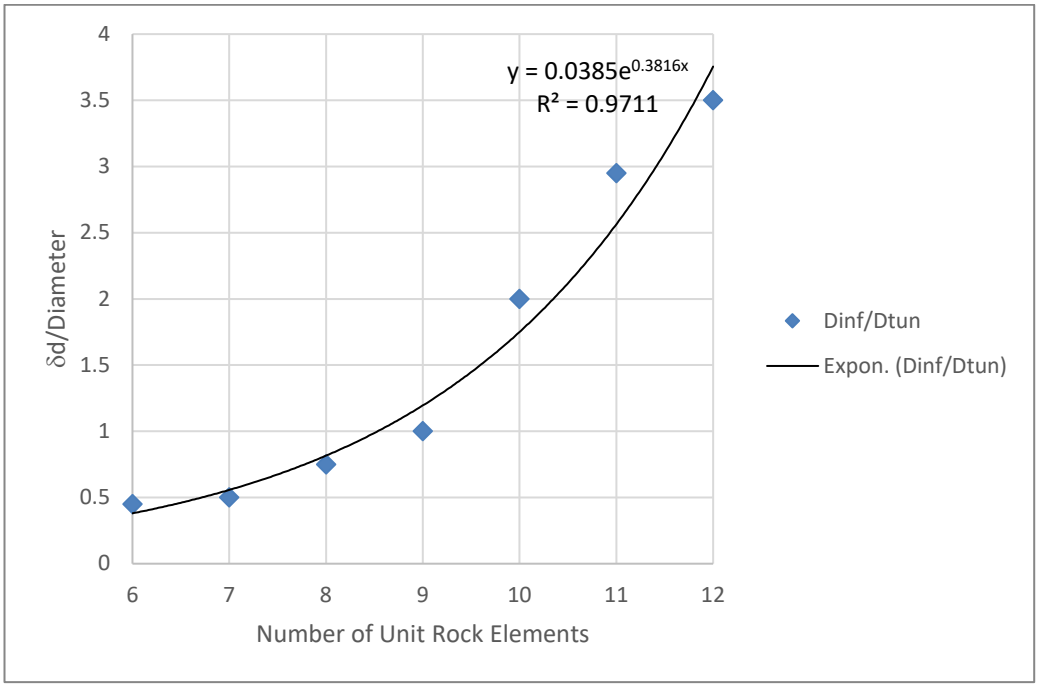

Figure 6.8. Plot of influence diameter with Joint Dip Angle = 45 degrees

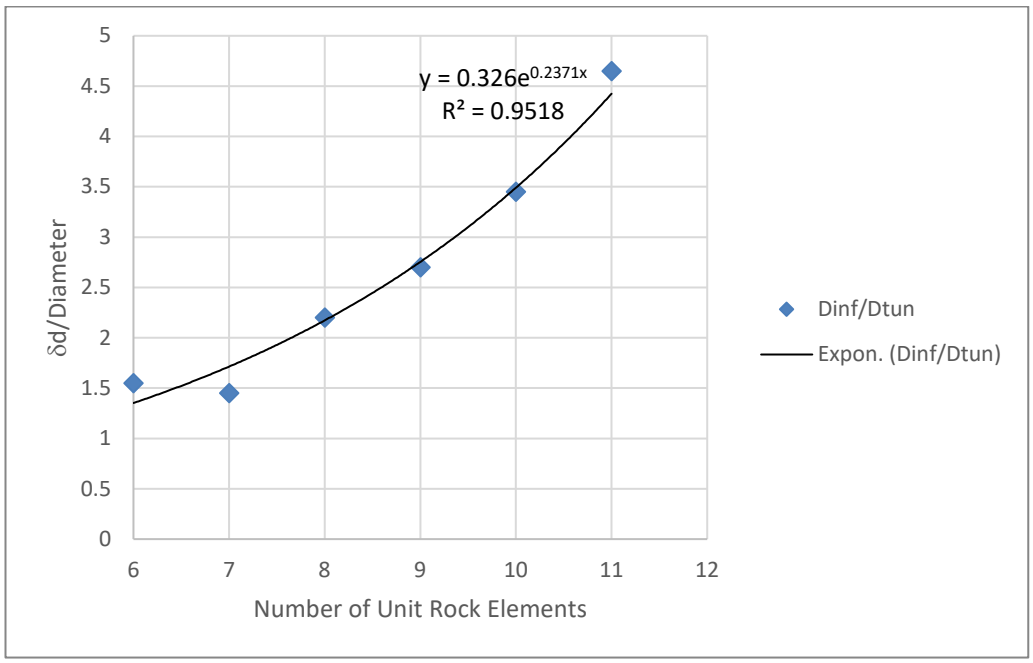

Figure 6.9. Plot of influence diameter with Joint Dip Angle = 60 degrees

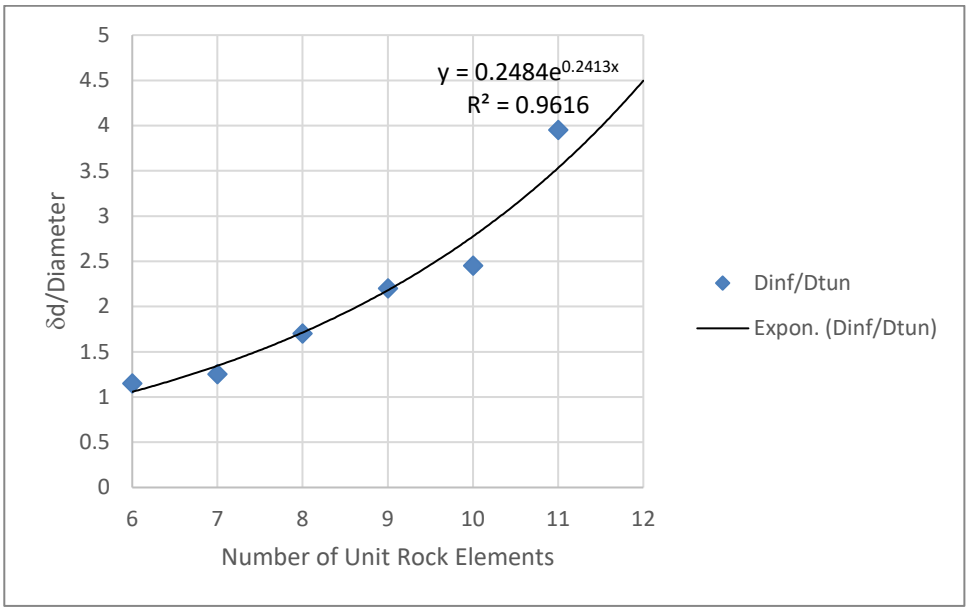

Figure 6.10. Plot of influence diameter with Joint Dip Angle = 75 degrees

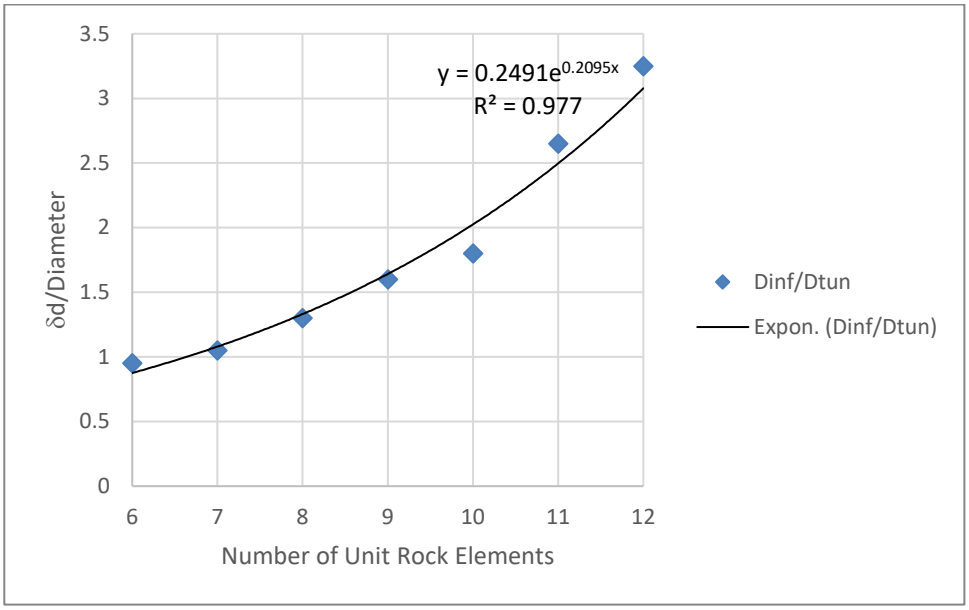

Figure 6.11. Plot of influence diameter with Joint Dip Angle = 75 degrees

The results indicate that 45 degrees is the safest dip angle in tunneling where 30 and 60 degrees of joint orientation may become potential danger in the structure. With increasing diameter, the effect of the number of joints becomes more appropriate. One of the main results is that when the top of the tunnel has more than 8-9 joint sets, the influenced diameter increases rapidly with exponential function. The graphs with exponential functions given above for each joint orientation indicates that the number of joints at the top of tunnel increases the trend line increases exponentially where 8-9 joint sets seems to be the critical number. This means protective zone may be thicker, but this bigger zone has to be remediated somehow where it will be not so easy and economical in real world. One diameter of influence zone with 6-8 number of joints can be accepted and reinforced by means of dowels, bolts etc. Second idea may come up that bigger tunnels or underground structures has to be excavated with splitted smaller parts even in central drift or side drift that will come up with 6-7 joint sets at heading part. On the other hand, this study would be useful to show that side drifts may be more useful since central drift or full face would affect bigger areas at the top. With the main idea of NATM, bigger diameter tunnels can be excavated with splitted parts taking care of influence zones by means of qualified personnel and useful engineering geological data. The engineering geology of the surrounding area of the underground structure is one of the key components in design and construction.

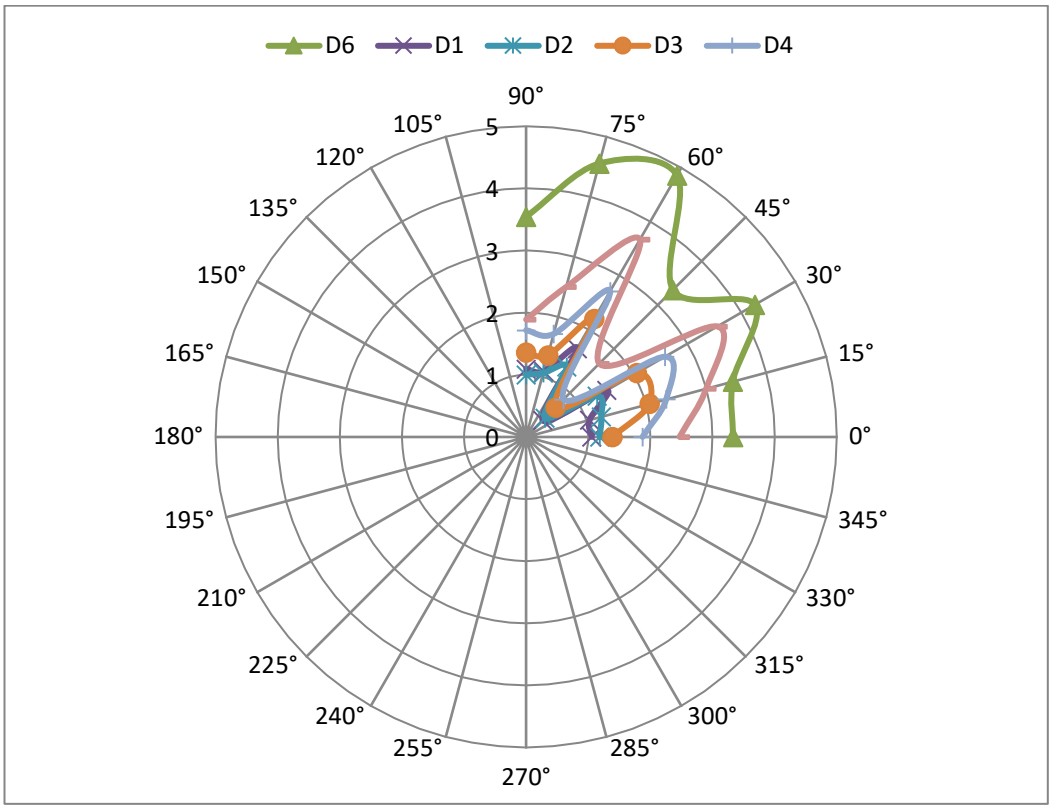

Figure 6.12. Polar Plot of Variation of influence diameter vs joint dip angle

The numerical results interpret very similar results with physical modelling where 45 degrees has the smallest influence zone and 60 degrees has the biggest influence zone. The reason for this type of behavior is that if the internal friction angles of both joint systems are almost same and the anisotropy s the conjugate of others. It can be said that shared anisotropy is obtained in this case. The strength reduction factor by means of numerical modelling gives interpretative results. The polar plot of discontinuities dip angles versus influence dimensionless ratio is given as Figure 6.12

Second general output from numerical results is that the bigger diameter the more influenced zone where 3-4 times the diameter was exceeded.

The results of numerical analysis are as follows; The first five sets of dip angles (zero to sixty degrees) behaved almost same with physical analysis. The last two sets of inclination

have the same inclination while dimensionless ratios of influence zone to diameter of the tunnel seems higher (almost two times) compared to physical tests.

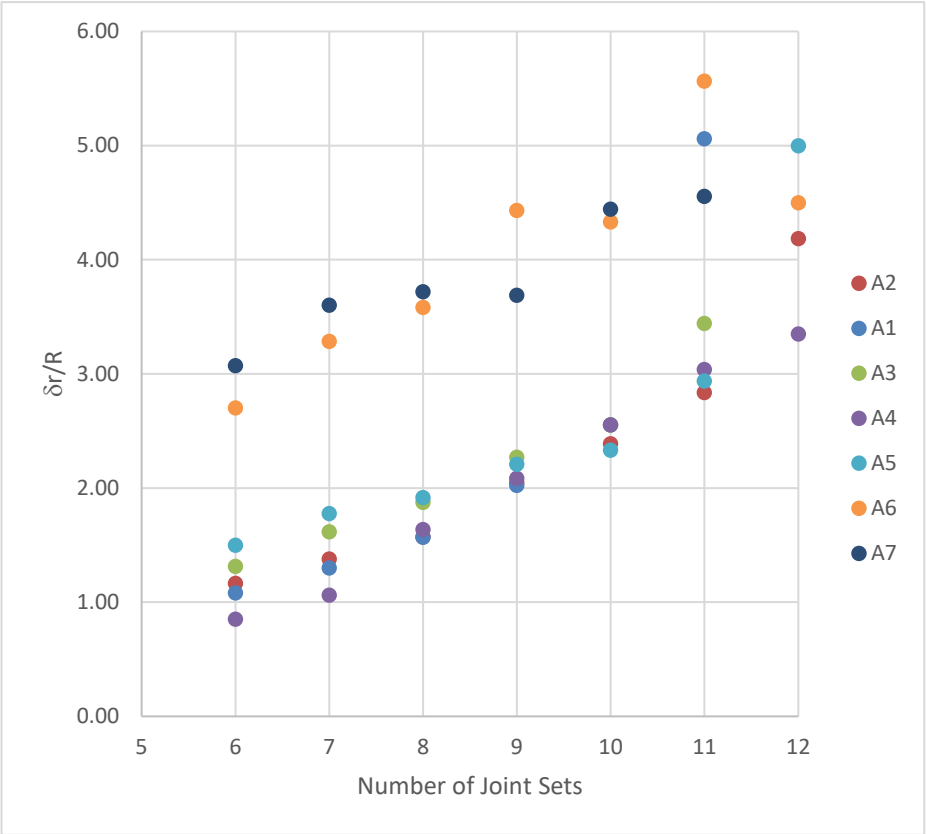

Figure 6.13. Plot of Variation of influence diameter vs joint dip angle - numerical results

As seen in Figure 6.13, the results of numerical analysis for higher dip angles (75-90) has a scatter when compared to physical results at thee angles. This was explained as the numerical results would have some boundary effect for some angles.

Figure 6.14 to Figure 6.20 were given to interpret the trend curve which is described as exponential functions. The R-squared values are mostly over 90%.

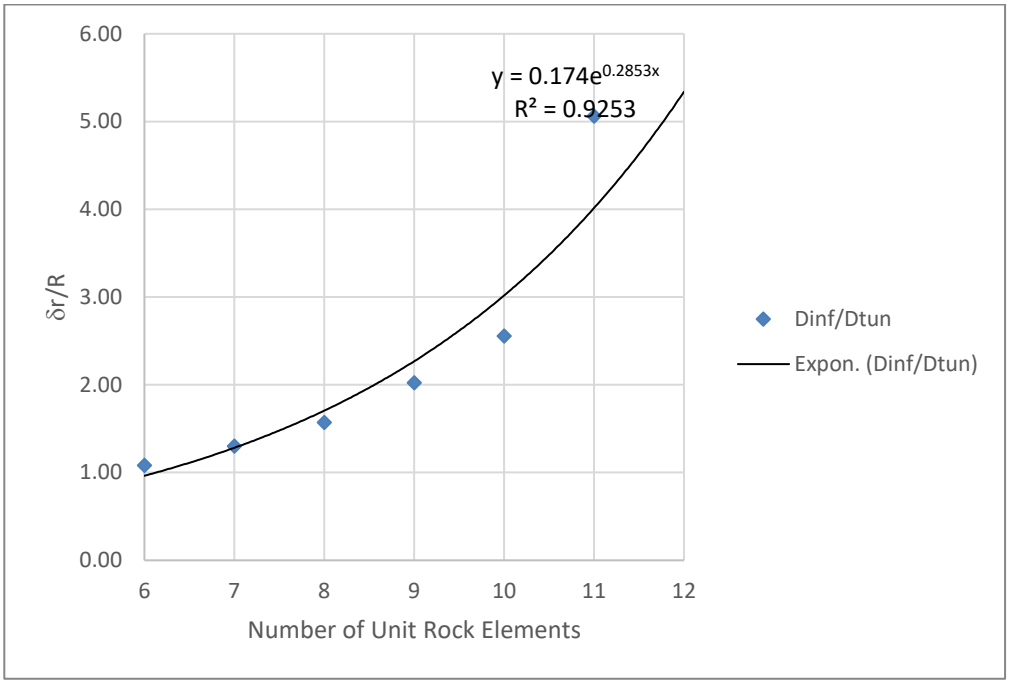

Figure 6.14 Plot of influence diameter with Joint Dip Angle = 0 degrees-numerical results

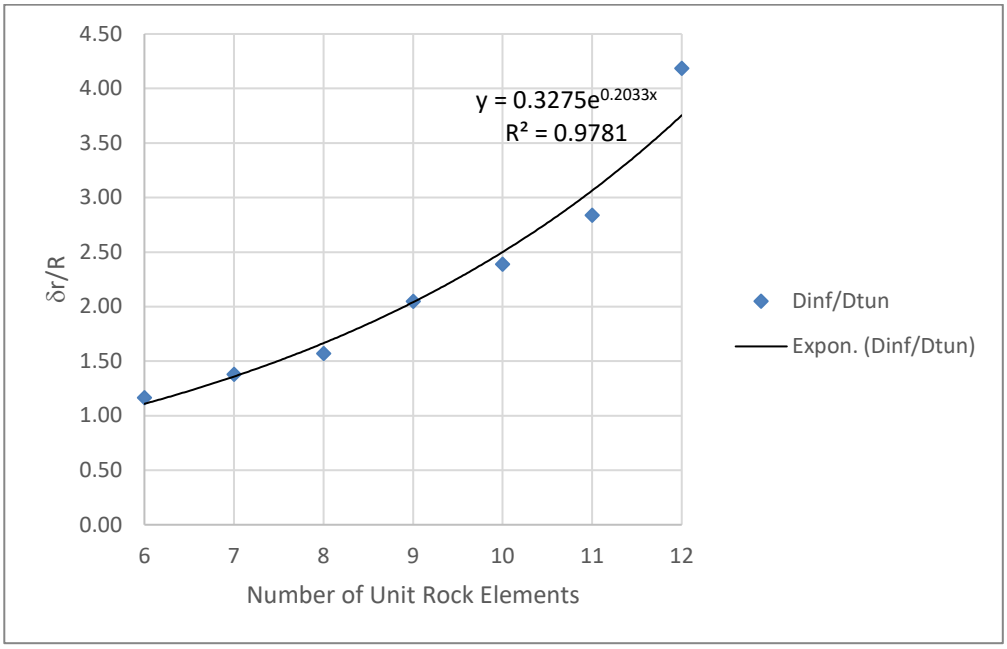

Figure 6.15 Plot of influence diameter with Joint Dip Angle = 15 degrees-numerical results

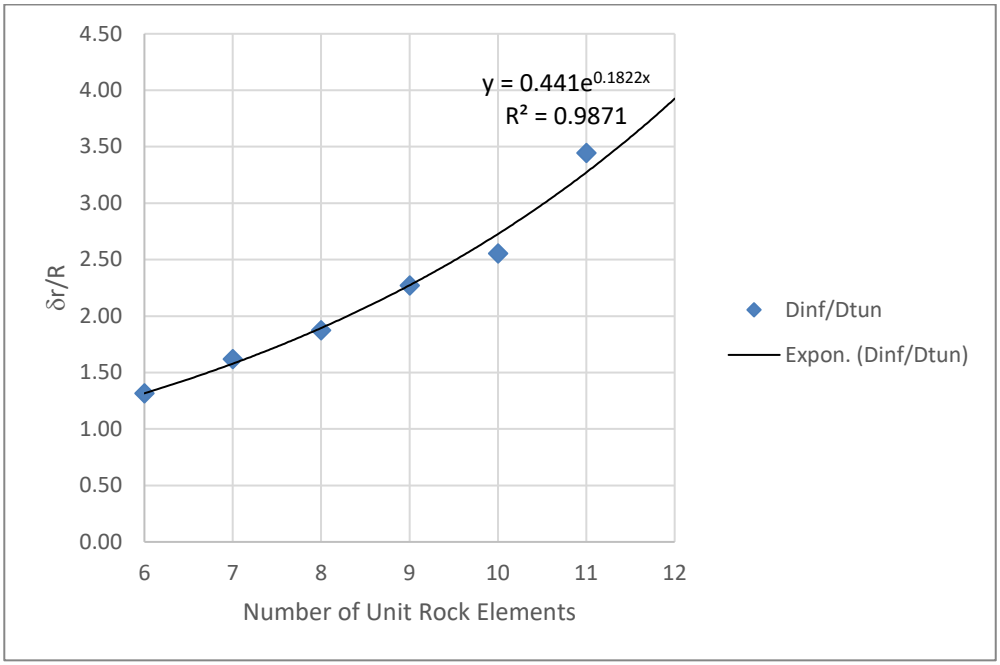

Figure 6.16 Plot of influence diameter with Joint Dip Angle = 30 degrees-numerical results

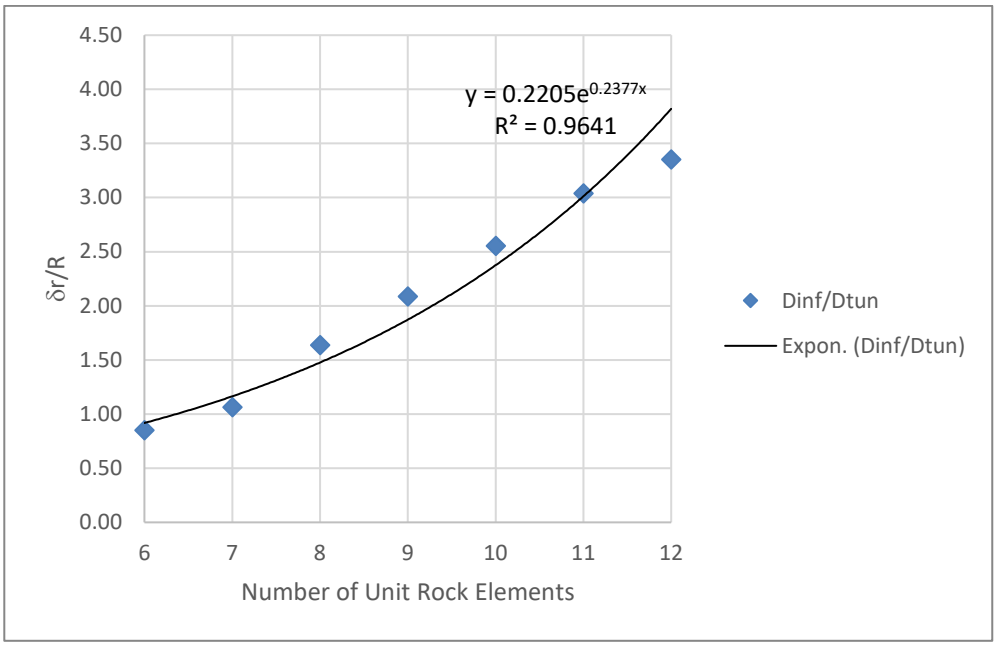

Figure 6.17 Plot of influence diameter with Joint Dip Angle = 45 degrees-numerical results

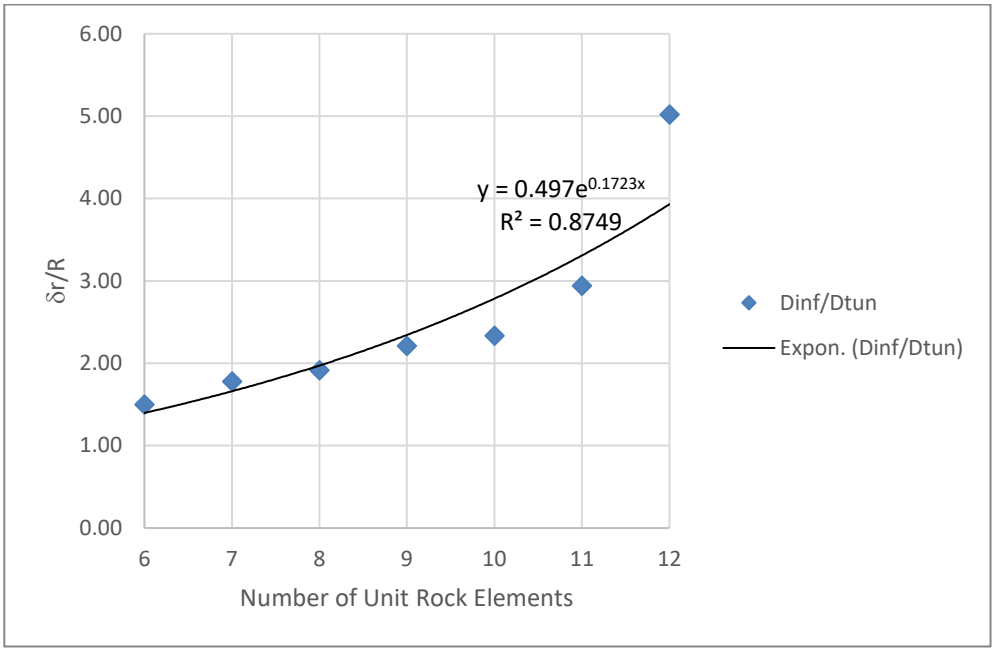

Figure 6.18 Plot of influence diameter with Joint Dip Angle = 60 degrees-numerical results

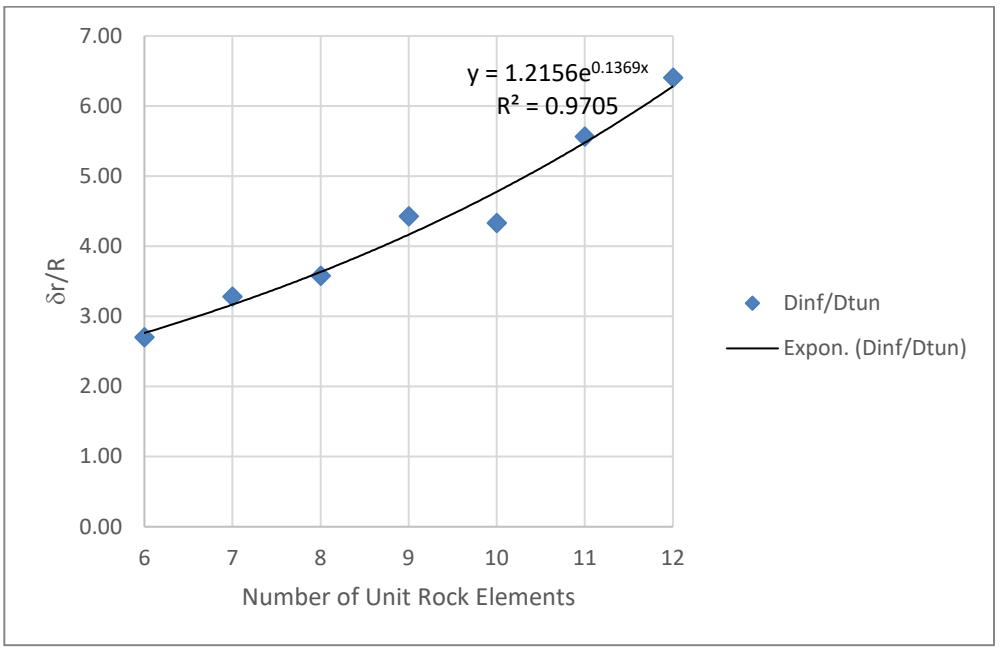

Figure 6.19 Plot of influence diameter with Joint Dip Angle = 75 degrees-numerical results

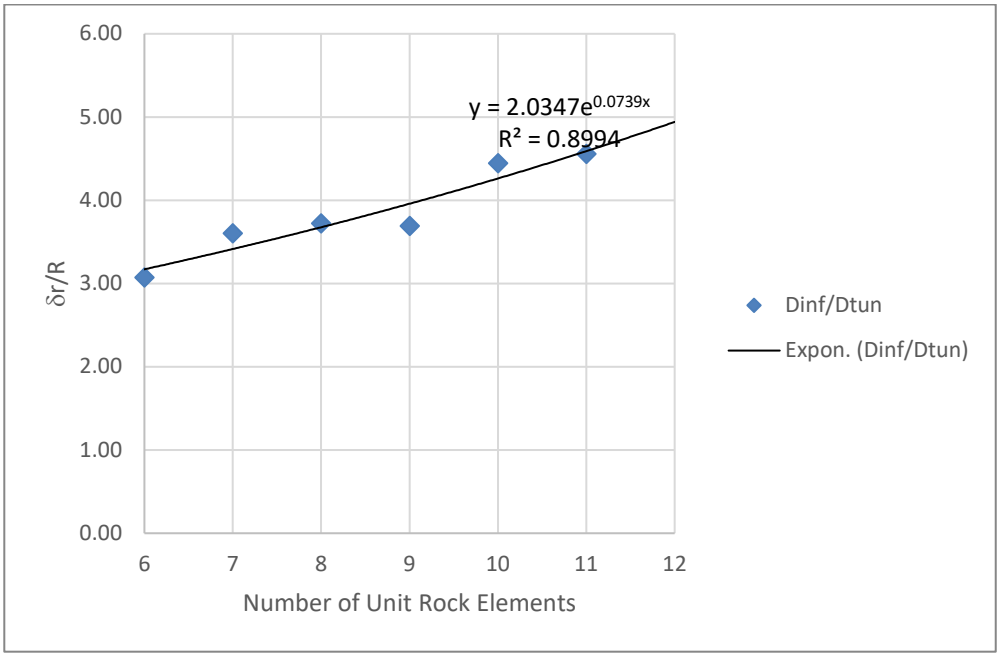

Figure 6.20 Plot of influence diameter with Joint Dip Angle = 90 degrees-numerical results

The results of numerical analysis indicate that the influence zone obtained from numerical model have comparable trends to the influence zone obtained from physical models. However, the dimensionless ratios are a little higher (1.1 – 1.15 times) compared to physical models.

7 CONCLUSIONS & DISCUSSIONS

In this study a base friction analyses concept was used to analyze the failure mechanisms of underground openings under anisotropic joint conditions. The geometry of the opening and the orientation of the joints were chosen as the critical factors which effect the failure criteria. Base friction was selected as a tool since it is practical and inexpensive way to simulate the jointed rock media. It also provides to illustrate the failure phenomena of the jointed rock mass as similar as possible to the real world.

Base friction technique was used successfully to determine the jointed rock media and analyzing the movement behavior of discontinuous rock masses. Even though the method is versatile and powerful, its limitations are also known and cannot be overlooked. It only provides a two-dimensional media and no strain measurements can be taken.

One of the goals of the study was to present the joint effects on underground structures since the generally accepted design criteria is based on continuum modelling. The jointed rock models are quasi continuum to discrete and show different behavior when loaded.

Karaca 1991 was studied jointed rock environment but he concluded that the primary influenced zone was up to radius of a circular tunnel. With this study, it is also evident that the influence zone was affected by the number of joints and their orientation and the continuum mechanics is not valid for general concept of design in underground structures.

The results of anisotropy due to dip of the joints also confirms the study by Müller et all. 1973, that the minimum disturbance is valid with 45 degrees of blocks since interlocking stresses occur under that angles. The variation of this study is that it is already confirmed with a tunnel structure where Müller and his colleagues performed these on triaxial tests in the laboratory.

The joint dip angles and the numbers of joints on the top of tunnel structures are the main issues where the rock can behave as discrete. This will affect the influence zone of the opening.

The dip angle of 60 or 90-60= 30 degrees for the jointed model interpreted the highest deformation influence zone in the physical models. The results of numerical models have a scatter in 75 and 90 degrees (compared to horizontal).

The ratio of diameter of influence zone to underground opening is mainly keen on the number of joint spacing at the head part of the opening. Generally speaking, the idea of one diameter influence zone is not valid and it increases by an exponential function with increase of number of joints.

Big span of underground structures can be excavated by means of NATM philosophy with circular cross sections and by knowing the interaction of tunnel with number and orientation of joints.

This thesis was only adopted $\kappa=1$ (through going joints) type of jointed structure where $\kappa=0.5$ (non through going joints) also can be studied for the future work to make interaction clearer in the design.

Influence zone of the rock environment was found to be directly interrelated with the dimensions of excavation versus number of joint sets. This mean without an Engineering Geological assessment at site, the underground structure may cause big problems with recent design methods. More joint sets with big diameter means higher influence zone that may affect more than 3-4 times (up to 5-6 diameter minimum with this study) diameter of the tunnel.

The results of both physical and numerical studies indicated that when the number of joint sets at the crown of the tunnel (here circular geometry) increases, the possibility of the failure increases.

The result is that the increment in joint sets leads the tunnel structure to have a big influence zone where it generally exceeds two or more diameters for 8-9 numbers of joint sets. Literature survey has some studies on anisotropy and in some cases of tunneling. However, the interrelations of geology (number of joint sets), influence zone with respect to diameter and its modeling is presented as a new contribution in this study.

The results of the physical analysis indicate that the orientation of failure is in same manner with numerical models based on finite element approach where the influence zone adaptations seems a little smaller (almost 0.85-0.9 times) when compared to physical models.

Another inference from numerical models is that the effect of joint geometry and the segmental geometry of rock pieces is important since the geometry of anisotropy of the affected zone can be evaluated more clearly. It is evident that the influenced area by means of technical interference differs with the joint orientation which is be acceptable with selected model.

It has to be noted that the limitation of model material is important in the result evaluation since the model material was accepted as elastic in behavior. Second reminder need to call that the geometry was selected as circular in order to get ratio-less assessment.

8 REFERENCES

1. Ashby J.P., 1971, *Sliding and toppling models of failure in models and jointed rock slopes*, MS. Thesis, London University (Imperial College), London.

2. Barton, N., 1979, “Model Studies of Very Large Underground Openings at Shallow Depth”, *Proceedings of Forth Congress International Society of Rock Mechanics*, Montreux, Vol. 1, pp. 583-590.

3. Barton, N., and H. Hansteen, 1979, “Very Large Span Openings at Shallow Depth: Deformation Magnitudes from Jointed Models and F.E. analysis", in A.C. Maevis and W.A., Hustrulid (eds.), *Forth Rapid Excavation and Tunneling Conference, RETC*; Atlanta Georgia, Vol. 2, pp. 1131-1353, American Institute of Mining, Metallurgical, and Petroleum Engineers, New York.

4. Bienawski, Z.T., 1969, “Deformational Behavior of Fractured Rock Under Multiaxial Compression”, *Proceedings of International Conference on Structure, Solid Mech. and Engineering Design*; Southampton, England, April 1969

5. Bieniawski, Z.T., 1984, *Rock Mechanics Design in Mining and Tunneling*, Balkema Publications, Amsterdam.

6. Bray, J.W. and R. E. Goodman, 1981, “The Theory of Base Friction Models”, *International Journal of Rock Mechanics,* Vol. 18, Issue 6, pp. 453-468, December.

7. Egger, P., 1973, “Einfluß des Post-Failure-Verhaltens von Fels auf den Tunnelausbau (unter Besonderer Berücksichtigung des Ankerausbaues)”, Veröff. Inst. Boden- und. Felsmechanik, Univ. Karlsruhe, H.57.

8. Egger, P., 1983, “Roof Stability of Shallow Tunnels in Isotropic and Jointed Rock”, Proceedings of Fifth International Society for Rock Mechanics and Rock Engineering, Melbourne, 10-15 April, pp. 295-301.

9. Engesser, F., 1882, *Uber den Erddruck Gegen Minere Stützwlinde Tunnelwönde*, Bauzeitung.

10. Erguvanli, K., Goodman R.E., 1972, "Applications of Models to Engineering Geology for Rock Excavations", *Bulletin of Association of Engineering Geology*, Vol. 9, pp. 89-104, London.

11. Fenner, R., 1938, *Untersuchungen tur Erkenntnis des Gebirgsdruckes*. Glückauf Jg. 74 Heft 32 - 33.

12. Fumagalli, E., 1973, *Statical and Geomechanical Models*, Springer-Verlag Wien, Vienna.

13. Fumagalli, E., 1979, *Model simulation of rock mechanics problems, Rock Mechanics in Engineering Practice*, John Wiley& Sons, Reprinted (1979).

14. Goodman, R. E. and G. H. Shi, 1985, *Block Theory and its Application to Rock Engineering,* Prentice-Hall International, London.

15. Goodman, R.E., 1976, *Methods of Geological Engineering in Discontinuous Rock*, West Publishing Company, pp. 277-299.

16. Goricki, A., 1999, *Base Friction Versuche für Felsmechanische Kluftkörpermodelle*, M.S Thesis, TU-Graz

17. Hammah, R. E., Yacoub, T. , Corkum, B. and J. H. Curran, 2008, "The Practical Modelling of Discontinuous Rock Masses with Finite Element Analysis" The 42nd U.S. Rock Mechanics Symposium (USRMS), 29 June-2 July, San Francisco, Californiaç

18. Hayashi, M., 1966, "Strength and dilatancy of brittle jointed mass – The extreme value stochastics and anisotropic failure mechanism" , *Proceedings of the First Congress of the International Society of Rock Mechanics*, Lisbon, Vol. 3, No. I, pp. 295-302

19. Heim, A., 1905, “Geologische Nachlese”, *Viertel jahresschrift der Naturforschungsgesellschaft*, Zürich, pp. 1-22.

20. Heuer, R. E. and A. J. Jr. Hendron, 1971, “Geomechanical Model Study of the Behavior of Underground Openings in Rock Subjected to Static Loads”. *Report 2. Tests on Unlined Openings in Intact Rock,* Illinois Univ. Urbana Dept. of Civil Engineering.

21. Jing, L., 2003, “A Review of Techniques, Advances and Outstanding Issues in Numerical Modelling for Rock Mechanics and Rock Engineering”, *International Journal of Rock Mechanics and Mining Sciences*. Vol. 40, Issue 3, April 2003, pp. 283-353.

22. John, K. W., 1969, “Festigkeit und Verformbarkeit von Druckfesten, Regelmäßig Gefügten Diskontinuen”, *Veröff. Inst. für Boden und Felsmechanik*, Universität Karlsruhe, Heft 37.

23. K.G.M., 2005, *NATM Uygulamalı Yeraltı Tünel İşleri Teknik Şartnamesi*, T.C. Bayındırlık ve İskân Bakanlığı, Karayolları Genel Müdürlüğü, Ankara.

24. Karaca, M. and P. Egger, 1993, “Failure Phenomena Around Shallow Tunnels in Jointed Rock”, in Pasamehmetoglu et. al. (eds), *Proceedings of the Assessment and Prevention of Failure Phenomena in Rock Engineering*, pp 381-388, Balkema, Rotterdam.

25. Karaca, M.A., 1991, *Stabilite des Tunnels a Faible Profondeur en Milieu Discontinu*, Ph.D. Dissertation, Ecole Polytechnique Fédérale de Lausanne.

26. Karakus, M. and R. J. Fowell, 2004, “An Insight into the New Australian Tunneling Method (NATM)”, *ROCKMEC'2004: The Seventh Regional Rock Mechanics Symposium*, Sivas, 21-22 October 2004, Turkey

27. Kastner, H., 1971, *Statik des Tunnel- und Stollenbaues auf der Grundlage Geomechanischer Erkenntnisse*, Springer Verlag, Berlin.

28. Kommerell, O., 1940, *Statische Berechnung von Tunnelmauerwerk*. Berlin.

29. Kovari, K., 1993, “Erroneous concepts behind NATM”, *Lecture given at Rabcewicz Colloquium*, Zurich.

30. Krsmanovic, D. and S. Milic, 1964, “Model Experiments on Pressure Distribution in Some Cases of a Discontinuum”, *Felsmechanik. und Ing. Geologie*, Supplement I, pp. 72-87.

31. Kuznecov, G. N., 1964, *Modellversuche zum Einflusse der Gesteinszerkluftung auf die Pfeilerstandfestigkeit beim Kammerabbau*, Bericht 5, International Buro für Gebirgsmechanik Leipzig, pp. 133-149.

32. Lajtai, E.Z., 1967, “The influence of interlocking rock discontinuities on compressive strength (model experiments)”. *Rock Mech. Eng. Geol.* Vol. 5, pp. 217-228.

33. Lajtai, E.Z., 1969, "Strength of Discontinuous Rocks in Direct Shear", Geotechnique, Vol. 19, No. 2, pp. 218-233.

34. Lajtai, E.Z., 1969a, "Shear Strength of Weakness Planes in Rock", *International Journal of Rock Mechanics and Mining Science*, Vol. 6, pp. 499-515.

35. Leon, A. and F. Willheim, 1912, “Über die Zerstörung in tunnelartig gelochten Gesteinen”, *Österreichische Wochenschrift für den öffentlichen Baudienst, Amtliches Fachblatt, Herausgegeben von k.k. Ministerium der Oeffentlichen Arbeiten*, XVI. Jahrgang.

36. Liu, Chi-Hong, 2003, *Base Friction Modeling of Discontinuous Rock Masses*, M.S. Thesis, University of Hong Kong.

37. Mahmutoğlu, Y. and M. Vardar, 1992, “Kaya Mekaniği Problemlerinin Çözümünde Model Malzemesi Tasarımı ve Üretilmesi”, *Mühendislik Jeolojisi Türk Milli Komitesi Bülteni*, Yıl 13, Sayı 13, Ankara.

38. Meguid, M.A., Saada, O., Nunes M.A. and J. Mattar, 2008, “Physical Modeling of Tunnels in Soft Ground: A Review”, *Tunneling and Underground Space Technology*, Vol. 23, Issue 2, March 2008, pp. 185-198.

39. Müller, L. and E. Fecker, 1978, "Grundgedanken und Grundsaetze der Neuen Österreichischen Tunnelbauweise" *Grundlagen und Anwendung der Felsmechanik: Felsmechanik Colloquium*, Karlsruhe, pp. 247-62, Trans Tech. Publications, Clausthal.

40. Müller, L. and F. Pacher, 1965, “Modellversuche zur Klärung der Bruchgefahr Geklüfteter Medien”, *Felsmechanik. und. Ing. Geol., Suppl. II*, Issue 13, pp. 7-24, Vienna,

41. Müller, L. and N. Rengers, 1969. “Kinematische Versuche an Geomechanischen Modellen” *Rock Mechanics, Suppl. I,* Issue 10, pp. 20-31, Vienna.

42. Müller, L., 1969, *Fundamentals of Rock Mechanics*: Lectures Held at the Department for Mechanics of Deformable Bodies, September, Udine.

43. Müller, L., 1978, *Der Felsbau. Bd. III: Tunnelbau,* Ferdinand Enke, Stuttgart.

44. Müller, L., Baudendistel, M. and H. Malina, 1970, “Der Einfluß des Flächengefüges auf die Standfestigkeit eines Untertage-Krafthauses” *Second Congress International Society for Rock Mechanics*, pp. 1-10, Belgrad.

45. Müller, L., Tess, C., Fecker E. and K.Müller, 1973, “Kriterien zur Erkennung der Bruchgefahr geklüfteter Medien — Ein Versuch”, *Rock Mechanics, Suppl. 2*, Issue 18, pp 71-92, Vienna.

46. Müller, L.-Salzburg and E. Fecker, 1978, “Fundamental Ideas and Principles of the New Austrian Tunneling Method”, *Grundlagen und Anwendung der Felsmechanik*, Felsmechanik Kolloqium Karlsruhe, pp. 1-10.

47. Müller-Salzburg, L., Sauer, G. and M. Vardar, 1978, "Dreidimensionale Spannungsumlagerungsprozesse im Bereich der Ortsbrust." in Müller L. (eds) *Geologische Vorerkundung. Tunnelbau — Bergbau — Gebirgssicherung — Kraftwerksbau / Geological Reconnaissance. Tunneling — Mining — Rock Support — Power Plant Construction. Rock Mechanics*, Vol. 7, Springer, Vienna.

48. OeGG, 2008, *Guideline for the Geotechnical Design of Underground Structures with Cyclic Excavation*. 2nd Revised Edition, The Austrian Society for Geomechanics, Salzburg/Austria.

49. ÖGG, 2001, Österreichische Gesellschaft für Geomechanik (eds.), *Richtlinie für die Geomechanische Planung von Untertagebauarbeiten mit Zyklischem Vortrieb*, Salzburg.

50. ÖGG, 2008, *Richtlinie für die geotechnische Planung von Untertagebauten mit Zyklischem Vortrieb*. Österreichische Gesellschaft für Geomechanik, Salzburg.

51. ÖNORM B2203, 2001, *Underground works – Works Contract – Part 1: Cyclic Driving (Conventional Tunneling)*.

52. ÖNORM B2203/1, 2005. *Untertagebauarbeiten – Werkvertragsnorm. Teil I: Zyklischer Vortrieb, 2001; Teil II: Kontinuierlicher Vortrieb.* Österreichisches Normungsinstitut, Vienna, 2005.

53. Pacher, F., 1963, "Deformationsmessungen im Versuchsstollen als Mittel zur Erforschung des Gebirgsverhaltens und zur Bemessung des Ausbaues" *14th Symposium of the Austrian Regional Group of the International Society for Rock Mechanics,* 27-28 September 1963, Salzburg

54. Palmström, A., 1993, "The New Austrian Tunnelling Method", *Conference on Fjellsprengningsteknikk, Bergmekanikk, Geoteknikk*, Oslo, pp. 31.1 – 31.20

55. Rabcewicz, L. and J. Golser, 1973, "Principles of Dimensioning the Supporting System for the New Austrian Tunneling Method", *Water Power*, pp. 88-93, March.

56. Rabcewicz, L. V., 1957, “Die Ankerung im Tunnelbau Ersetzt Bisher Gebrauchlice Einbaumethoden”, Bauzeitung 75 Nr. 9.

57. Rabcewicz, L., 1944, *Gebirgsdruck und Tunnelbau*, Springer - Verlag Vienna

58. Rabcewicz, L., 1964, “The New Austrian Tunneling Method, Part one”, *Water Power,* pp. 453-457, November.

59. Rabcewicz, L., 1964, “The New Austrian Tunneling Method, Part two”, *Water Power*, pp. 511-515, December.

60. Rabcewicz, L., 1965, “The New Austrian Tunneling Method, Part Three”, *Water Power*, pp. 19-24. January.

61. Rabcewicz, L., 1973, “Yeni Avusturya Yöntemi İle Tünel Açımında Tahkimat Sisteminin Boyutlandırma Esasları”, Çeviri: Meran Pakel, Water Power Dergisi, Mart.

62. Reik, G. and F. J. Hesselmann, 1981, “Verfahren zur Ermittlung der Gebirgsfestigkeit von Sedimentgesteine”, *Österreichische Gesellschaft für Geomechanik (Hrsg.): Ingenieurgeologie und Geomechanik im Talsperren- und Tunnelbau*, Springer, Vienna.

63. Reik, G., 1977, “Methoden zur Ermittlung der Felsmasseneigenschaften Geklüfteter Sedimentgesteine” *Jahresbericht 1976 des Sonderforschungsbereiches 77 Felsmechanik*" Universität Karlsruhe, pp. 94-115.

64. Ritter, W., 1879, *Die Statik der Tunnelgewölbe*, Berlin

65. Sauer, G., 1975, *Entwicklung und Aufbau einer Versuchsanlage zur Durchführung dreidimensionaler Modellversuche in Geklüfteten Medien*, Jahresbericht, Universität Karlsruhe, pp. 189-220.

66. Sauer, G., 1976, “Spannungsumlagerung und Oberflächensenkung beim Vortrieb von Tunneln mit geringer Überdeckung” *Inst. Boden und Felsmech.* Uni. Klie Heft 67

67. Schmid, J., 1926, *Statische Grenzprobleme in kreis-förmig durchörterten Gebirge*. Springer Verlag, Berlin.

68. Schubert, G., 2004, *Grundlagen der NATM*, Skriptum, TU Graz Institute Für FelsMechanik und Tunnelbau.

69. Schubert, W, Goricki, A., and G. Riedmüller, 2010, *Guideline for The Geomechanical Design of Underground Structures,* Austrian Society for Geomechanics, Vienna.

70. Schubert, W. and G. M. Vavrovsky, 1996, *Die Neue Osterreichische Tunnelbaumethode*, Österreichische Ingenieur- und Architekten-Zeitschrift (ÖIAZ), 141, Heft 7-8.

71. Schubert, W., 1994, "Gebirgsdruck und Tunnelbau – aus der Sicht von Rabcewicz 1944", *Felsbau*, Vol. 12 Issue 5, pp. 303-305, Vienna.

72. Schubert, W., 2002, *Grundlagen der New Austrian Tunnelling Method*, Technische Universität Graz, Institute für Felsmechanik und Tunnelbau,

73. Schubert, W., 2015, *Development and Background of NATM*, Graz University of Technology, Austrian Tunneling Seminar, Ankara.

74. Sharma, B., 1976, "Model Tests for Slope Tunnels in Jointed Rocks", *Rock Mechanics Suppl. V*, Springer Verlag, pp. 179–190, Vienna.

75. Shen, B., and N. Barton, 1997, "The Disturbed Zone Around Tunnels in Jointed Rock Masses, Technical Note", *International Journal of Rock Mechanics & Mining Sciences*, Vol. 34: 1, pp. 117-125, January.

76. Spang R. M., 1976, *Möglichkeiten und Grenzen des Base Friction Konzepts*, Rock Mechanics and Rock Engineering, Volume 8, Issue 3, pp 185–198, September.

77. Stini, J., 1950, *Tunnel-baugeologie*. Springer Verlag. Wien,

78. Stipek, W., 2012, “50 Years of NATM: Experience Reports”, *International Tunneling Association,* Austria,

79. Terzaghi, K., 1946, “Rock Defects and Loads on Tunnel Support”, *Rock Tunneling with Steel Supports,* Commercial Shearing & Stamping Company, Youngstown, Ohio.

80. Trompeter, W. H., 1899, *Die Expansivkraft im Gestein als Hauptursache der Bewegung des den Bergbau umgebenden Gebirges*. Essen.

81. Tsesarsky, M., 2005, *Stability of Underground Openings in Stratified and Jointed Rock*, Ph.D. Dissertation, Ben Gurion University of the Negev.

82. UK Health & Safety Executive, 2014, *Safety of New Austrian Tunnelling Method (NATM) Tunnels*,

83. Vardar, M., 1977, *Zeiteinfluss auf das Bruchverhalten des Gebirges in der Umgebung von Tunneln*, Fakultät für Bauingenieur-und Vermessungswesen der Universität Karlsruhe (TH), pp. 1-26

84. Vardar, M., 1979, “Yeraltı Kaya Yapıları Mekaniğindeki Son Gelişmeler”, *Mühendislik Jeolojisi Türk Milli Komitesi Bülteni*, Yıl 2, Sayı 2, Ankara.

85. Vardar, M., 1981, "Kayanın Zamana Bağlı Kırılma Davranışlarının Madenlerdeki Kaya Yapılarının Stabilitesine Olan Etkisi", Türkiye VII. Madencilik Kongresi, pp. 85-100, Ankara.

86. Vardar, M., 1981, “Tünel İnşaatı için Kaya (Dağ) Sınıflamaları”, *Mühendislik Jeolojisi Türk Milli Komitesi Bülteni*, Yıl 4, Sayı 4, Ankara.

87. Vardar, M., 1983, “Kaya Anizotropisi ve Kayanın Kırılma Direncindeki Değişimler”, *Mühendislik Jeolojisi Türk Milli Komitesi Bülteni,* Yıl 5, Sayı 5, Ankara.

88. Vardar, M., 1994, “Istanbul Metrosu Örneğinde Kaya Mekaniği Parametrelerinin Uygulama ve Planlamadaki Yeri”, T.M.M.O.B. Maden Mühendisleri Odası Ulaşımda Yeraltı Kazıları 1. Sempozyumu, pp. 13-24, Istanbul.

89. Vardar, M., 1994, “Metro Tünellerinde Duraylılığın Korunması ve Sağlanması, Sağlamlaştırma-Destekleme-Iyileştirme”, T.M.M.O.B. Maden Mühendisleri Odası Ulaşımda Yeraltı Kazıları 1. Sempozyumu, pp. 39-48, Istanbul.

90. Vardar, M., 1999, *Kaya Yapıları Mekaniği Yüksek Lisans Ders Notları,* Istanbul Teknik Universitesi, Istanbul.

91. Vardar, M., 2004, *Kaya Mekaniği Ders Notları*, Istanbul Teknik Üniversitesi, Maden Fakültesi, Uygulamalı Jeoloji Anabilim Dalı, Istanbul

92. Vardar, M., 2005, *Time Dependent Stability Problems in Tunnels and Time Dependent Behavior of the Rock Mass*, ITA / AITES Training Course Tunnel Engineering,

93. Wiesmann, E. 1909, Ein Beitrag zur Frage der Gebirgs- und Gesteinsfestigkeit “, *In: Schweizerische Bauzeitung*, Bd. LIII, Nr. 13

94. Wiesmann, E., 1912, “Über Gebirgsdruck”, *In: Schweizerische Bauzeitung*, Bd. LX, Nr. 7, Nr. 8.

95. Wittke W. and C. Louis, 1968, “Modell Versuche zur Durchströmung Klüftiger Medien” *Felsmechanik und Ingenieurgeologie*, Suppl. IV, pp. 52 – 78.

96. Yeung, M. R., and L. L. Leong, 1997, “Effects of Joint Attributes on Tunnel Stability”, *International Journal of Rock Mechanics and Mining Sciences,* Vol. 34, Issues 3–4, April–June 1997, pp. 348.e1-348.e18

97. Yu, C.W. and J.C. Chern, 2007, “Expert System for D&B Tunnel Construction”, in Barták, Hrdina, Romancov & Zlámal (eds.), *Underground Space – the 4th Dimension of Metropolises*, Taylor & Francis Group, London,